Climate Change Impacts on Climate Variables for a Deep Geological Repository (South Bruce Study Area)

NWMO-TR-2020-09 December 2020

Patrick Breach, Janya Kelly, Sean Capstick

Golder Associates Ltd

NUCLEAR WASTE MANAGEMENT ORGANIZATION
SOCIÉTÉ DE GESTION DES DÉCHETS NUCLÉAIRES

Nuclear Waste Management Organization
22 St. Clair Avenue East, 6th Floor
Toronto, Ontario
M4T 2S3
Canada

Tel: 416-934-9814
Web: www.nwmo.ca

Climate Change Impacts on Climate Variables for a Deep Geological Repository (South Bruce Study Area)

NWMO-TR-2020-09

December 2020

Patrick Breach, Janya Kelly, Sean Capstick
Golder Associates Ltd

Document History

Title:	Climate Change Impacts on Climate Variables for a Deep Geological Repository (South Bruce Study Area)		
Report Number:	NWMO-TR-2020-09		
Revision:	R000	Date:	December 2020
Golder Associates Ltd			
Authored by:	Patrick Breach, Golder Associates Ltd		
Verified by:	Janya Kelly, Golder Associates Ltd		
Approved by:	Sean Capstick, Golder Associates Ltd		
Nuclear Waste Management Organization			
Reviewed by:	Helen Leung, Jeremy Chen, Kelly Liberda and Melissa Mayhew		
Accepted by:	Paul Gierszewski		

Revision Summary		
Revision Number	**Date**	**Description of Changes/Improvements**
R000	2020-12-14	First issue

ABSTRACT

Title: **Climate Change Impacts on Climate Variables for a Deep Geological Repository (South Bruce Study Area)**
Report No.: **NWMO-TR-2020-09**
Author(s): Patrick Breach, Janya Kelly, Sean Capstick
Company: Golder Associates Ltd
Date: December 2020

The Nuclear Waste Management Organization (NWMO) completed a literature review on climate change impacts and developed a preferred method to assess the climate change impacts on probable maximum precipitation (PMP). The objective of this study is to apply the preferred method to assess the climate change impacts on the PMP and Intensity-Duration-Frequency (IDF) amounts for a case study (South Bruce study area) during currently planned Deep Geological Repository (DGR) implementation periods for used fuel. Additional climate variables including monthly temperature and precipitation statistics, World Meteorological Organization (WMO) climate indices, potential evapotranspiration, drought index, wind speed and relative humidity have been included to provide more context to the climate change projections given for extreme rainfall. Daily timeseries for the current climate and future projections have been developed to support climate change impact studies at the site.

The results have been presented for a range of global climate models within the ensemble and are expressed in terms of percentiles, so that the level of acceptable risk can be selected by using the desired percentile. Climate extreme projections for the 2050s and 2080s are indicating a future that is likely to be wetter, which is consistent with the current and future climate projections. Both the 1-day PMP values and the 1-day rainfall events are projected to increase during the 2050s and 2080s at the 50th percentile level.

There is a level of inherent uncertainty when projecting future climate; however, the approach taken in this study aims to address this uncertainty by relying on a multi-model ensemble and providing percentiles. The estimated percent changes to precipitation through the PMP and IDF curves have been described in terms of percentiles, allowing for different levels of acceptable risk. The additional climate variables also carry uncertainty related to the multi-model ensemble, which is expressed using percentiles. In addition, the qualitative analyses for relative humidity and wind speed also carry uncertainty through the use of available data taken from the literature, or from data sources that may not be as applicable to the site compared to the downscaled multi-model ensemble used for precipitation and temperature variables.

The selection of future projections for a climate change risk assessment should be based on the balance between the extra investment and consequential risks.

Based on Golder's experience in climate change projections, the proposed approaches are considered best guidance for the industry.

TABLE OF CONTENTS

LIST OF TABLES

Page

LIST OF FIGURES

Page

GLOSSARY OF TERMINOLOGY AND ABBREVIATIONS

Term/Acronym	Definition
AD	Anderson-Darling
AHCCD	Adjusted and Homogenized Canadian Climate Data
AMS	Annual Maximum Series
AR5	Fifth Assessment Report
BCCAQ	Bias Correction/Constructed Analogues with Quantile mapping reordering
CC	Climate Change
CCCR	Canada's Changing Climate Report
CDF	Cumulative Density Function
CMIP	Climate Model Intercomparison Project
CS	Climate Station
CSA	Canadian Standards Association
DAD	Duration-Area Depth
DGR	Deep Geologic Repository
ECCC	Environment and Climate Change Canada
ECMWF	European Centre for Medium-Range Weather Forecasts
ECP	Extended Concentration Pathways
ETCCDI	Expert Team on Climate Change Detection and Indices
EQM	Equidistant Quantile Matching
EV1	Extreme-Value Type 1 Distribution (Gumbel)
EV2	Extreme-Value Type 2 Distribution (Fréchet)
EV3	Extreme-Value Type 3 Distribution (Weibull)
GCM	Global Climate Model
GEV	Generalized Extreme Value
IDF	Intensity-Duration-Frequency
IPCC	Intergovernmental Panel on Climate Change

Term/Acronym	Definition
KS	Kolmogorov-Smirnov
LOCA	Localized Constructed Analogues
LP3	Log-Pearson Type 3
MERRA	Modern-Era Retrospective analysis for Research and Applications
MNRF	Ministry of Natural Resources and Forestry
MTO	Ministry of Transportation Ontario
NASA	National Aeronautics and Space Administration
NWMO	Nuclear Waste Management Organization
OCDP	Ontario Climate Data Portal
OFAT	Ontario Flow Assessment Tool
OMNR	Ontario Ministry of Natural Resources
PDF	Probability Density Function
PE3	Pearson Type 3
PMP	Probable Maximum Precipitation
PPT	Precipitation
PWC	Precipitable Water Content
PWM	Probability Weighted Moment
QDM	Quantile Delta Mapping
RCP	Representative Concentration Pathway
RCS	Regional Climate Station
RM	Ratio Method
SPEI	Standardized Precipitation and Evapotranspiration Index
SRES	Special Report on Emissions Scenarios
UNEP	United Nations Environment Program
WCRP	World Climate Research Program
WMO	World Meteorological Organization

1. INTRODUCTION

A changing climate within Ontario's watersheds may present physical risks to infrastructure if designs do not consider the impacts of these changes. Golder Associates Ltd. (Golder) was retained to apply the developed methodology by the Nuclear Waste Management Organization (NWMO) in Wood (2019) to assess the impacts of climate change on probable maximum precipitation (PMP) events for two study areas for a Deep Geologic Repository (DGR) for used fuel. In addition to the assessment of future PMP events, future Intensity-Duration-Frequency (IDF) values are estimated for a range of return periods varying from 2 to 2000-year return periods. Additional climate variables including seasonal, annual, and monthly temperature and precipitation statistics are calculated along with derived climate variables including rain and snow, snow depth, potential evapotranspiration, drought index, and qualitative information for wind speed and relative humidity.

Previous studies undertaken within the Ontario Power Generation's DGR Project for low and intermediate level radioactive waste at the Bruce nuclear site have evaluated the potential for flooding to impact the operations of the DGR based on the current climate (AMEC 2011). In the future, projected higher temperatures may change the capacity of the atmosphere to hold water, potentially resulting in more frequent and intense storms. This projected change in climate may increase vulnerabilities to potential climate extremes at the two DGR study areas (i.e., Ignace and South Bruce) for used fuel. Siting the potential placement of the DGR within these two study areas must consider the range of credible storms within the watershed to appropriately design the associated storm water management system. Therefore, the first step towards potential placement of the DGR is to understand how the projected changes in climate may impact PMP and IDF values at the study areas using the method developed in Wood (2019).

This report documents the climate change impacts on IDF, PMP, and additional climate variables in the South Bruce study area. The approach and methodology are summarized first to characterize the current and future climate conditions in the South Bruce study area (Section 2). Detailed descriptions of the data sources and approaches used for both the climate baseline and future climate projections are provided in Appendix A. Next, for the baseline and future climate conditions, IDF, PMP, and additional climate variable values are estimated respectively in Section 3 and Section 4. Detailed statistics for PMP, IDF, and additional climate estimates are given in Appendix B, while daily current and future climate timeseries for the additional climate variables are provided in Appendix C. A qualitative climate assessment for considering the projected changes in PMP, IDF and additional climate variables beyond the year 2100 is given in Section 5. Uncertainty of climate change projections and recommendations on how to use the data are discussed in Section 6 and Section 7, respectively. Finally, conclusions and recommendations are provided in Section 8.

2. APPROACH AND METHODOLOGY ON PMP, IDF, AND ADDITIONAL CLIMATE VARIABLE ANALYSES

Understanding what the current climate conditions of the study area are and understanding how they are projected to change under future climate change are fundamental to the following approach. The discussion of climate vulnerability is focused around rainfall events, namely PMP and IDF values with different return periods and durations. Contextual climate information is also provided for additional climate variables. The approach follows the key steps in Figure 1. The following sections provide high level overviews of the methodologies used to develop the current climate and future projected climate datasets used in this assessment. More detailed information on each methodology is provided in Appendix A.

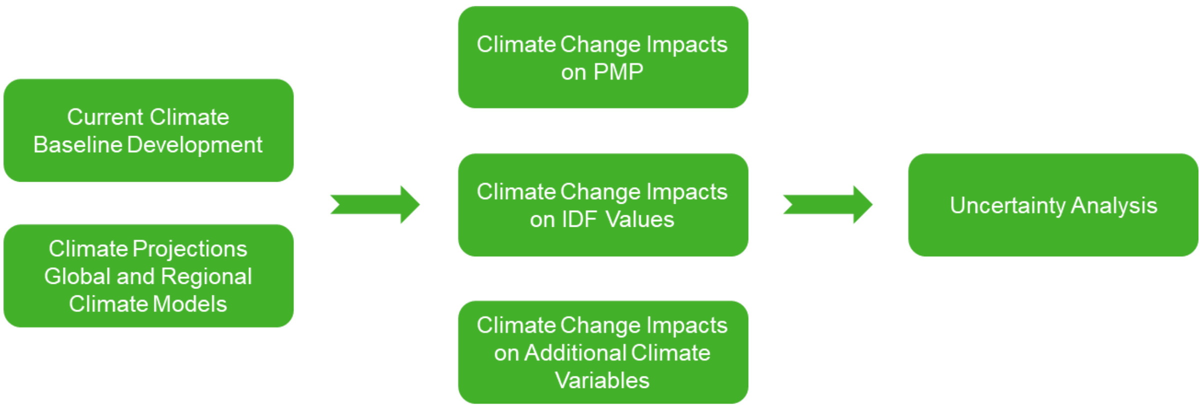

Figure 1: High Level Step-Wise Approach

2.1 Current Climate Methodology on PMP, IDF, and Additional Climate Variable Analyses

Understanding the current climate and current climate trends is important when evaluating current design parameters. Where available, the climate baseline is grounded in observations from local climate observation stations. The baseline is established using available local climate stations and/or publicly available nearby regional climate stations infilled with reanalysis data whenever possible (to meet data completeness requirements, such as only considering observations where at least 90% observations are available in any given year or month). Before infilling, the reanalysis data are compared and correlated to available regional climate stations.

Reanalysis data from Version 2 of the National Aeronautics and Space Administration's (NASA's) Modern-Era Retrospective analysis for Research and Applications (MERRA-2) and the European Centre for Medium-Range Weather Forecasts (ECMWF) Re-Analysis (ERA5) data are used to represent current climate or to infill the missing data from observations. R-squared (R^2) statistics is calculated between MERRA-2 and ERA5 and is used to complete missing historical observed dataset. The R^2, also known as coefficient of determination, provides a measure of how well observed outcomes are replicated by the regression line fitted. It ranges from 0 to 1, 1 being a perfect fit.

Using the daily current climate baseline precipitation, the PMP is calculated according to Hershfield Method (Chapter 4 in WMO 2009a) and the DAD (duration-area-depth) curves discussed in Appendix A of this report. A second method (the Transposition method) relies on observations of significant storms nearby the study area and is accomplished by construction of DAD curves. Using the same daily current climate baseline precipitation, IDF values are then calculated for various durations (1-day through 120-day) and return periods (1 in 100 years and 1 in 500 years). PMP is calculated for 1-day, 2-day, and 3-day durations. The IDF values for the current climate are calculated by adjusting a statistical distribution to the Annual Maximum Series (AMS) based on daily observed data. The AMS is a record of the largest 1-day rainfall for each year in a series and is calculated by extracting the maximum value of the daily precipitation series for each year. Three statistical distributions (Gumbel, Generalized Extreme Value – GEV, Pearson/Log-Pearson Type 3) are tested against the available data and the parameters are estimated using the method of L-moments (Hosking and Wallis 1997), following the approach adopted by Environment and Climate Change Canada - ECCC (ECCC 2019).

Annual and monthly temperature and precipitation statistics are calculated by resampling the daily current climate dataset. Derived variables including rain, snow, snow depth, drought index, World Meteorology Organization (WMO) climate indices, and potential evapotranspiration use precipitation and temperature values from the current climate dataset. Rain, snow and snow depth are calculated using methods adopted by ECCC, drought index is calculated using the Standardized Precipitation and Evapotranspiration Index (SPEI) method of Vicente-Serrano et al. (2010), WMO Indices are calculated using the methods of WMO (2009b), and potential evapotranspiration is calculated using the Hargreaves method (Hargreaves and Samani 1985). A high-level flowchart with the analyses conducted is presented in Figure 2.

The detailed description of the methods is presented in Appendix A.2.

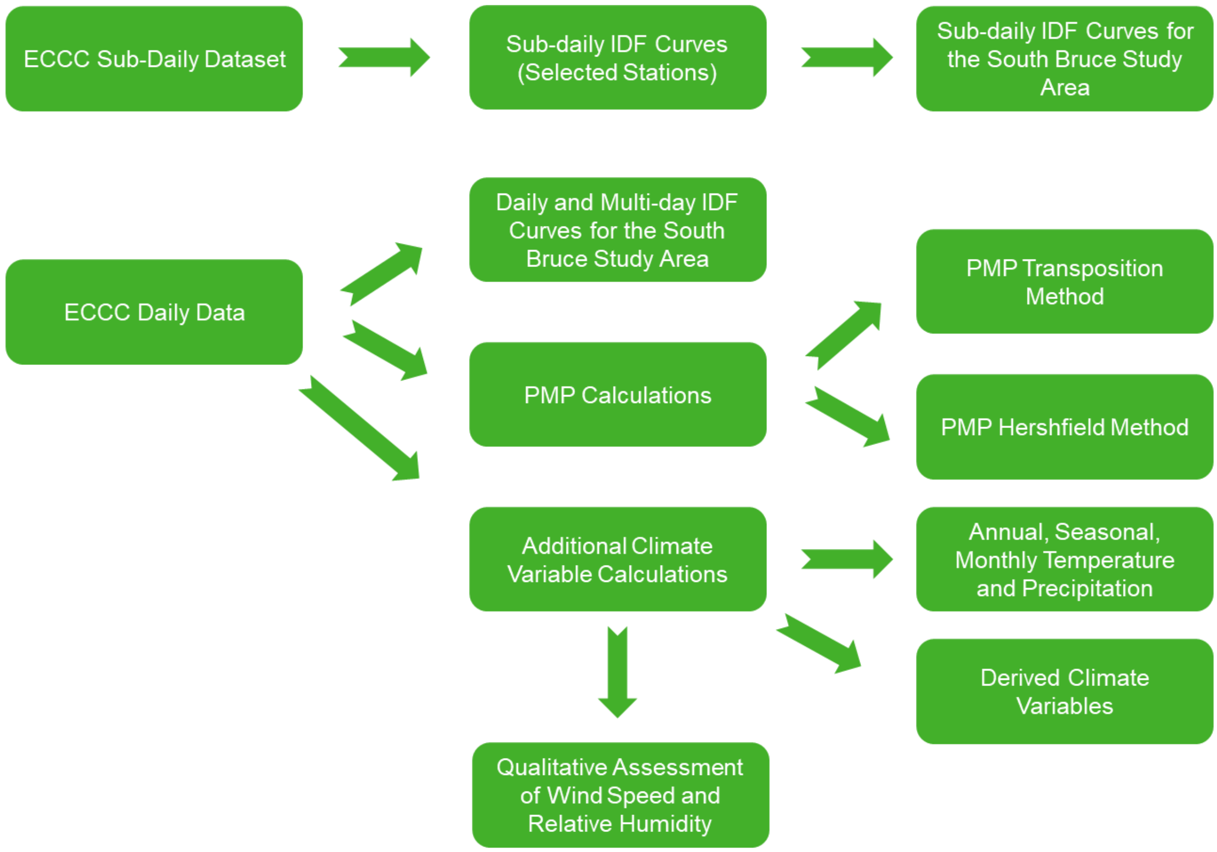

Figure 2: High-Level Summary of Evaluation of Current Climate on PMP, IDF, and Additional Climate Variable Analyses

2.2 Future Climate Methodology on PMP, IDF, and Additional Climate Variable Analyses

The approach to evaluating future climate impacts on precipitation uses the state of science and publicly available climate projections to complete the climate change impact assessment on the PMP and the IDF values. The range of projected future climate depends on the emission scenario used to project the future climate conditions as well as selected global climate model (GCM). Since no one model or climate scenario can be viewed as completely accurate, the Intergovernmental Panel on Climate Change (IPCC) recommends that climate change assessments use as many models and climate scenarios as possible, or a “multi-model ensemble”. For this reason, the multi-model ensemble approach is used here to describe the probable range of results using percentile levels. Changes to both PMP and IDF curves are expressed as percent changes from the model baseline. For the additional climate variables, temperature-based statistics and the WMO indices are expressed as absolute changes while all other variables are expressed as percentage changes.

For this study, Golder developed methods to extract climate data (precipitation and temperature) from the multi-model ensemble for model baseline (1979-2019), the mid-century (2041- 2070), and end-of-century (2071 through to 2100) time periods for the PMP, IDF, and additional climate variables. The baseline period of 1979 to 2019 was selected based on a combination of data availability constraints, as well as the need for high quality precipitation observations to allow for more accurate analysis of precipitation extremes in the form of PMP and IDF curves. The future time periods of 2041 to 2070 (2050s) and 2071 to 2100 (2080s), chosen to be a length of 30 years (minimum number of years needed to represent a climate normal as recommended by the World Meteorological Organization (WMO)), represent the changes in climate for mid-century and end of century time periods and are applicable to the site characterization, construction and operational periods. Currently, downscaled climate projections only extend out to the year 2100, making the 2071 to 2100 time period the furthest point into the future for detailed assessment. A qualitative assessment is provided for time periods beyond 2100 to cover the monitoring and decommissioning periods for the project. Emission scenarios RCP 2.6, RCP 4.5, and RCP 8.5 from the IPCC Fifth Assessment Report (AR5) (IPCC 2013) are used to describe the model baseline, mid-century and end-of-century time periods. The qualitative assessment past 2100 relies on projections available in literature.

Daily downscaled climate projections for precipitation and minimum and maximum temperature are obtained for the multi-model ensemble. This ensemble consists of statistically downscaled climate scenarios that correspond to a particular GCM for a given Representative Concentration Pathway (RCP). These daily time-series are then used in conjunction with methods for estimating PMP, snowfall, and moisture to establish initial ranges for PMP-related variables (based on literature values and results from historic analysis of PMPs), including precipitable water and moisture content, and rainfall. Ranges for previously identified ancillary factors (such as snowpack and snowmelt) are also established. The ranges are then presented as percent changes between the baseline period and the selected future periods across all GCMs and RCPs.

Using the historic data and GCM ensemble results, projections for future IDF values are developed. These projections can be used to understand aspects of the PMP storm (including sub-daily rainfall distribution) and how the PMP storm compares to more frequent design storms typically used in non-critical infrastructure design. These IDF values are done using two methods currently used by Golder to estimate the changes to IDF distributions: (1) Quantile Delta Mapping (QDM) method and; (2) the Ratio Method (RM).

A high-level flowchart with the PMP and IDF analyses conducted is presented in Figure 3. The future projected changes in PMP are calculated using the moisture maximization method and the Hershfield method. The moisture maximization method is not used for current climate conditions, since it produces an analogous vapour pressure result (rather than an absolute rainfall depth value), and can only be used to estimate the change in PMP (i.e., based on change in vapour pressure) rather than provide an absolute value. Comparing the modelled future climate to modelled baseline produces changes in specific humidity, so it can be used to estimate percent change in PMP depths between baseline and future conditions. Ensemble statistics in terms of percentiles are calculated across the results from both methods. The daily rain and snowmelt projected changes are calculated using the same methodology as for the current climate but applied to all ensemble members and presented using percentiles across the ensemble.

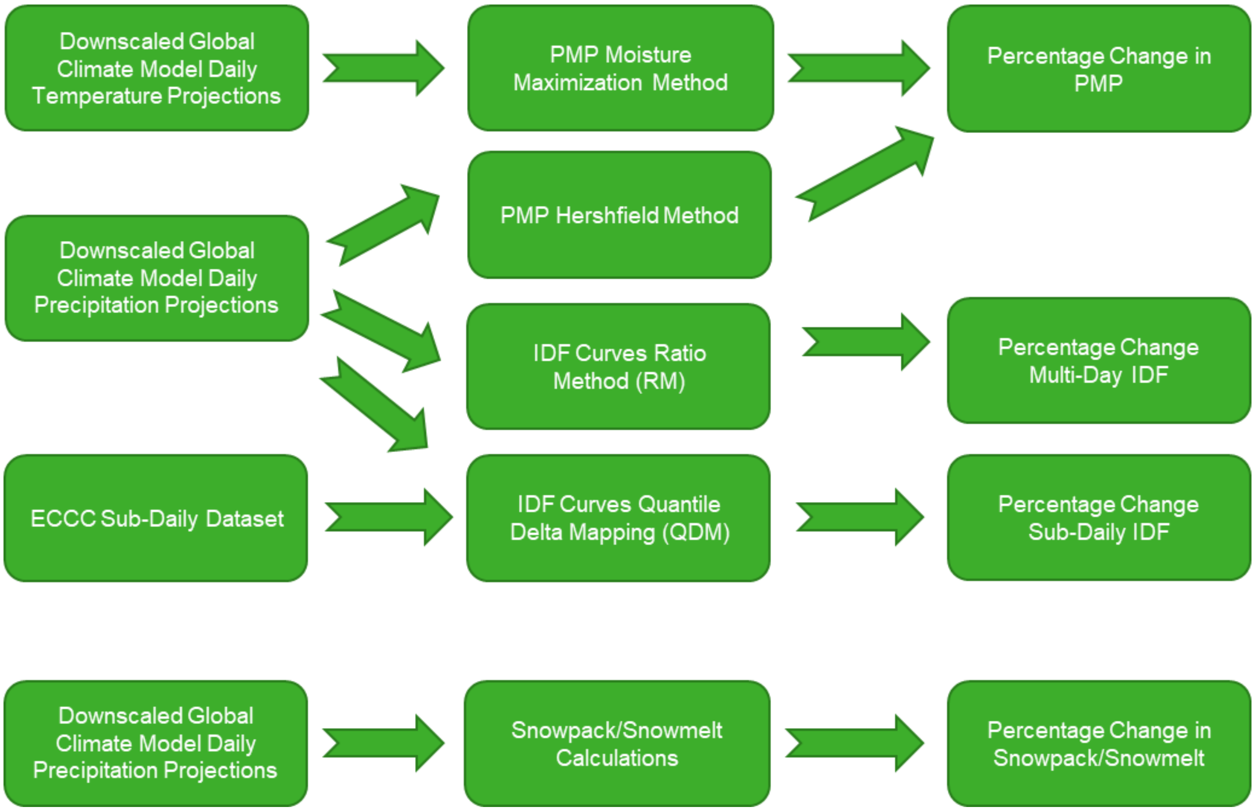

Figure 3: High-Level Summary of Evaluation of Future Climate on PMP and IDF Estimates

In Figure 4, the analyses conducted for the additional climate variables and how they relate to one another are presented. Future change in rain, snow, snow depth, WMO climate indices, and potential evapotranspiration are derived from both precipitation and temperature values from the downscaled climate projections. The drought index is estimated using the Standardized Precipitation and Evapotranspiration Index (SPEI), which incorporates precipitation projections and potential evapotranspiration derived from the temperature projections. Qualitative analyses are carried out for wind speed and relative humidity, as these variables are not included in the statistically downscaled model ensemble. Published values applicable to the South Bruce study are used to infer how these variables may change in the future.

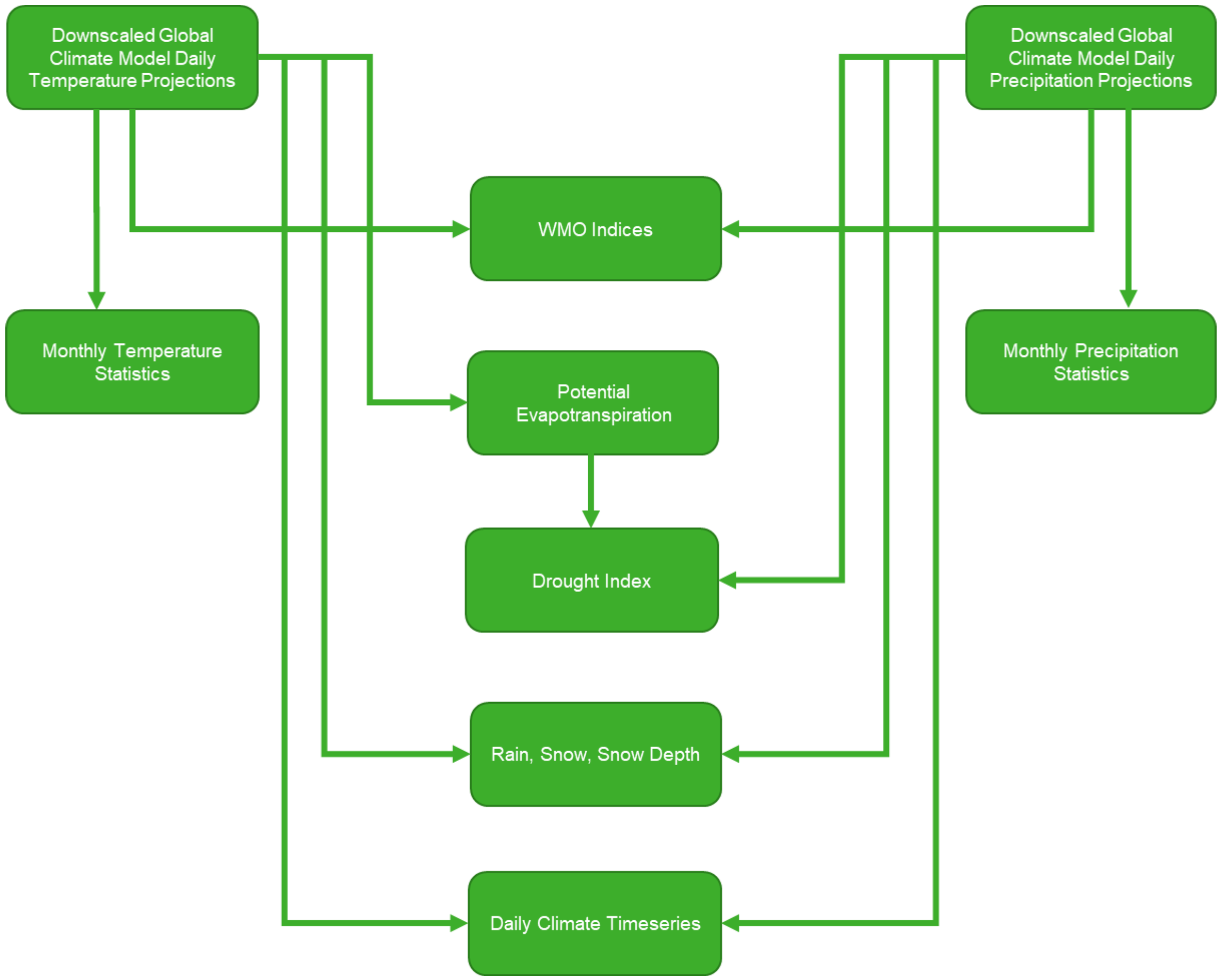

Figure 4: High-Level Summary of Evaluation of Future Climate on Additional Climate Variable Estimates

The detailed description of the methods for future climate is presented in Appendix A.3.

3. ANALYSES OF CURRENT CLIMATE ON PMP, IDF, AND ADDITIONAL CLIMATE VARIABLES

The following sections outline the development of the climate baseline and calculations of the baseline IDF curves and PMP. The baseline was developed using the high-level methodology described in Section 2.1. The detailed description of the methods is presented in Appendix A.2. Select tables presented in this section are coloured using a gradient to aid in the visual representation of the values. The colour gradients provide a relative indication of the highest (red) and lowest (green) values with transitional colours in between. Colours cannot be compared between tables, as the colour scale is relative to the values in each table.

3.1 Climate Baseline Development

The current climate baseline was developed using publicly available regional climate stations based on the methodology presented in Appendix A.2.

The following sections describe the three climate datasets used for the various analyses in this report:

1) Daily dataset to screen for significant storms for the Transposition method and the construction of the DAD curves as used in Wood (2019).
2) Daily infilled dataset at the South Bruce study area for the analysis of daily and multi-day IDF curves, the PMP statistical (Hershfield) method, and the analysis of rainfall on snow and snowpack.
3) Data from the ECCC Engineering Database for the calculation of the sub-daily IDF curves.

3.1.1 Daily Climate Dataset

The main criteria for the climate stations selected were the length of record (minimum 30 years of data), proximity to the study area, and the availability of continuous precipitation data. Other criteria are listed in Appendix A.2. All publicly available stations within about 50 km from the study area were considered for the analysis of regional storms. The candidate stations with daily data for the South Bruce study area were collected from Environment and Climate Change Canada (ECCC 2019a). The list of the selected stations is presented in Table 1 and the location of the stations relative to the study area is provided in Figure 5. These stations were primarily used to screen for significant storms in the study area and to assist in calculating the DAD curves. The data available for the DAD analysis are less critical, since the interest is in specific (large) events.

The climate stations described in Table 1 are used for identifying regional storm events, with a selected subset of these climate stations used to describe the site-level current climate conditions for the estimation of PMP and IDF statistics. Station selection to represent the study area of South Bruce applied the criteria in Appendix A.2 to the stations listed in Table 1. Through this process, the Wroxeter station was selected due to the availability of at least 30 years of recent continuous data as well as close proximity, similar elevation, and geographical siting (i.e., distance to Lake Huron) to the study area.

The criteria of a 30-year climate record eliminated Harriston and Jamestown stations. Kincardine station was eliminated due to very close proximity to Lake Huron which will likely influence precipitation patterns. Lucknow, Ayton, Paisley, and Durham station were eliminated due to a lack of recent data (records ending over 15 years prior to present day). The remaining stations included Blyth, Hanover, and Wroxeter which all had data availability above 95% for precipitation. Of these three stations trade-offs between elevation difference and distance from the study area, observed temperature availability, and recentness of data were assessed. Wroxeter has an elevation difference of only 15 m, was closest to the site (18.6 km), and had the most recent data, but no temperature data was available. Hanover station had high data availability for temperature and was close to the site, but also had the largest elevation difference and less recent data (records ending in 2008). Blyth station had very high data availability for both precipitation and temperature, and almost identical elevation compared to the study area, but was also the farthest (36.3 km).

Due to the focus of extreme precipitation statistics in this report, Wroxeter station was selected as it would likely be the most representative of current climate precipitation for the study area, being the closest station with the most recent data despite not having temperature observations. Compared to the localized nature of precipitation, temperature patterns vary on a more regional scale. In addition, temperature estimates that are slightly too low or high will not impact PMP and IDF statistics. Therefore, temperature estimates may be obtained from other nearby climate stations or through high resolution reanalysis datasets as a proxy for local observations (see Section 3.1.2). In this case, temperature data was obtained from the ERA5 reanalysis dataset to match the time period of precipitation observations from the Wroxeter station, as Hanover and Blyth climate stations have data series ending in 2008 and 2010, respectively.

An additional dataset was selected from the ECCC Engineering Database for the sub-daily IDF curves as noted in Table 1 (notes column). The selected station for sub-daily IDF analysis is discussed in Section 3.1.3.

Table 1: Climate Station Properties

Station Name	Climate ID	Latitude and Longitude	Elevation (masl [1])	Distance from Site (km)	Distance from Lake Huron (km)	Years Available	Notes
South Bruce Study Area	—	44.02, -81.21	350	—	38.5	—	Location of study area included for comparison
AYTON	6110439	44.08, -80.83	361.0	30.9	57.7	1988-1993	Used to screen for large storms
BLYTH	6120819	43.72, -81.38	350.5	36.3	27.5	1959-2010	Used to screen for large storms
DURHAM	6112171	44.18, -80.82	384.0	35.6	46.9	1882-2003	Used to screen for large storms
HANOVER	6113329	44.12, -81.01	270.0	19.2	48.0	1972-2008	Used to screen for large storms
HARRISTON	614CCNR	43.90, -80.80	401.0	35.5	73.2	1992-1995	Used to screen for large storms
JAMESTOWN	6143905	43.80, -81.18	319.0	24.8	43.4	2006-2015	Used to screen for large storms
KINCARDINE	6124127	44.17, -81.62	200.0	36.8	2.3	1870-2020	Used to screen for large storms
LUCKNOW	6124700	43.95, -81.50	289.6	24.8	17.0	1885-1993	Used to screen for large storms
MOUNT FOREST [2]	6145504	43.98, -80.75	415.0	37.0	74.6	1962-2016	Used for sub-daily IDF
PAISLEY	6126210	44.27, -81.37	244.1	30.4	17.2	1961-1992	Used for screen large storms
WROXETER	6129660	43.86, -81.15	335.0	18.6	45.5	1966-2020	Used for screen large storms and define the baseline at South Bruce study area, PMP estimates and daily/multi-day IDF Curves

Notes: [1] Meters above sea level.
[2] Included in the Engineering Dataset for Sub-Daily IDF curves analysis.

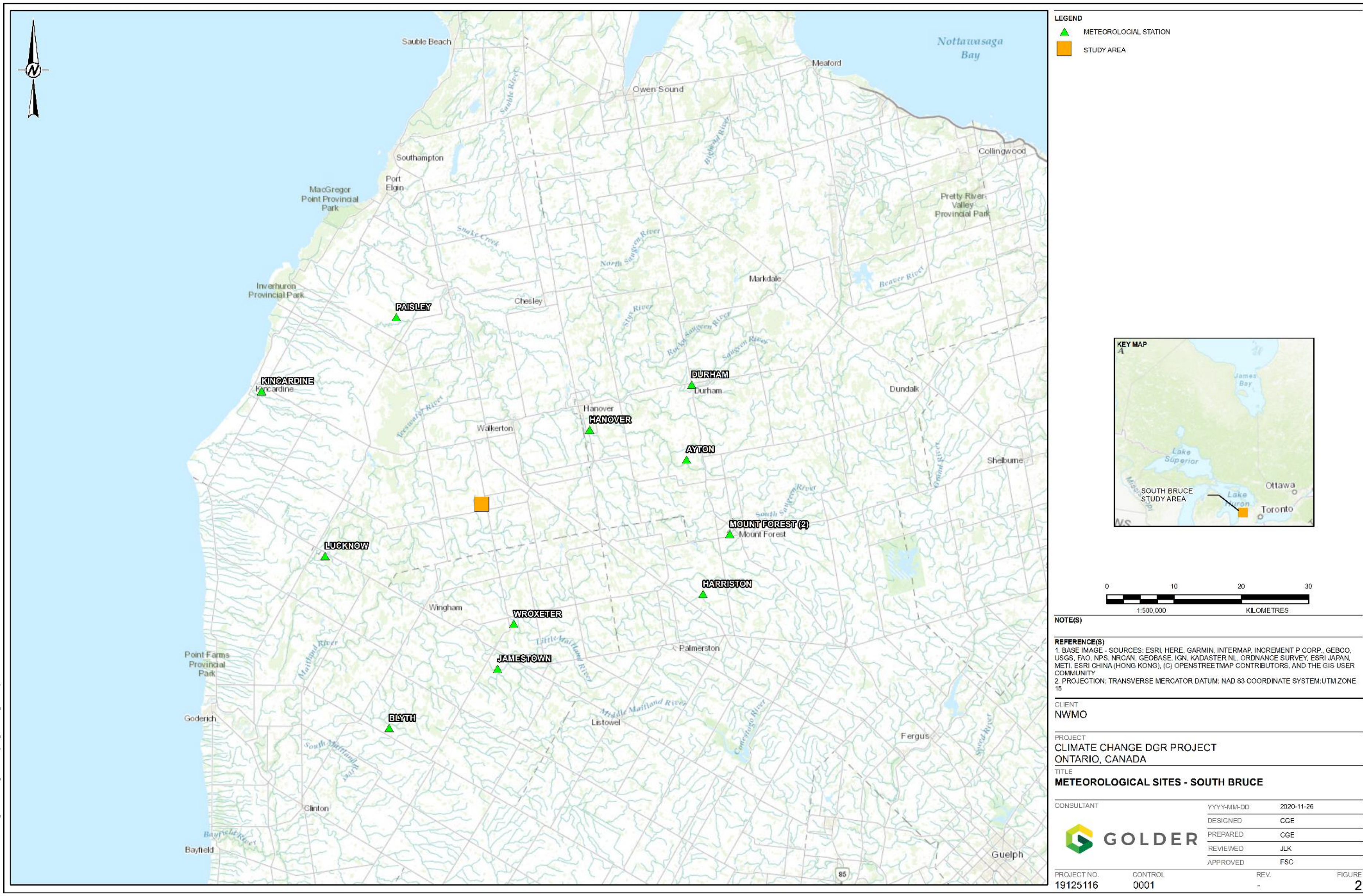

Figure 5: Map of South Bruce Study Area Location and Regional Climate Stations

3.1.2 Daily Infilled Dataset Series for the South Bruce Study Area

A daily dataset was defined for the South Bruce study area using Wroxeter (6129660) station to calculate the daily and multi-day IDF curves, PMP, and rainfall on snow analysis. The Wroxeter station has records dating back to 1966 and ending in 2020. Only years and months with at least 90% of the precipitation data available were considered (see Appendix A.2). A total of 24 months in the 54-year record were found to have less than 90% data availability. These months were primarily found in the years 1966, 1969, 1977, 2008, and 2009. These missing periods were infilled using reanalysis data to develop a continuous record. Observational data was not used for infilling of missing data at the Wroxeter station, due to lack of data for the year 2008 and later at climate stations in the region. No consistent trends were found in the missing data that could introduce bias in the representation of months or seasons.

Reanalysis data from MERRA-2 and ERA5 are only available from 1981 and 1979 onwards, respectively; therefore, infilling is not possible before these years. For Wroxeter station, ERA5 and MERRA-2 were both tested against the concurrent period from 1981 to 2019. This was done by:

1) Establishing concurrent periods between observations and reanalysis data, including only the months which are within the 90% data availability criterion of the observed data.
2) Comparing the monthly and annual variation of precipitation between observations and reanalysis datasets for the concurrent periods.
3) Calculation and comparison of R^2 statistic between the observed data and both ERA5 and MERRA-2 reanalysis datasets for the concurrent periods.

The reanalysis dataset that has the highest level of correlation (R^2 statistic) and the ability to capture the monthly and annual variation of the observed data was used for infilling.

A comparison of temperature and precipitation statistics on a monthly and annual time scale was conducted for Wroxeter, Blyth, and Hanover climate stations as well as the MERRA-2 and ERA5 reanalysis datasets (Figure 6 to Figure 9). This was done for the concurrent period of observations between the climate stations from 1991 to 2017, to examine regional variation in temperature and precipitation, and how this is captured by the reanalysis data. Comparison of the annual averaged monthly total precipitation (Figure 6) shows that MERRA-2 consistently underestimates monthly total precipitation at the Wroxeter station, while ERA-5 generally shows closer values to Wroxeter with slight overestimation in the summer months. Both MERRA-2 and ERA5 appear to capture interannual variability in annual total precipitation (Figure 7); however, MERRA-2 tends to underestimate while ERA5 shows much closer values. Linear regression of monthly total precipitation shows that ERA-5 presents a better agreement with observations from Wroxeter station, with an R-squared (R^2) statistic of 0.53, while MERRA-2 was lower at 0.40. Therefore, infilling of precipitation was accomplished using the ERA5 dataset by first applying a bias correction using the linear regression relationship then substituting for the missing values. Although the correlation coefficient is relatively low for both reanalysis datasets, the impact of including this data for infilling is expected to be minor as only 3% of the data was infilled, and bias correction was performed (Table 2). More details on the infilling process are discussed in Appendix A.2.1. Due to the presence of gaps in the Wroxeter station data prior to 1979, the current climate baseline period is established as 1979 to 2019. This will ensure that all missing data can be infilled using the ERA5 reanalysis data. Screening of storms for DAD curve development used the time period of 1870 to 2020 in order to capture all available data for major storm events in the region.

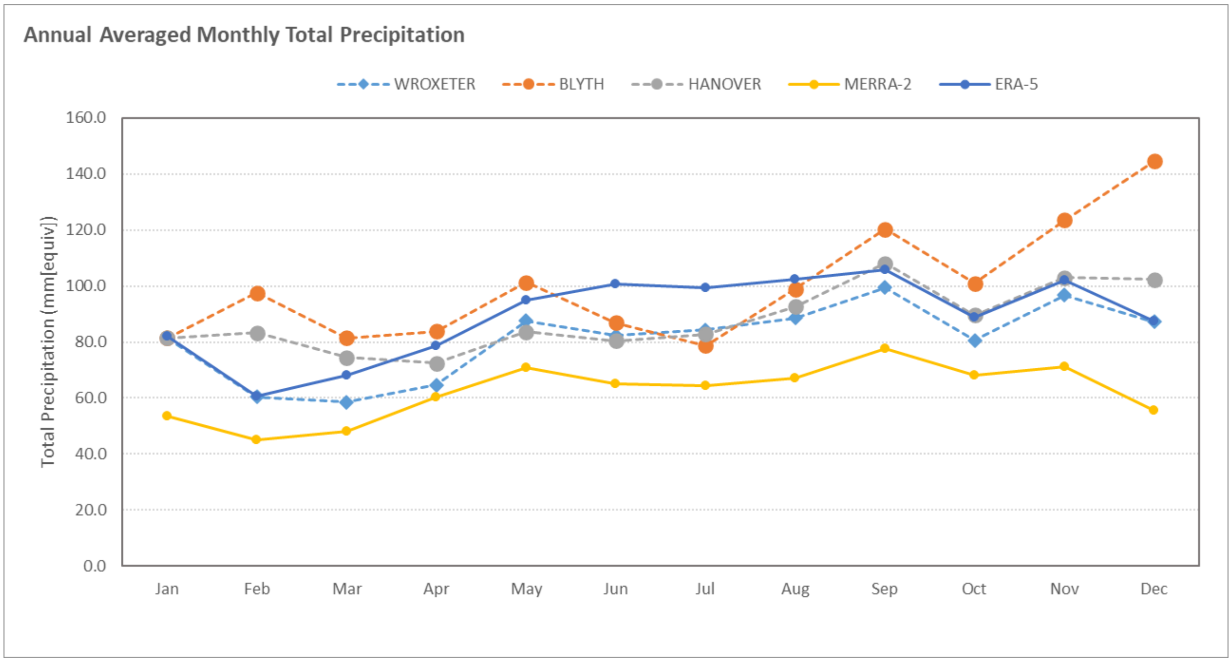

Figure 6: Comparison of Mean Monthly Total Precipitation for Concurrent Periods between Climate Stations and Reanalysis Data

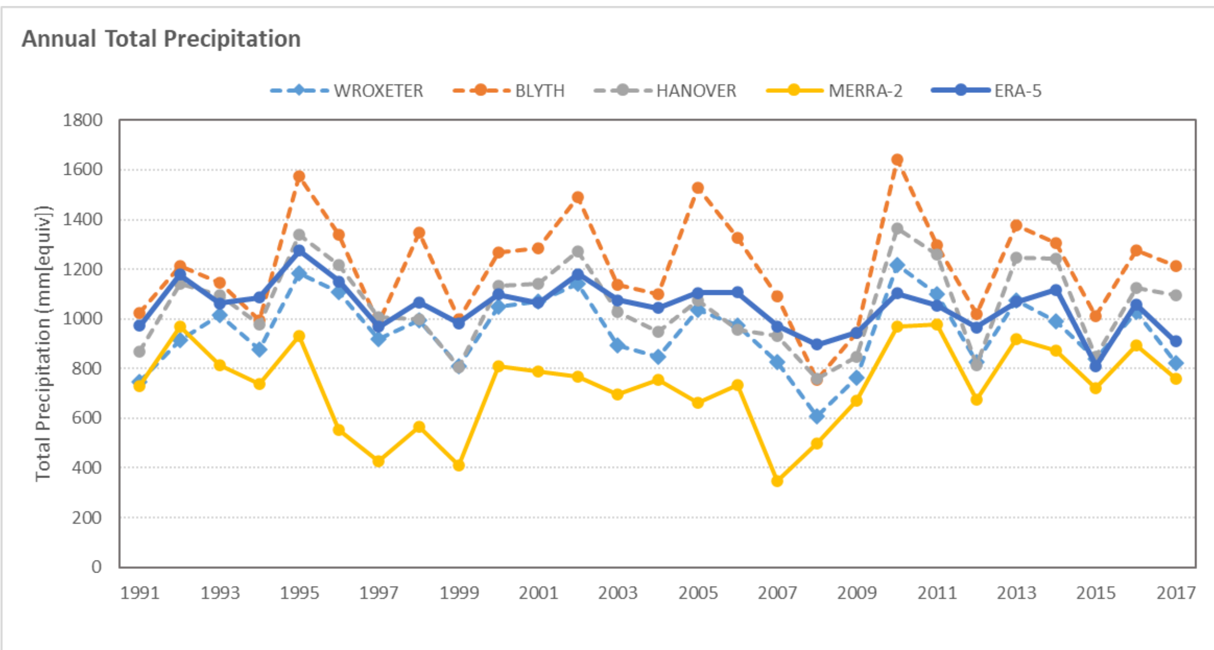

Figure 7: Comparison of Annual Total Precipitation for Concurrent Periods between Climate Stations and Reanalysis Data

Table 2: Correlation between Wroxeter (6129660) station and ERA-5 reanalysis during 1979-2019

Climate Variable	Percentage Infilled	Daily R^2	Infilling Equation
Daily Maximum Temperature	100%	—	Infilled=1.000 x ERA-5
Daily Minimum Temperature	100%	—	Infilled=1.000 x ERA-5
Daily Mean Temperature	100%	—	Infilled=1.000 x ERA-5
Daily Total Precipitation	3%	0.533	Infilled=0.795 x ERA-5

Temperature observations are not available from the Wroxeter station; therefore, temperature values were taken from another nearby regional climate station or based solely on reanalysis data. Comparison of annual average monthly mean temperature and annual average mean temperature for nearby regional climate stations and reanalysis datasets are shown in Figure 8 and Figure 9, with no corrections made to account for differences in station elevation. In Figure 8, it is shown that the seasonal variation in temperatures is fairly consistent in the region, with Hanover having slightly lower values on average likely due to its location at a higher latitude compared to Blyth. ERA-5 mean temperatures are slightly higher than Blyth in the spring months and lower during late summer to early fall. Similarly, Figure 9 shows Hanover station with lower annual average temperatures, while both ERA-5 and MERRA-2 show similar values compared to Blyth and capture interannual variation of mean temperature in the region. In summary, both reanalysis datasets capture seasonal and interannual variations of mean temperature. However, the ERA-5 dataset was used for infilling the Wroxeter station for consistency with precipitation infilling: an earlier starting year (1979 versus 1981), and the ability to extract values closer to the site due to higher resolution than MERRA-2 (0.25°x0.25° compared to 0.5°x0.625°).

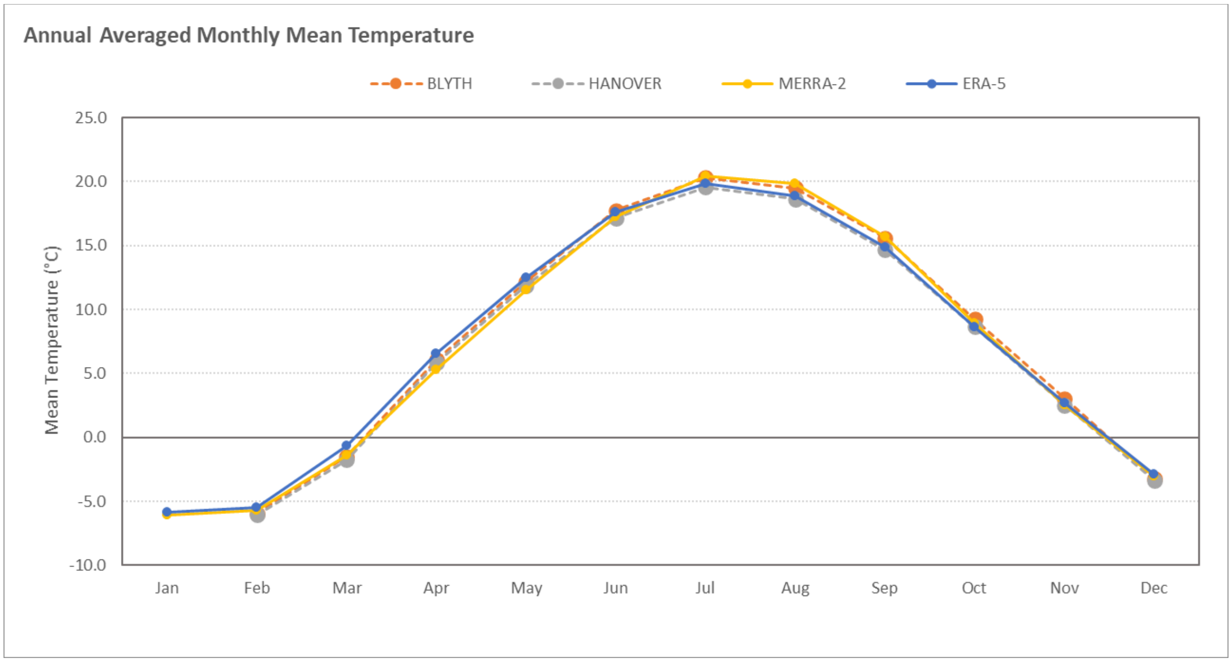

Figure 8: Comparison of Annual Averaged Monthly Mean Temperature for Concurrent Periods between Climate Stations and Reanalysis Data

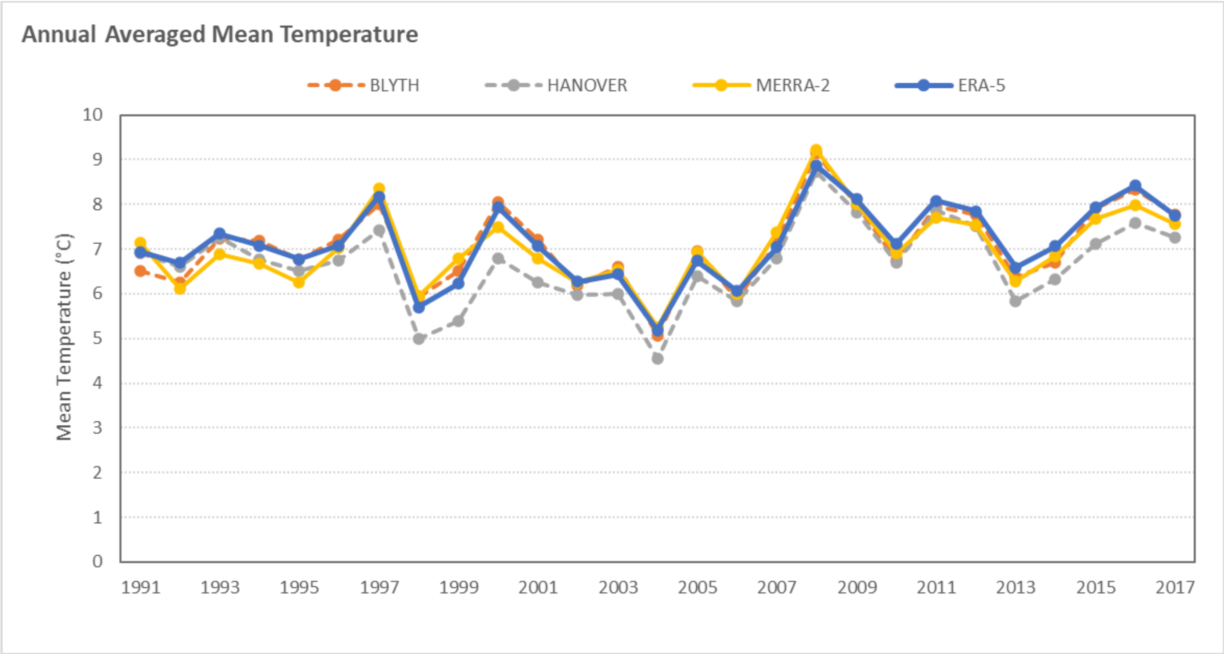

Figure 9: Comparison of Annual Averaged Mean Temperature for Concurrent Periods between Climate Stations and Reanalysis Data

The equations used for infilling precipitation and temperature variables are provided in Table 2. Bias correction was not performed for temperature variables, as there is no observed analog at the Wroxeter station to build the linear regression relationship. However, the low amount of variability in monthly mean temperature across climate stations and the reanalysis datasets demonstrates that bias correction is not needed (Figure 8). The resulting current climate baseline dataset includes daily total precipitation, minimum, maximum, and mean temperature for a total of 41 years from 1979 to 2019. Table 3 and Figure 10 highlight the annual maximum values of daily total precipitation to be used for analysis of precipitation extremes. The current climate dataset developed in this work provides a representative baseline for the South Bruce study area. Climate statistics may be calculated from this baseline, and future projected changes in climate may be applied to these statistics.

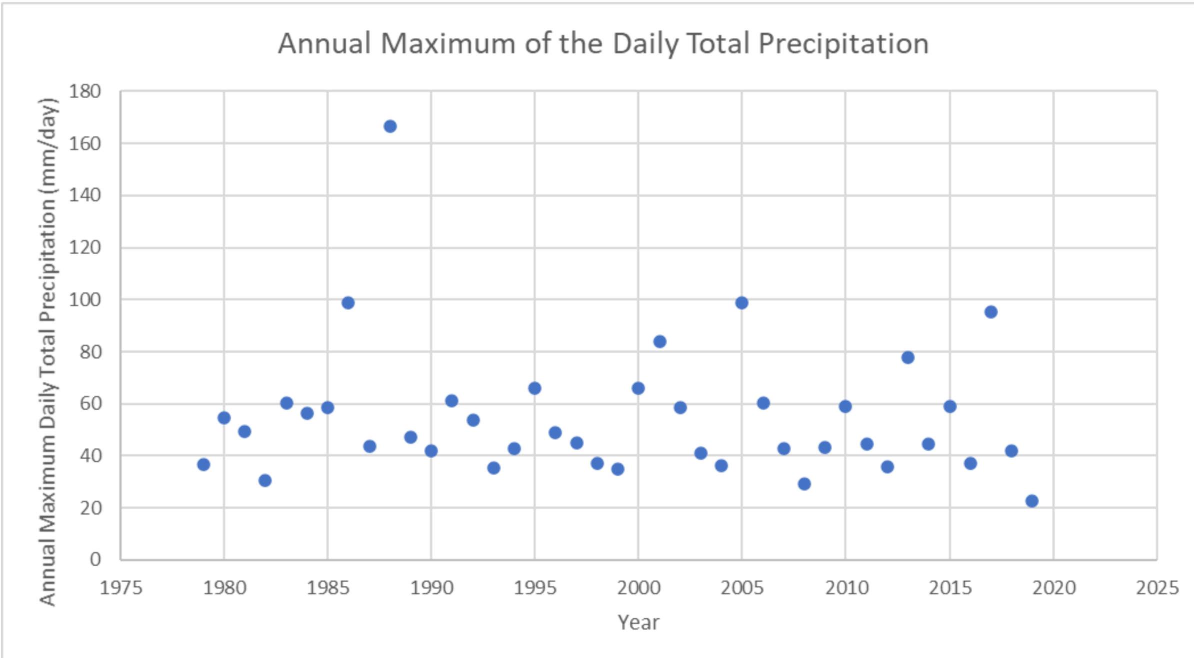

Figure 10: Annual Maximum of the Daily Total Precipitation Series for Wroxeter (6129660)

Table 3: Annual Maximum of the Daily Total Precipitation Series for Wroxeter (6129660)

Year	PPT (mm)	Year	[1]PPT (mm)	Year	PPT (mm)	Year	PPT (mm)
1979	36.8	1993	35.4	1952	45.2	2007	43
1980	54.6	1994	42.6	1953	78.0	2008	29.2
1981	49.2	1995	66	1954	33.5	2009	43.2
1982	30.5	1996	49	1956	28.2	2010	59
1983	60.3	1997	45	1957	44.5	2011	44.6
1984	56.2	1998	37	1958	49.0	2012	36
1985	58.7	1999	35	1960	38.9	2013	77.6
1986	99	2000	66	1961	36.3	2014	44.4
1987	43.6	2001	84	1962	73.2	2015	58.8
1988	166.4	2002	58.6	1963	56.4	2016	37
1989	47.1	2003	41	1964	44.5	2017	95.4
1990	41.8	2004	36.4	1965	57.4	2018	42
1991	61	2005	98.6	1966	27.9	2019	22.6
1992	53.9	2006	60.4	1967	31.8	—	—

Note: (1) PPT denotes the annual maximum daily total precipitation (mm).

3.1.3 IDF Engineering Dataset

In the region of the South Bruce study area, there are only 6 climate stations with sub-daily rainfall data available within a 75 km radius (Table 4). Of these 6 stations there are 2 with less than 30 years of available data (Grand Valley WPCP and Glen Allan). These stations were excluded from further analysis, as longer timeseries are preferred for the estimation of IDF statistics in order to better capture higher return period events and better capture the range of recorded storm events. Two of the remaining stations are in very close proximity to Lake Huron (Goderich and Owen Sound MOE) and were excluded due to the potential for lake effects on observed rainfall values. Of the final two stations, Stratford WWTP is located the farthest away from the study at 74.4 km, and Mount Forest (AUT) is the closest to the study area at 37 km. Convective rainfall events occurring on scales of 10-100 km are likely to be responsible for extreme precipitation amounts for durations of less than 2 hours in Ontario (CSA 2019). Therefore, Mount Forest (AUT) – 6145504, the closest of the two remaining stations, was selected to represent the South Bruce study area.

The data from the ECCC IDF Engineering dataset are provided in the form of preprocessed annual maximum series (AMS) for selected sub-daily durations and are verified by ECCC for quality assurance (ECCC 2019b).

Table 4: Stations from the Engineering Data Set for Sub-daily IDF Curves

Name	Climate ID	Years Available	Elevation (masl)	Latitude and Longitude	Distance from South Bruce Study Area (km)
GLEN ALLAN	6142803	1960-1970	400	43.68, -80.71	54.9
GODERICH	6122847	1970-2016	214	43.77, -81.72	49.8
GRAND VALLEY WPCP	6142991	1976-1991	465	43.88, -80.33	71.9
MOUNT FOREST (AUT)	6145504	1962-2016	415	43.98, -80.75	37.0
OWEN SOUND MOE	6116132	1965-2006	179	44.58, -80.93	66.1
STRATFORD WWTP	6148105	1966-2004	345	43.37, -81.00	74.4

3.2 Baseline IDF Curves

IDF curves were calculated using the selected stations in the baseline development for return periods ranging from 2-year to 2000-year. The IDF curves were compared to other available IDF values for the region, including historical precipitation trends. Two distinct analyses are presented in the next sections. The first analysis (Sections 3.2.1 to 3.2.2) using the sub-daily ECCC Engineering Database are interpolated sub-daily IDF curves for Mount Forest (AUT) station and includes a comparison to other sources. The second analysis using the Annual Maximum of the Daily Total Precipitation time series calculates the daily and multi-day IDF curves for the South Bruce study area (Section 3.2.3).

3.2.1 Sub-daily IDF Curves for the Selected Stations

Three statistical tests including the Anderson-Darling, Chi-squared and Kolmogorov-Smirnov tests were used to select the best statistical distribution to fit the data from the four distributions- Gumbel (EV1), Generalized Extreme Value (GEV), Pearson Type 3 (PE3), and Log-Pearson type 3 (LP3) as described in Appendix A.2.2.3. This approach ensures that the most suitable distribution is used to fit the IDF curves to the Mount Forest (AUT) climate station, i.e., better fitted to the observations. Only the Mount Forest station was included in this analysis, as it has been identified as the only station with sub-daily rainfall information that may be deemed representative of the South Bruce study area (Section 3.1.3).

Table 5 presents the results of each statistical test for the Mount Forest (AUT) climate station. The table shows how many times the distribution was selected for each of the sub-daily durations. The most frequent distribution was then used for all sub-daily durations and the selected return periods. The GEV distribution was found to be the best fit for 6 out of 9 sub-daily durations. Results of the fitted GEV curve for return periods ranging from 2 to 2000 years for sub-daily durations 5 minutes to 24 hours are shown in Table 6.

It should be noted that for return periods beyond 100 years, there are instances where an event with a longer duration may have a higher value than an event with a duration that is shorter. This is due to slight differences in the fitted distribution for a given duration, as return periods beyond 100 years are extracting values from the extreme right rail of the distribution. If a shorter duration for the same return period has a higher precipitation value than the duration of interest, the greater of the two values should be selected as a conservative measure.

Table 5: Best Distribution for Mount Forest (AUT) Station (Number of Times Selected for the Sub-Daily Durations)

Station	Distributions			
	GEV	EV1	PE3	LP3
6145504 – MOUNT FOREST (AUT)	6	0	2	1

Table 6: IDF Curves for Mount Forest (AUT) Station – GEV Distribution (mm)

Return Period (years)	5 min	10 min	15 min	30 min	1-hour	2-hour	6-hour	12-hour	24-hour
2	8.8	12.9	15.3	20.1	24.7	30.6	38.1	43.7	49.4
5	10.8	15.5	18.6	25.5	32.6	39.8	48.6	55.5	63.4
10	12.1	16.7	20.3	28.9	38.1	45.4	56.4	63.3	72.6
20	13.2	17.7	21.6	32.2	43.4	50.6	64.5	70.6	81.4
50	14.6	18.6	23.0	36.4	50.6	56.9	75.9	80.0	92.7
100	15.5	19.1	23.8	39.5	56.1	61.4	85.3	86.9	101.2
200	16.4	19.5	24.5	42.5	61.7	65.7	95.4	93.8	109.7
500	17.4	20.0	25.2	46.4	69.4	71.0	110.0	102.7	120.7
1,000	18.2	20.2	25.6	49.4	75.3	74.7	122.1	109.4	129.1
2,000	18.9	20.4	26.0	52.2	81.4	78.3	135.1	116.0	137.4

3.2.2 Comparison with Other Sources

The above stations were compared with publicly available external tools and portals to confirm that the results presented in the previous section were in line with other sources. The following sources were used in the comparison:

- **IDF_CC Tool**: The tool used Gumbel and GEV distribution with the method of moments and L-moments respectively to calculate the baseline values. The tool only calculates return periods up to 100-year.
- **MTO Lookup tool**: The tool used Gumbel with the method of moments to calculate the baseline values for the IDF curves. The tool only calculates return periods up to 100-year and uses an interpolation methodology.

Only the 100-year return periods and 24-hour duration were used for comparison, as presented in Table 7. The estimates generated by Golder are in line with the IDF tool for the Mount Forest (AUT) station. The comparison with the MTO tool shows a larger value that may be attributed to the spatial interpolation of the MTO tool.

Table 7: IDF Curves Comparison with Other Sources – 100-Year Return Period for 24-Hour Duration

Station	Golder	IDF_CC Tool		MTO IDF Tool	
	(mm)	(mm)	(%)	(mm)	(%)
6145504 – MOUNT FOREST (AUT)	101.2	101.2	0%	133.3	31.7%

3.2.3 Daily and Multi-Day IDF Curve for the South Bruce Study Area

The data source for this analysis is the daily baseline time series defined in Section 3.1.2. The daily and multi-day IDF curves were calculated for the same return periods used for the IDF curves in the previous section. Based on the goodness of fit tests, the Log-Pearson Type 3 (LP3) distribution was selected to calculate the curves. The results are shown in Table 8 for selected durations up to 120-days. The 1-day IDF curve was converted to 24-hours duration (using the 1.13 ratio recommended by the World Meteorological Organization 2019). Daily rainfall can be calculated for two different periods: 24-hour rainfall and 1-day rainfall. The 24-hour rainfall is calculated as the maximum rainfall during a moving block of 24 hours, while the 1-day rainfall is calculated as the maximum rainfall during the period from midnight of one day to midnight of the next. Due to the differences in the method of calculation, there are typically differences in the values, with the 24-hour rainfall often being higher (moving block allows for greater capture of storms). The 24-hour IDF curve for South Bruce study area (using daily precipitation from the Wroxeter climate station) is shown in Table 9. The IDF values presented in Table 9 are significantly higher than the 24-hour IDF values shown for Mount Forest climate station (Table 6). The precipitation data from these climate stations represent the best available observations for sub-daily annual maximums and daily precipitation totals. The difference in these values can be attributed to measurements taken at different locations, the application of the 1.13 rule for conversion of daily to 24-hour durations, and shape of the fitted IDF curves. Therefore, it is recommended the most conservative values be used between Table 6 and Table 9 to represent the 24-hour IDF curve for the South Bruce study area.

Table 8: Daily and Multi-day IDF Curves for the South Bruce Study Area (mm)

Return Period (years)	1-Day	2-Day	3-Day	4-Day	5-Day	6-Day	7-Day	10-Day	20-Day	30-Day	50-Day	75-Day	90-Day	120-Day
2	51.1	59.0	65.3	69.4	73.7	79.6	83.9	96.8	134.3	168.6	235.0	308.9	351.0	434.0
5	71.1	79.6	85.7	90.1	94.8	101.7	106.5	123.6	164.4	204.7	284.3	367.8	414.3	503.4
10	84.3	93.3	99.2	103.9	108.7	116.3	121.5	141.3	184.4	228.5	316.9	406.8	456.1	549.3
20	97.1	106.5	112.1	117.1	122.1	130.4	135.9	158.3	203.5	251.4	348.2	444.3	496.3	593.4
50	113.5	123.5	128.9	134.1	139.4	148.5	154.5	180.3	228.3	281.1	388.7	492.7	548.3	650.4
100	125.8	136.2	141.4	146.9	152.4	162.1	168.4	196.8	246.9	303.3	419.0	529.0	587.2	693.2
200	138.1	148.9	153.9	159.6	165.3	175.7	182.3	213.2	265.4	325.4	449.3	565.2	626.0	735.8
500	154.3	165.6	170.5	176.4	182.4	193.6	200.6	234.9	289.8	354.6	489.2	612.9	677.2	792.0
1,000	166.6	178.3	182.9	189.1	195.3	207.1	214.5	251.2	308.3	376.6	519.3	649.0	715.9	834.4
2,000	178.8	190.9	195.4	201.8	208.2	220.6	228.3	267.6	326.7	398.7	549.5	685.1	754.6	876.9

Table 9: 24-hour IDF Curve for the South Bruce Study Area

Return Period (years)	24-Hours [(1)] (mm)
2	57.7
5	80.3
10	95.3
20	109.7
50	128.3
100	142.2
200	156.1
500	174.4
1,000	188.2
2,000	202.0

Note: [(1)] Converted to 24-hours duration using the 1.13 WMO ratio.

3.3 Baseline PMP Calculations

Using the stations listed in Table 1, DAD curves and PMP values were calculated for the desired duration periods (24-hour, 1-day, 2-day, and 3-day). The PMP values were calculated specifically for the South Bruce study area using the precipitation series defined in Section 3.1.2 of this report for the Hershfield method and cross validated using two different methods, the PMP Hershfield and the Transposition (DAD curves).

3.3.1 Historical Storms for the Transposition Method

All periods for the stations (Table 1) were screened for large events, including the most recent observations. The periods covered by the stations is from 1870 to 2019. All precipitation events higher than 95 mm/day with 4 or more stations contributing to the event were preselected and screened. This was done to capture a set of large storm events in the region where enough data is available from multiple stations for DAD curve development. A total of 10 events were registered under these criteria and are shown in Table 10. Wroxeter (6129660) station recorded the largest event with a 1-day value of 166.4 mm, while Blyth (6120819) station most frequently recorded the largest value compared to the other stations across the events.

The storm event occurring on September 10th and 11th of 1986 has the highest average precipitation amount across the stations. This event is well documented, as it was associated with a large tropical air mass from the Pacific Ocean reaching Central Lower Michigan where it was rapidly uplifted to produce a band of storms over a large area (Torregrossa 2016). The result of which was record breaking rainfall across Michigan and southwestern Ontario. Over a two-day period, some areas of Michigan experienced close to 250 mm of rainfall and 177 mm in Exeter, Ontario, producing severe flooding and high river flows (Brown 1996; Torregrossa 2016). The total precipitation at Wroxeter (6129660) station recorded for this event (99 mm on September 10th and 21.6 mm on September 11th) is much less than the peak value for this station mentioned previously (166.4 mm). This highlights the regional variation in precipitation for the South Bruce study area, and the need to consider multiple storm events in the construction of the DAD curves.

No significant storm events where registered on the stations from 2008 to present (based on the observations screened). The composite DAD curve was constructed using all of the major storms provided in Table 10 and compared to the results from the site specific Hershfield method for the South Bruce study area.

Table 10: Total Precipitation of Major Storm Events Recorded in Region of South Bruce from 1870 to 2019 (mm)

Date of Peak	AYTON (6110439)	DURHAM (6112171)	HANOVER (6113329)	BLYTH (6120819)	KINCARDINE (6124127)	LUCKNOW (6124700)	PAISLEY (6126210)	WROXETER (6129660)	JAMESTOWN (6143905)	HARRISTON (614CCNR)	HANOVER (6113329)
1964-08-02	—	36.1	—	86.6	—	2.8	117.6	—	—	—	—
1975-08-23	—	31.8	82.8	112.3	—	1.8	100.6	109.2	—	—	—
1977-08-16	—	63.5	95.8	78	—	99.8	58.4	80	—	—	—
1986-09-10	—	81.6	68.8	137	—	70	69.4	99	—	—	—
1986-09-11	—	77.4	63.3	39.5	—	100	79	21.6	—	—	—
1988-07-30	24.2	10	8.5	12.5	—	19	20.6	166.4	—	—	24.2
1995-06-02	—	14.2	17.9	76.5	5.4	—	—	65	—	96.2	—
2005-07-16	—	—	22.4	63	20.2	—	—	98.6	—	—	—
2008-03-31	—	—	48	134	33	—	—	25.2	0	—	—
2008-09-30	—	—	6	102	3.2	—	—	—	8.1	—	—

3.3.2 Estimates of PMP with the Hershfield method

For the estimate of the PMP using the Hershfield method as described by the World Meteorological Organization (WMO 2009a), the daily baseline time series prepared for the South Bruce study area as described in Section 3.1.2 was used. The results using the baseline time series were compared to the calculations from the DAD curves for the Transposition method in the next section. The 1-day PMP value found was 405.2 mm (Table 11), which results in 457.9 mm for the 24-hour duration PMP using the 1.13 conversion factor (from daily to 24-hour rainfall events) recommended by the WMO. The 2-day and 3-day PMP values for the same location were calculated to be less than the 24-hour day value based on the statistical relationships with the observed data; however, this is physically unrealistic. This occurs due to low variability in the 1 to 3-day durations, suggesting that most extreme events in the South Bruce study area are associated with relatively short durations of rainfall. Due to the data limitations the greater value was used for PMP durations less than or equal to the duration of interest. If the 2- and 3- day PMP value is key to design parameters, additional statistical assessment may be required that is outside the scope of this assessment.

Table 11: PMP Summary for Statistical Method for the South Bruce Study Area

Duration	PMP (mm)
1-Day	405.2
24-Hour (1)	457.9
2-Day	*457.9
3-Day	*457.9

(1) Converted from daily to 24-hour duration using the 1.13 ratio recommended by the WMO (2009a).

* 2- and 3-day PMP calculated as 425.1 mm and 417.4 mm. Therefore, the 24-hour value is used to represent these durations.

3.3.3 Development of DAD Curves in Estimate of PMP with the Transposition Method

The DAD curves were developed using the Transposition method described in Appendix A.2.3. For the development of the DAD curves for the South Bruce study area, multiple major storm events needed to be considered, as there is not one major event that dominates all recorded precipitation in the region. Therefore, all major storms presented in Table 10 identified in the nearby climate stations were used to develop a composite DAD curve for the South Bruce study area. For each storm, the center was assumed to occur at the station with the highest 1-day reading. DAD curves were estimated separately for each storm event and then compiled together by taking the maximum of all the curves to develop a composite DAD curve for the study area.

The original DAD curves were constructed as shown in Table 12. The original DAD curves and consequent PMP values were multiplied by the maximization factor (used to maximize the screened observed storm) and transposition factor (used to transpose the values of the PMP to the South Bruce study area), using the precipitable water content as described in Appendix A.2.3.2 (Table 13). The maximization factor for each storm event was obtained using the 12-hour persistent dew point map from Figure 3.6 in OMNR (2006) for the month of June and the maximum daily mean temperature as a proxy for the dew point for each storm. The transposition factors for each storm (as defined in Appendix A.2.3.2) were found by using the map from Figure 3.6 in OMNR (2006). The storm maximization factors were calculated and applied to the original DAD curves shown in Table 11 to arrive at the adjusted DAD curves for South Bruce (Figure 11 and Table 12). In Figure 11 the points represent the transposed and maximized storm events while the lines represent envelopment curves used to bound all of the points. The resulting DAD curves are composite DAD curves that incorporate all the major historical events described in Table 10. The data points used to plot the curves as well as the maximization and transposition factors calculated for South Bruce are provided in Appendix B.

Table 12: Original Composite DAD Curves for South Bruce Regional Storms

Area (km^2)	PMP (mm)			
	1-Day	2-Day	3-Day	24-Hour
25	166.4	182.3	184.4	188.1
100	161.6	182.1	184.3	182.6
500	139.9	181.4	183.5	158.1
1,000	131.1	180.5	182.6	148.1
2,000	125.5	178.7	180.8	141.8
5,000	111.3	173.6	175.6	125.7
10,000	102.2	165.7	167.6	115.5

Table 13: Storm Maximization and Transposition Factors for South Bruce Major Storm Events

Storm Event	Maximization Factor	Transposition Factor
1964-08-02	1.44	1.01
1975-08-23	2.20	0.98
1977-08-16	1.85	0.99
1986-09-10	1.71	0.98
1986-09-11	1.56	0.98
1988-07-30	1.20	0.99
1995-06-02	1.51	1.00
2005-07-16	1.11	0.99
2008-03-31	2.79	0.98
2008-09-30	2.99	0.98

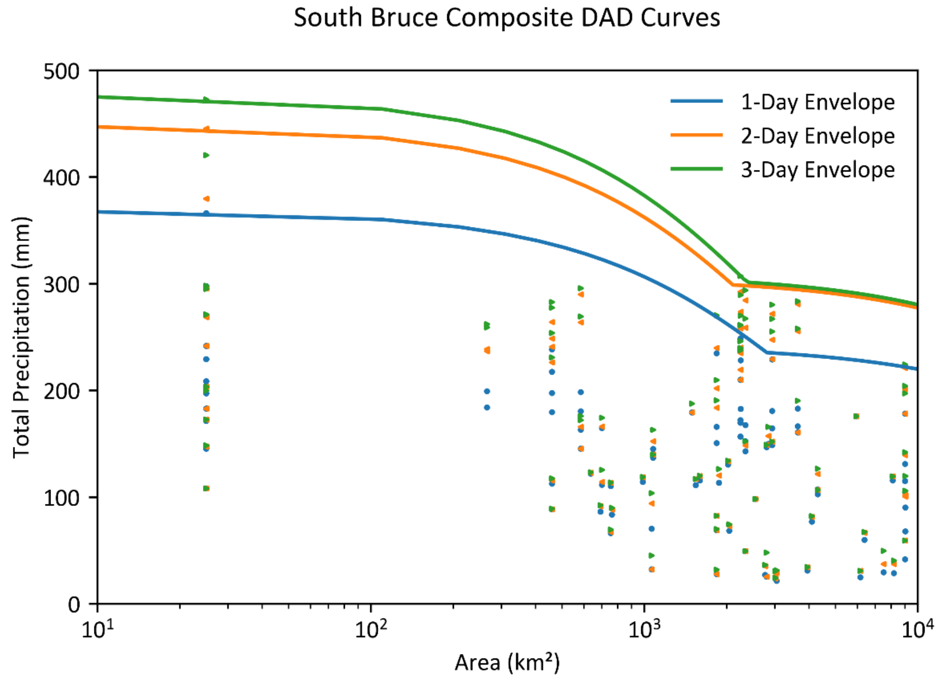

Figure 11: Adjusted Composite DAD Curves for South Bruce Study Area, 1-, 2- and 3-Day Duration

Table 14: Adjusted DAD Curves for the South Bruce Study Area

Area (km²)	PMP (mm)			
	1-Day	**2-Day**	**3-Day**	**24-hour (1)**
25	366.3	445.9	472.8	413.9
100	360.8	438.1	464.4	407.8
500	334.5	400.9	424.0	377.9
1,000	306.5	362.5	382.5	346.3
2,000	262.5	304.1	319.8	296.6
5,000	230.5	290.7	293.7	260.5
10,000	220.1	277.5	280.3	248.7

(1) Converted to 24-hour using 1.13 ratio recommend by the WMO (2009a).

3.3.4 PMP Comparison

The PMP value from the DAD curves varies with the area under consideration. The minimum bounding circle enclosing the stations for which major storms were identified (Table 9) covers an area of approximately 4,111 km². However, if the Saugeen watershed for which South Bruce is located is considered, this would correspond to an area of 4,025 km². For this watershed area, the PMP from the DAD curves corresponds to 240.9 mm and 272.2 mm for 1-day and 24-hour durations (linearly interpolating from Table 14). This is significantly less than that obtain from the Hershfield method, corresponding to the PMP value of 405.2 mm and 457.9 mm for the 1-day and 24-hour durations. This is due to the Hershfield method yielding point estimates of PMP rather than one that considers PMP over a given areal extent. Because of this, the PMP from the DAD curves at the lowest areal extent of 25 km^2 is most similar to that obtained through the Hershfield method at 366.3 mm and 413.9 mm for 1-day and 24-hour durations. It is recommended a conservative approach be taken such that the greater value between methods should be used for a given duration.

The values of the PMP calculated were compared with other sources, including OMNR (2006), for validation. The PMP values were calculated by OMNR as an average by group of watersheds in Ontario as opposed to specific locations or storms. The South Bruce study area is in the South-Central watershed and the 24-hour PMP is estimated at 462 mm. This is in line with the estimate of 457.9 mm for the same duration using the Hershfield method. The bolded values in Table 15 are recommended for use in the South Bruce study area as they represent the most conservative estimates of PMP for the 24-hour and 1-day durations.

Table 15: PMP Comparison for the South Bruce Study Area

Duration	PMP (mm)		
	Golder – Transposition (1)	Golder - Hershfield	OMNR (2006)
24-hour	413.9	457.9	**462**
1-day	366.3	**405.2**	—

(1) For watershed areal extent of 25 km^2.

3.3.5 Sub-Daily PMP Estimates

The hourly precipitation data are not available from ECCC; therefore, the sub-daily PMP was estimated using ratios obtained for the IDF curves for the sub-daily durations, from 5 minutes to 12 hours as described in Appendix A.2.3.3 (Table 16). The ratios were calculated using 24-hour duration and 100-year return period from the sub-daily IDF curves calculated for the South Bruce study area in Section 3.2.1. The 100-year return period was selected since it provides a more realistic and reliable estimate among sub-daily durations than higher return periods. This is because the shape of the fitted distributions can be more variable across durations at higher return periods, while the 100-year return period allows for a clear relationship to be shown across durations. The ratios were applied to the 24-hours PMP values obtained by the Hershfield method (Section 3.3.2) and the Transposition method (Section 3.3.3); the results are presented in Table 17 and Table 18. There are some uncertainties associated with the approach used to come up with the sub-daily values, since the actual sub-daily storm distribution may differ from the storm distribution derived using the adopted method.

Table 16: Conversion Ratios from 24-hour to Sub-daily PMP

Duration	5-min	10-min	15-min	30-min	1-hour	2-hour	6-hour	12-hour
Ratio	0.153	0.189	0.235	0.390	0.554	0.607	0.843	0.859

Table 17: Estimated Sub-Daily PMP Values for the South Bruce Study Area – Hershfield Method

Duration	PMP (mm)
5-Min	70.1
10-Min	86.5
15-Min	107.6
30-Min	178.7
1-Hour	253.8
2-Hour	277.8
6-Hour	385.9
12-Hour	393.3
24-Hour	457.9
1-Day	405.2

Table 18: Estimated Sub-Daily PMP Values for the South Bruce Study Area – Transposition Method

Area (km^2)	PMP (mm)									
	1-Day	24-Hour	12-Hour	6-Hour	2-Hour	1-Hour	30-Min	15-Min	10-Min	5-Min
25	366.3	413.9	355.5	348.8	251.1	229.4	161.5	97.3	78.2	63.3
100	360.8	407.8	350.2	343.6	247.4	226.0	159.1	95.8	77.0	62.4
500	334.5	377.9	324.6	318.5	229.3	209.5	147.5	88.8	71.4	57.8
1,000	306.5	346.3	297.4	291.8	210.1	192.0	135.1	81.4	65.4	53.0
2,000	262.5	296.6	254.8	250.0	179.9	164.4	115.7	69.7	56.0	45.4
5,000	230.5	260.5	223.7	219.6	158.0	144.4	101.7	61.2	49.2	39.9
10,000	220.1	248.7	213.6	209.6	150.8	137.8	97.0	58.5	47.0	38.1

3.4 Rainfall on Snow

The analysis of rain on snow included the combined effect of precipitation as rainfall and the melting of accumulated snow. This analysis was conducted for the Wroxeter station using the baseline daily total precipitation and daily temperature time series defined for the South Bruce study area, as described in Section 3.1.2. The rain on snow requires the concurrent daily total precipitation and temperature data from the current climate baseline. The procedure used for the calculation of the rainfall on snow results presented in this report followed the methodology adopted by ECCC (Louie and Hogg 1980), and the steps adapted are detailed in Appendix A.2.4. A snowpack accumulation and snowmelt model (Pysklywec et al. 1968) were used to estimate the depth of equivalent rainfall converted from the snowpack accumulation for the South Bruce study area. A probability distribution (Gumbel) was used to calculate the estimates for selected return periods and presented in Table 19. The 1-day snowpack accumulation was calculated with the same distribution are presented in Table 20. The rain on snow projections can assist in hydrological modeling for flood assessments, dam safety assessments, storage requirements and others. For shorter durations, i.e., the 1-day 100-year return period rain on snow event was calculated at 85.3 mm, indicating that extreme rainfall events are predominant over the combined rainfall and snowmelt events based on the analysis of the historical observations. Longer duration events of 20-days or more and high return periods (100-year or more) may be useful for hydrological analysis when volumetric capacity is an important variable to consider.

3.5 Baseline Additional Climate Variables

To provide more context for the extreme rainfall projections in Sections 3.2 and 3.3, additional climate variables were analyzed for the South Bruce study area. These include annual and monthly temperature and precipitation statistics from which seasonal variation can be inferred. Derived climate variables are also provided, including WMO indices, rain and snow, snow depth, potential evapotranspiration, drought index, and qualitative information for wind speed and relative humidity. The information for wind speed and relative humidity variables may be interpreted qualitatively, as alternative datasets were used due to limited available data for the South Bruce study area. The period of 1979 to 2019 was used to maintain consistency with the period used for PMP and IDF estimates (Sections 3.3 and 3.2), although this may impact estimates of trends in the WMO indices. Additional climate variables provided for the study area will allow for further understanding of the current climate conditions and may be used to support additional studies relating to site hydrology and ecology, for example.

3.5.1 Precipitation and Temperature

Daily precipitation and mean temperature variables were used to estimate annual and monthly mean, minimum, and maximum statistics, highlighting the climate variation over a year at the site. Annually, the average total precipitation for the South Bruce study are is 988.6 mm, ranging from 627 mm to 1382.7 mm. The mean total precipitation values range from 61.7 mm to 95.3 mm with the wettest months of the year occurring from late summer through to fall (Table 21). The months of February and March are typically the driest months of the year with mean total precipitation values of 63.1 mm and 61.7 mm. The wettest month on record was in September 1986 with 251.7 mm and the driest month on record was in July 1989 with 2.0 mm.

Table 19: Rainfall on Snow for the South Bruce Study Area (mm)

Return Period (years)	1-Day	2-Day	3-Day	4-Day	5-Day	6-Day	7-Day	10-Day	20-Day	30-Day	50-Day	75-Day	90-Day	120-Day
2	43.3	59.2	71.5	80.7	91.0	99.0	106.3	126.5	167.0	201.9	264.4	333.7	372.0	436.6
5	54.5	73.1	90.2	103.3	118.0	129.4	138.9	168.1	219.1	261.0	324.3	398.0	434.4	507.4
10	62.0	82.3	102.6	118.3	135.8	149.5	160.5	195.7	253.6	300.2	363.9	440.6	475.7	554.2
20	69.1	91.2	114.5	132.7	152.9	168.8	181.2	222.1	286.8	337.7	401.9	481.4	515.3	599.2
50	78.3	102.6	129.9	151.4	175.0	193.8	207.9	256.4	329.6	386.3	451.1	534.3	566.6	657.4
100	85.3	111.2	141.4	165.3	191.6	212.5	228.0	282.0	361.7	422.7	487.9	573.9	605.1	700.9
200	92.2	119.7	152.9	179.2	208.1	231.2	248.0	307.6	393.7	459.0	524.7	613.4	643.4	744.4
500	101.2	131.0	168.0	197.6	229.9	255.8	274.4	341.3	435.9	506.9	573.1	665.5	693.9	801.7
1,000	108.1	139.5	179.5	211.5	246.4	274.4	294.3	366.8	467.9	543.0	609.7	704.9	732.1	845.0
2,000	115.0	148.0	190.9	225.3	262.9	293.0	314.3	392.3	499.7	579.2	646.3	744.2	770.3	888.3

Table 20: 1-Day Snowpack Accumulation for the South Bruce Study Area (mm)

Return Period (years)	2	5	10	20	50	100	200	500	1,000	2,000
1-Day	138.1	196.2	234.7	271.6	319.4	355.2	390.9	438.0	473.6	509.1

Table 21: Mean, Minimum, and Maximum of Monthly Total Precipitation for the Baseline Period from 1979 to 2019 (mm) for the South Bruce Study Area

Month	Mean	Minimum	Maximum
January	83.1	39.9	159.4
February	63.1	17.2	140.5
March	61.7	14.6	178.3
April	75.7	16.4	169.2
May	84.6	14.4	205.2
June	86.9	24.3	206.4
July	85.0	2.0	213.4
August	86.3	35.2	192.2
September	95.3	24.8	251.7
October	87.7	25.4	213.2
November	90.8	26.6	170.5
December	88.4	29.4	163.3
Annual	988.6	627.0	1382.7

Mean temperature was used for the calculation of the annual and monthly statistics (Table 22). The annual average temperature was calculated as 7.3°C ranging from 5.9°C to 9.1°C. The warmest month on average is the month of July with a mean temperature of 20°C, and the coldest is the month of January with a mean temperature of -6.1°C. The coldest monthly temperature occurred in February 2015 with a minimum monthly temperature of -13.7°C, while the warmest monthly temperature occurred in July 2011 with a maximum monthly temperature of 22.2°C.

Table 22: Mean, Minimum, and Maximum of Monthly Mean Temperature for the Baseline Period from 1979 to 2019 (°C)

Month	Mean	Minimum	Maximum
January	-6.1	-12.5	-0.8
February	-5.7	-13.7	-0.7
March	-0.6	-6.0	6.7
April	6.3	1.9	9.9
May	12.9	8.1	16.3
June	17.6	14.4	21.5
July	20.0	16.8	22.2
August	19.0	16.6	21.5
September	15.1	12.4	18.0
October	8.7	5.8	12.9
November	2.7	-0.7	6.2
December	-2.7	-10.2	3.2
Annual	7.3	5.9	9.1

3.5.2 WMO Climate Indices

The World Meteorological Organizations (WMO's) Expert Team on Climate Change Detection and Indices (ETCCDI; WMO 2009b) recommends using 27 climate extreme indices as a means of summarizing daily temperature and precipitation statistics, focusing primarily on aspects of climate extremes. They have been developed to allow consistent comparison of climate conditions on an international basis. For the following assessment, the WMO climate indices were calculated for the current climate baseline period using the 27 indices, as described in Appendix A. Two analyses for the WMO indices were completed. In the first, the minimum, maximum, mean and median values for each of the 27 indices were calculated over the entire period (Table 23). In the second, the long-term averages and trends were calculated based on the annual values of each of the indices (Table 24).

As shown in Table 23, the number of heavy precipitation days (R10) (i.e., daily precipitation greater than 10 mm) is approximately 33.9 days per year on average, ranging from 19 to 48 days during the current climate baseline period. Based on the R10 value, there are at a minimum, 19 days in each year corresponding to precipitation greater than 10 mm. Maximum one-day (RX1day) and five-day (Rx5day) precipitation events were 54.8 mm and 77.6 mm on average, corresponding to a 2 to 5 year return period event based on the current climate IDF curves developed in Section 3.2.3. Compared with the monthly total precipitation in Section 3.5.1, the average annual maximum five-day event is less than what is received in most months on average. This indicates that monthly rainfall amounts are typically made up of a series of wet periods as opposed to one major event. The precipitation during the extremely wet days (R99p) (i.e., the annual total precipitation when daily precipitation is greater than the 99th percentile) could be up to a maximum of 293.2 mm. The number of consecutive dry days (CDD) ranges from 10 days to 31 days per year, with an average of 17.4 days.

The highest (TXx) and lowest (TXn) recorded daily maximum temperature is 34.7°C and -20.4°C, respectively. The highest (TNx) and lowest (TNn) recorded daily minimum temperature are 26.6°C and -31.6°C, respectively. The range of extreme daily temperatures is almost double of that shown in the monthly statistics for mean temperature in Section 3.5.1. This indicates that the daily temperatures show a high degree of variation compared to the monthly averages.

The long-term averages and trends over the current climate baseline period were calculated for the WMO indices using the methodology outlined in Appendix A. For each of the 27 indices, the climate normal, decadal trend, and statistical significance of the trend were calculated. For each of the 27 indices, the climate normal, decadal trend, and statistical significance of the trend were calculated. The climate normal is used to establish the current conditions, while the decadal trend indicates the direction and magnitude of how the indices are changing on average over a ten-year period. The analysis assessed the statistical significance at the 90th, 95th, 99th and 99.9th percentile levels. Below the 90^{th} percentile level a trend is deemed to be "not statistically significant", while trends that are 0 when rounded to the first decimal place are labelled as "no apparent trend". The long-term averages and trends are presented in Table 24.

No statistically significant trends in precipitation were found during the current climate baseline period. Significant trends in precipitation may be present at the South Bruce study area; however, the trends cannot be distinguished from the variability in the precipitation events. This indicates that there is uncertainty in how precipitation extremes are changing for the South Bruce study area over the current climate baseline period.

Significant trends related to temperature extremes indicate that daily minimum temperatures, warm nights (days where daily minimum temperature is greater than 90th percentile), and warm days (percentage of days when the daily maximum temperature is greater than the 90th percentile) are increasing. Cold nights (days where daily minimum temperature is less than 10th percentile), frost days (annual count when the daily minimum temperature is less than 0°C), and cool days (days with greater than 25°C daily maximum temperature) have a decreasing trend.

Table 23: WMO Indices for Current Climate Extremes

ID	Indicator Name	Units	Min	Max	Mean	Median
CDD	Consecutive dry days	Days	10.0	31.0	17.4	16.0
CSDI	Cold spell duration indicator	Days	0.0	8.0	1.0	0.0
CWD	Consecutive wet days	Days	3.0	13.0	6.2	6.0
DTR	Diurnal temperature range	ºC	4.8	9.6	7.1	7.0
FD0	Frost days	Days	112.0	159.0	137.9	137.0
GSL	Growing season Length	Days	179.0	253.0	217.2	217.0
ID0	Ice days	Days	34.0	82.0	63.6	64.0
PRCPTOT	Annual total wet-day precipitation	mm	627.0	1365.8	984.1	993.6
R10	Number of heavy precipitation days	Days	19.0	48.0	33.9	35.0
R20	Number of very heavy precipitation days	Days	4.0	16.0	9.5	10.0
R95p	Very wet days	mm	0.0	460.4	200.5	208.2
R99p	Extremely wet days	mm	0.0	293.2	64.6	47.1
R30MM	Number of days above 30 mm	Days	0.0	8.0	3.1	3.0
RX1day	Max 1-day precipitation amount	mm	22.6	166.4	54.8	47.1
Rx5day	Max 5-day precipitation amount	mm	45.0	171.4	77.6	71.0
SDII	Simple daily intensity index	mm/day	6.2	11.6	8.6	8.7
SU25	Summer days	Days	22.0	73.0	47.0	45.0
TN10p	Cool nights	% of Days	3.5	17.7	10.3	10.6
TN90p	Warm nights	% of Days	4.0	16.0	10.4	10.8
TNn	Minimum of daily minimum temperature	ºC	-31.6	-18.7	-24.8	-24.3
TNx	Maximum of daily minimum temperature	ºC	19.8	26.6	22.9	22.9
TR20	Tropical nights	Days	0.0	18.0	8.1	7.0
TX10p	Cool days	% of Days	3.7	19.0	10.4	10.3
TX90p	Warm days	% of Days	3.7	19.2	10.4	10.4
TXn	Minimum of daily maximum temperature	ºC	-20.4	-7.5	-14.1	-13.9
TXx	Maximum of daily maximum temperature	ºC	29.6	34.7	31.7	31.8
WSDI	Warm spell duration indicator	Days	0.0	16.0	3.1	0.0

These significant temperature trends detected indicate that days with low temperature are becoming less frequent (fewer frost days, cold nights, and cool days, increasing minimum temperatures), with more warm days. In the South Bruce study area, significant trends were only detected for extreme cold temperatures as opposed to extreme hot temperatures. This is consistent with the trends established in Bush and Lemmen (2019), which shows that indices for extreme cold temperatures have increased more rapidly than indices of extreme hot temperatures in Ontario. Therefore, changes in extreme hot temperatures may be occurring at a slower rate than the extreme cold temperatures at the study area, but they are not statistically significant over the current climate baseline.

Table 24: Long-term Averages and Trends of WMO Indices for Current Climate Extremes

Climate Indices	Units	Mean	Decadal Trend	Statistical Significance
Consecutive dry days	Days	17.4	0.0	no apparent trend
Cold spell duration indicator	Days	1.0	0.0	no apparent trend
Consecutive wet days	Days	6.2	0.0	no apparent trend
Diurnal temperature range	ºC	8.7	-0.1	not statistically significant
Frost days	Days	137.9	-3.3	significant at the 95th percentile
Growing season length	Days	217.2	-0.7	not statistically significant
Ice days	Days	63.6	0.0	no apparent trend
Annual total wet-day precipitation	mm	984.1	+9.3	not statistically significant
Number of heavy precipitation days	Days	33.9	0.0	no apparent trend
Number of very heavy precipitation days	Days	9.5	0.0	no apparent trend
Very wet days	mm	200.5	-11.8	not statistically significant
Extremely wet days	mm	64.6	-0.4	not statistically significant
Number of days above 25 mm	Days	3.1	0.0	no apparent trend
Max 1-day precipitation amount	mm	54.8	-1.2	not statistically significant
Max 5-day precipitation amount	mm	77.6	-2.8	not statistically significant
Simple daily intensity index	mm/day	8.6	-0.2	not statistically significant
Summer days	Days	47.0	+2.5	not statistically significant
Cool nights	% of Days	10.3	-1.9	significant at the 99.9th percentile
Warm nights	% of Days	10.4	+0.9	significant at the 90th percentile
Min Tmin	ºC	-24.8	+0.3	not statistically significant
Max Tmin	ºC	22.9	+0.4	significant at the 90th percentile
Tropical nights	Days	8.1	+0.8	not statistically significant
Cool days	% of Days	10.4	-1.0	significant at the 90th percentile
Warm days	% of Days	10.4	+1.1	significant at the 90th percentile
Min Tmax	ºC	-14.1	+0.7	significant at the 90th percentile
Max Tmax	ºC	31.7	+0.2	not statistically significant
Warm spell duration indicator	Days	3.1	0.0	no apparent trend

3.5.3 Potential Evapotranspiration

Estimates of potential evapotranspiration can provide an indication of how much water is lost to the atmosphere through evaporation and transpiration processes at a given location without soil moisture limitations. The Hargreaves equation (Hargreaves and Samani 1985) was selected to provide consistency between the current climate observations and future climate projections. Monthly potential evapotranspiration estimates for the South Bruce study area are provided in Table 25. Potential evapotranspiration calculated using the current climate baseline temperatures is provided as a daily time series in Appendix C.

Table 25: Potential Evapotranspiration for the South Bruce Study Area on a Monthly Timescale for the Baseline Period from 1979 to 2019

Month	Potential Monthly Evapotranspiration (mm)
January	10.7
February	15.7
March	38.5
April	72.0
May	113.1
June	130.9
July	136.6
August	114.0
September	78.4
October	43.5
November	20.3
December	11.4
Annual	785.3

The greatest monthly evapotranspiration rates occur in July at 136.6 mm, which was shown to also have the highest mean monthly temperatures (Table 22). Most of the evapotranspiration occurs in the late spring to summer months of May to August. The lowest evapotranspiration rates occur in January at an average of 10.7 mm where temperatures are consistently low.

For comparison, Hember et al. (2017) have calculated monthly potential evapotranspiration across North America using six different methods for the period of 1971-2000. The range of results for the South Bruce study area estimated from the provided maps is from 3 mm/day to 4.5 mm/day for the average daily potential evapotranspiration between May and September. Using the estimates provided in Table 25, the mean daily evapotranspiration rate for this time period corresponds to 3.7 mm/day, which is within the range given by Hember et al. (2017), despite the use of different methods and time periods. The Hargreaves method used in this report only requires temperature climate variables as inputs and was selected to provide a consistent method for future projections. Although it appears to perform well for the South Bruce study area, if a more comprehensive assessment is needed, then the method should be checked against other methods that use additional climate variables to confirm the validity of this approach. For example, Penman-Monteith based methods incorporate the effects of wind speed and relative humidity which were not included here.

Sublimation is not included directly in the Hargreaves method; however, the functional form includes the diurnal temperature range, allowing for some potential evapotranspiration to occur in the winter months which includes sublimation (see Appendix A.2.5.3). It is not anticipated that this effect will result in a large absolute difference in potential evapotranspiration (PET) over the winter months, as this is when PET is lowest throughout the year.

Annual potential evapotranspiration is lower than mean annual precipitation (Table 21), indicating an annual surplus of water for the study area. Ideal conditions are needed for potential evaporation to occur. If actual conditions are different from the ideal conditions (e.g., increased cloud cover limiting the solar radiation, elevated humidity limiting the amount of moisture the air can hold), the actual evapotranspiration will be lower than potential evapotranspiration. The difference between the potential and actual evapotranspiration also supports annual surplus conditions as with less water lost to evapotranspiration.

3.5.4 Drought Index

The drought index was estimated using the standard precipitation and evapotranspiration index (SPEI) of Vincente-Serrano et al. (2010), which is based on the standard precipitation index described in WMO (2012). This method illustrates the number of standard deviations the monthly net precipitation (precipitation less evapotranspiration) is from the median. By using net precipitation, both precipitation and temperature influence the drought index instead of only precipitation. The SPEI was calculated on a monthly timescale using a 12-month calculation interval (see Appendix A.3.6.4). Annual values are not provided for the drought index, as for a given month the calculated value is dependent on the previous twelve months; therefore, an aggregated annual value is not meaningful. The mean of all the calculated values is 0 and the standard deviation is 1 due to the normalization step of the method.

The distribution of SPEI is provided using a set of percentiles across each calendar month in the current climate baseline (Table 26). The values for SPEI can be interpreted using the classification scheme discussed in Appendix A.2.5.4. SPEI values between -1 and 1 are classified as near-normal, between 1 to 1.49 and -1 to -1.49 are moderately wet and moderately dry, and between 1.5 to 1.99 and -1.5 to -1.99 are severely wet and severely dry. Extremely wet and dry conditions are represented by a value of 2 and -2 respectively.

At the 50th percentile, only minor variations in drought occur in a given month, with some months being under a small deficit (negative net precipitation greater than -1) while others are in a small surplus (positive net precipitation less than 1). The minimum values reveal that the most significant drought events have occurred in March with a value of -1.92, which does not exceed the threshold for extremely dry conditions (-2 or less). The wettest months (maximum values) were found to correspond with spring rainfall in April and March, as well as fall storms in September.

Extreme drought periods (-2 or greater) have not occurred in the baseline period (1979 to 2019) at the South Bruce study area following the SPEI thresholds. Extremely wet conditions (2 or greater) have occurred; however, this is only in the maximum value of the indicated calendar months and not at the 90th percentile. Therefore, extreme surplus conditions occur relatively infrequently.

Table 26: Drought on a Monthly Timescale for the South Bruce Study Area

Month	Min	10%	25%	50%	75%	90%	Max	Mean	Std. Dev.
January	-1.37	-1.22	-0.74	-0.06	0.43	1.45	1.89	0.00	1.04
February	-1.58	-1.43	-0.77	0.19	0.65	1.24	1.66	0.00	1.04
March	-1.92	-1.33	-0.62	0.13	1.02	1.05	1.26	0.00	1.04
April	-1.52	-1.01	-0.79	-0.34	0.59	1.34	2.04	0.00	1.04
May	-1.61	-1.12	-0.67	-0.12	0.56	1.42	2.05	0.00	1.04
June	-1.49	-1.02	-0.93	0.05	0.79	1.21	1.91	0.00	1.04
July	-1.69	-1.48	-0.66	0.02	0.58	1.18	1.74	0.00	1.04
August	-1.38	-1.28	-0.79	0.10	0.81	1.42	1.65	0.00	1.04
September	-1.61	-1.09	-0.70	-0.19	0.61	1.04	2.21	0.00	1.04
October	-1.50	-1.43	-0.44	0.14	0.63	1.02	1.99	0.00	1.04
November	-1.56	-1.15	-0.88	0.08	0.36	1.51	1.55	0.00	1.04
December	-1.46	-1.18	-0.62	-0.15	0.43	1.52	1.92	0.00	1.04

Note: Percentiles are calculated across calendar months to illustrate the distribution of SPEI values.

3.5.5 Wind Speed and Relative Humidity

Climate normals from ECCC for wind speed and relative humidity are not available directly for the South Bruce study area or any of the stations listed in Table 1. However, climate normals for the 1981 to 2010 period were available for WIARTON A (6119500) from ECCC (2020). The applicability of these climate normals to the South Bruce study area depends on geographical siting including the distance from the site, elevation difference, and latitude. This information is given below in Table 27. The station is located a considerable distance away from the site (79.3 km) with an elevation difference of 127.8 m and is significantly closer to Lake Huron. In terms of latitude, WIARTON A is located 0.71 degrees north of the study area. Despite the differences, the station represents the closest observed wind speed and relative humidity climate normals to the South Bruce study area. Observations are preferred over data that has been spatially interpolated or modelled in reanalysis datasets for wind speed and relative humidity variables as information from neighboring climate stations can be sparse and wind speed is not well represented in climate models. Therefore, the values provided should be interpreted qualitatively for the South Bruce study area.

Table 27: Selected Climate Stations for Relative Humidity and Wind Speed Climate Normals

Station Name	Climate ID	Latitude and Longitude	Elevation (masl)	Distance from Site (km)	Distance from Lake Huron (km)	Climate Normal Period
South Bruce Study Area	—	44.02, -81.21	350	—	38.5	—
WIARTON A	6119500	44.73, -81.11	222.2	79.3	16.6	1981-2010

Wind speed and monthly average relative humidity normals are provided for the WIARTON A station (Table 28). The mean, maximum hourly, and gust windspeed for WIARTON A (6119500) varies from 9.8 km/h to 16 km/h, 56 km/h to 84 km/h, and 93 km/h to 126 km/h respectively across calendar months, measured 10 m from the ground surface. Monthly average relative humidity is generally higher in the morning than mid-day, with a range of 78.8% to 89.2% at 6 am and 58.7% to 77.6% at 3 pm. It should be noted that due to the proximity of this climate station to Lake Huron, it is likely that wind speeds and relative humidity values are greater than what would be expected at the South Bruce study area.

Trend analyses have been conducted using daily mean windspeed timeseries across Canada (Wan et al. 2010). In the region of the South Bruce study area, a downward trend was found in the linear trends of homogenized monthly wind speeds for the period of 1953 to 2010. Downward trends were also found across seasons. This indicates that the climate normals for the wind speeds mentioned above are not stationary. Updated climate normals, as they are released, should be reviewed for changes in the wind speed observations provided.

Table 28: Wind Speed and Relative Humidity Data for WIARTON A (6119500) Station from 1981-2010 Canadian Climate Normals

Month	Average Wind Speed (km/h)	Maximum Hourly Wind Speed (km/h)	Gust Wind Speed (km/h)(1)	Average Relative Humidity at 6 am (%)	Average Relative Humidity at 3 pm (%)
January	16.0	76	108	81.7	77.3
February	14.4	68	96	80.5	72.0
March	13.7	84	108	79.3	64.9
April	14.1	68	126	78.8	58.7
May	11.6	64	104	81.1	59.0
June	9.8	61	93	86.0	62.7
July	9.8	56	105	86.8	61.6
August	10.0	80	119	89.2	63.9
September	11.6	64	113	87.5	65.5
October	14.0	74	102	82.7	67.5
November	15.4	80	111	81.4	73.0
December	15.8	76	111	82.6	77.6
Annual	13.0	84	126	83.1	67.0

(1) Gust wind speed is the instantaneous peak wind speed recorded in each calendar month.

4. ANALYSES OF FUTURE CLIMATE ON PMP, IDF, AND ADDITIONAL CLIMATE VARIABLE ESTIMATES

The following sections build on the current climate descriptions in Section 3 by providing the projected changes under future climate conditions for two future time horizons (2050s and 2080s) relative to the model baseline period of 1979 to 2019. The model baseline is based on projections from the GCMs for the same time period as the observations used to form the current climate baseline. The projected changes in climate are presented as the percentage change from the model baseline with guidance on how to apply the changes to the observed current climate baseline in order to obtain absolute values for future climate. Section 4.1 provides a description of future climate conditions used to estimate the potential changes in IDF curve and PMP estimates which are later discussed in Sections 4.2 and 4.3. Rain on snow estimates are discussed in Section 4.4, and the additional climate variables are presented in Section 4.5. In all sections, projections are provided in terms of percentiles measured over the 136-member multi-model ensemble. Select tables presented in this section are coloured using a gradient to aid in the visual representation of the values. The colour gradients provide a relative indication of the highest (red) and lowest (green) values with transitional colours in between. Colours cannot be compared between tables, as the colour scale is relative for each.

The following sections focus on the 50th percentile to illustrate general trends. The remaining percentiles are included in Appendix B. Daily future timeseries developed for the additional climate variables are provided in Appendix C. Guidance on applying the percentile changes to the observed current climate basis is provided in Section 4.1.

4.1 Future Climate Projections Datasets

Climate change has the potential to change future precipitation and temperature regimes that are important inputs for design purposes. Golder has followed the methodology developed in Wood (2019) to complete the climate change assessment presented in the following sections to aid in the design of deep geological repositories for nuclear waste. The development of a detailed future climate assessment helps support the consideration of climate change in such designs. This climate change assessment report summarizes future projected changes in climate with a focus on extreme precipitation events. Future projected changes in IDF curves, PMP and the additional climate variables (including annual and monthly temperature and precipitation statistics, WMO indices, rain and snow, snow depth, potential evapotranspiration, drought index, and qualitative information for wind speed and relative humidity) were estimated based on the best available climate science.

The IPCC is generally considered to be the definitive source of information related to past and future climate change as well as climate science. As an international body, the IPCC provides a common source of information relating to emission scenarios, provides third party reviews of models, and recommends approaches to document future climate projections. Periodically, the IPCC issues assessment reports summarizing the most current state of climate science. The Fifth Assessment Report (AR5) (IPCC 2013) represents the most current complete synthesis of information regarding climate change to date. The next assessment report (Sixth Assessment Report) is anticipated in 2022 and will build on the results from AR5. Future climate is typically projected using GCMs that involve the mathematical representation of global land, sea, and atmosphere interactions over a long time period. These GCMs have been developed by different government agencies but share common elements described by the IPCC. The IPCC does not run the models but acts as a clearinghouse for the distribution and sharing of the model forecasts. Future climate projections are made using scenarios that incorporate different representative concentrations pathways (RCPs) to drive the GCM simulations. The RCPs represent different trajectories for radiative forcing due to mainly anthropogenic influence on the climate cycle. The pathways are named after the radiative forcing projected to occur by 2100. Future climate projections are available from about 30 GCMs and four representative concentration pathways (RCP 2.6, RCP 4.5, RCP 6.0, and RCP 8.5) in AR5.

Downscaling procedures allow GCM model output to be represented at a finer spatial scale which better represents local climate. Statistical downscaling refines GCM projections by incorporating observed data, and statistical methods are applied to allow for a better match between local observed climate and historical GCM model output. These methods are then applied to future GCM projections which are assumed to be more representative of local climate. This report focuses on analysis using the statistically downscaled daily data using the Bias Correction/Construction Analogues with Quantile mapping reordering version 2 (BCCAQv2) model from ClimateData.ca (ClimateData 2019), and the Localized Constructed Analogues (LOCA) model from the GDO-DCP archive (Pierce et al. 2014; Reclamation 2013). Climate variables of daily minimum and maximum temperature and precipitation were obtained from these datasets. Three RCP scenarios (RCP 2.6, RCP 4.5, and RCP 8.5) are currently available from ClimateData.ca for the BCCAQv2 model and were used in this report, while only two RCP scenarios (RCP 4.5 and RCP 8.5) are available for LOCA. Details regarding the methodology, number of model projections, and resolution of both the BCCAQv2 and LOCA datasets are included in Appendix A.

Since no one model or climate scenario can be viewed as completely accurate, the IPCC recommends that climate change assessments use as many models and climate scenarios as possible, or a “multi-model ensemble”. For this reason, the multi-model ensemble approach is used to delineate the probable range of results using percentiles. The percentiles are used to show the distribution of projected changes. This allows for uncertainty in the projections to be understood, while the 50th percentile is used to illustrate general trends. For critical infrastructure, selection of future projections at higher percentiles and higher return periods should be considered. For example, for critical infrastructure whose failure is considered unacceptable, a 95th percentile could be considered over the typical 50th percentile. The projected changes in climate for the site were calculated using three separate time periods including:

- Model baseline (1979 to 2019) – this time-period represents the current climate conditions for which the changes are estimated using each member of the multi-model ensemble.
- Mid-century (2041 to 2070) – used to represent changes in climate projected for the near future.
- End-of-century (2071 to 2100) – used to represent the furthest projections into the future possible with the available climate model scenarios. Changes in climate are typically greater for this period compared to the mid-century for the RCP4.5 and RCP8.5 scenarios.
- Beyond 2100 - qualitative climate assessment (climate projections beyond 2100 are not currently available from ClimateData.ca) provided using the projected trends from the mid-century and end-of-century periods guided by literature.

Changes in climate for the mid-century and end-of-century future periods were calculated as percentage changes from the model baseline to avoid model bias influencing the results. Absolute values for the future climate projections can be obtained by applying the percentage changes to the observed data for a given percentile level from the multi-model ensemble as outlined in Appendix A (Sections A3.3 through A3.5).

The planned Project phases and how they correspond to the selected time periods are shown in Figure 12. The mid-century period coincides with part of the site characterization, preparation, and construction phase. The mid-century and part of the end of century time periods coincide with the operational period phase. Part of the end of century time period coincides with the extended monitoring period, and the qualitative climate assessment period corresponds with both the extended monitoring and decommissioning period Project phases. The extended monitoring and decommissioning periods extend past the year 2100 up to 2180.

Each of the Project phases coincides with part of the selected climate assessment periods. Percentiles from the multi-model ensembles for mid- and end-of-century may be selected in a way that accounts for how the Project phases and climate periods overlap. For example, a lower percentile may be used to cover the site characterization, preparation, and construction phase, as the mid-century period represents time horizon beyond this project phase. Similarly, a higher percentile may be used for the extended monitoring phase as it takes place after the end-of-century period. The 50th percentile level may be selected from the end-of century climate period to represent the operational project phase. Different percentile levels may be selected from the climate projections based on the level of associated risk for design purposes. For designs that are associated with a high level of risk, the 95th or 99th percentile level may be used. For project phases past 2100, a high percentile from the end-of-century climate period can be used for screening purposes. The qualitative climate assessment provides further guidance on how the climate may change past the year 2100.

The qualitative climate assessment period takes into consideration both the mid-century and end-of-century periods, as well as Extended Concentration Pathways (ECPs). ECPs have been developed by extending the RCP scenarios until the year 2300 using Earth Models of Intermediate Complexity (EMICs). The results of the EMIC extensions are consistent until 2300 with atmospheric-ocean general circulation models used in the IPCC fifth assessment report. Only global values are provided and are not directly applicable to the site; however, they provide qualitative trajectories of changes in temperature and precipitation in the far future.

The future projected changes in PMP were calculated using the Hershfield and moisture maximization methods. Future projected changes in IDF curves for sub-daily, daily, and multi-day durations were estimated using the Equidistant Quantile Mapping (EQM) method and the Ratio method. The same approach for estimating changes in IDF curves was applied to combined daily rain and snowmelt. Future projections are provided for additional climate variables including monthly precipitation and temperature statistics, WMO climate indices, potential evapotranspiration, and the drought index. Qualitative information on future wind speed and relative humidity is also provided. Daily future timeseries for rain, snow, and snow depth are developed in Section 4.5.1 and provided in Appendix C along with daily timeseries for potential evapotranspiration.

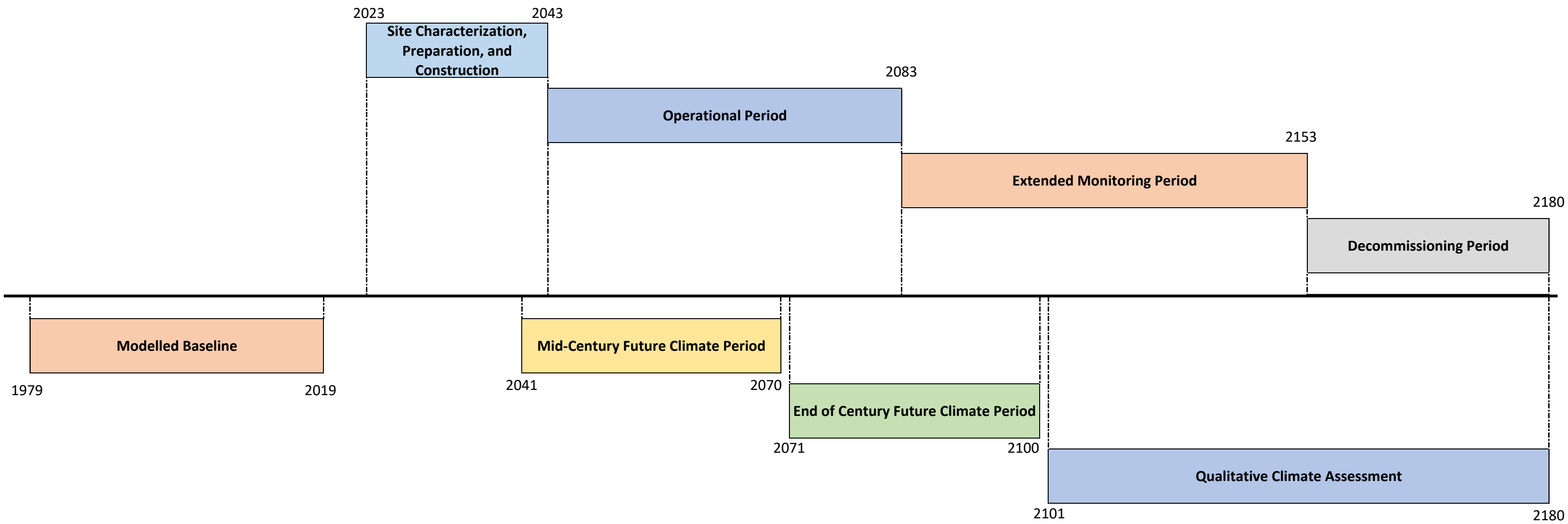

Figure 12: Overview of Project Phases and Selected Future Climate Periods

The ensemble approach was used for all future projections, providing the results for a range of percentiles which took multiple climate models, emission scenarios, and calculation methodologies into account. Details regarding the methodology for all the analyses provided in this report can be found in Appendix A. The following sections focus on the 50th percentile to illustrate general trends. The remaining percentiles are included in Appendix B.

4.2 Climate Change Impacts on IDF Curves

The percent changes in IDF conditions (future periods relative to model baseline) were estimated for different durations of extreme rainfall events. Selected results for the 50th percentile for the 2050s and 2080s climatic horizons are summarized in the following sub-sections. Detailed methodology for this section can be found in Section A.3.3. Additional results have been included in Appendix B in an Excel spreadsheet format. This format was selected to allow for the results to be more easily accessible and improve the readability of the report.

4.2.1 Percent Changes in Sub-Daily IDF Curves

Sub-daily IDF curves are generally used to size site infrastructure for catchments small enough that runoff from the catchment would peak in less than 24 hours.

Daily rainfall amounts are provided in the climate model ensemble; however, sub-daily rainfall in the future projections are not available. The change in sub-daily rainfall statistics can be inferred by examining the projected changes for the 1-day duration. A summary of the projected changes in 1-day rainfall for the 2-, 5-, 10-, 25-, 50-, 100-, 1000-, and 2000- year return period are presented here for the 2050s and 2080s (Table 29 and Table 30). In the 2050s, the 1-day rainfall amount is projected to increase between 7.5% to 18.9% for the 50th percentile across return periods, while in the 2080s this is projected to increase between 9.3% to 15.3%. At the 50th percentile, the greatest changes are shown for the highest return periods, indicating that rare extreme precipitation events will increase in magnitude. In general, the magnitude of daily precipitation events is expected to increase in the future; however, the projected changes for the highest return periods (200 to 2000 years) show greater percentage changes in the 2050s compared to the 2080s. Changes in sub-daily rainfall durations can be estimated by applying the changes in the 1-day rainfall amounts for the 2050s (Table 29) and 2080s (Table 30) to the observed sub-daily durations (Table 6).

Projections for the 10-, 20-, and 50-year 24- hour events are available in Canada's Changing Climate report for Ontario using a multi-model ensemble 29 global climate models for comparison (Bush and Lemmen 2019). A comparison of projected changes to those provided in this report is provided in Table 31. The values for the 2031 to 2050 time period in Bush and Lemmen (2019) are comparable to those for the 2041 to 2070 time period in this report. The values provided in this report for the 2071 to 2100 time period are within the range of those in Bush and Lemmen (2019). It should be noted that these values use global climate models that are not downscaled, have different time periods from those in this report, and present average values from the model ensemble as opposed to 50th percentile shown here. In general, the results shown in Table 29 and Table 30 are close to the range of projections made in Bush and Lemmen (2019).

Table 29: Summary of the Projected Changes (%) in 1-day Rainfall in 2050s for the South Bruce Study Area

Statistical indices	Return Period (years)									
	2	5	10	20	50	100	200	500	1000	2000
Minimum	-13.2%	-14.0%	-17.4%	-20.8%	-24.2%	-26.2%	-28.3%	-31.2%	-33.0%	-34.5%
5%	-6.1%	-5.0%	-6.0%	-8.1%	-9.6%	-11.4%	-13.8%	-15.5%	-16.6%	-18.4%
10%	-2.8%	-2.5%	-2.4%	-3.8%	-5.9%	-6.7%	-7.3%	-8.1%	-9.1%	-9.9%
25%	3.0%	2.9%	3.3%	3.3%	3.0%	2.6%	1.8%	0.8%	0.1%	-0.8%
50%	7.5%	8.3%	9.6%	11.8%	12.6%	13.4%	15.4%	16.3%	17.9%	18.9%
75%	13.7%	16.4%	18.2%	22.1%	26.1%	29.2%	31.4%	34.5%	36.7%	39.0%
90%	19.5%	26.2%	30.3%	34.0%	41.1%	43.5%	47.7%	55.6%	59.2%	65.5%
95%	23.3%	29.5%	35.4%	44.7%	57.2%	64.2%	70.8%	82.9%	92.0%	103.4%
99%	27.9%	40.2%	60.9%	104.8%	184.9%	247.6%	313.6%	398.2%	461.1%	524.3%
Maximum	32.8%	47.7%	84.8%	135.7%	316.1%	480.2%	659.2%	910.3%	1107.2 %	1308.0 %
Mean	8.1%	10.0%	12.2%	14.8%	18.8%	22.1%	25.4%	29.8%	33.2%	36.6%
Standard deviation	8.6%	10.9%	14.4%	20.7%	34.0%	46.7%	60.9%	81.1%	97.1%	113.4%

Table 30: Summary of the Projected Changes (%) in 1-day Rainfall in 2080s for the South Bruce Study Area

Statistical indices	Return Period (years)									
	2	5	10	20	50	100	200	500	1000	2000
Minimum	-11.9%	-11.8%	-13.9%	-20.5%	-28.0%	-32.6%	-36.5%	-40.9%	-43.7%	-46.1%
5%	-3.3%	-4.7%	-6.2%	-7.2%	-8.9%	-9.9%	-11.1%	-12.6%	-13.7%	-14.5%
10%	-1.6%	-1.3%	-1.8%	-3.6%	-4.6%	-6.3%	-8.3%	-8.9%	-9.4%	-9.6%
25%	2.2%	4.0%	4.0%	3.8%	3.1%	2.3%	1.6%	0.8%	-0.2%	-1.1%
50%	9.3%	10.6%	11.9%	12.5%	13.9%	14.4%	14.5%	14.7%	15.1%	15.3%
75%	17.5%	19.2%	21.9%	25.9%	27.6%	28.9%	31.5%	34.2%	35.0%	34.8%
90%	25.4%	28.9%	33.2%	36.7%	44.5%	51.2%	56.3%	61.5%	67.1%	69.7%
95%	32.5%	33.5%	37.0%	43.4%	54.2%	65.2%	77.2%	91.5%	98.3%	108.1%
99%	38.3%	47.4%	62.0%	89.1%	147.3%	192.5%	235.2%	292.7%	336.1%	367.9%
Maximum	47.9%	105.1%	145.3%	180.4%	253.4%	370.7%	496.6%	671.2%	807.2%	945.4%
Mean	10.7%	12.4%	14.1%	16.1%	19.0%	21.2%	23.5%	26.6%	28.9%	31.3%
Standard deviation	11.2%	13.1%	16.0%	21.0%	30.5%	39.1%	48.6%	62.0%	72.4%	83.1%

Table 31: Comparison of Projected Changes in 24-Hour Precipitation Events to Bush and Lemmen (2019)

Return Period (Years)	Bush and Lemmen (2019)		Golder	
	2031-2050	2081-2100	2041-2070	2071-2100
10	6% - 8.5%	5.3% - 20.5%	9.6%	11.9%
20	5.7% - 8.2%	5.1% - 20.1%	11.8%	12.5%
50	4.9% - 8.5%	7.6% - 20.1%	12.6%	13.9%

Changes in atmospheric processes driving extreme rainfall will unlikely be uniform in the future climate for sub-daily rainfall durations. However, climate models are not yet able to fully resolve convective processes responsible for generating extreme precipitation amounts on finer spatial scales and contributing to extreme precipitation in larger scale synoptic systems (CSA 2019). Despite this fact, climate projections generally support an increase in short duration rainfall in future climate within Canada (CSA 2019). Therefore, the projected changes in sub-daily rainfall based on the 1-day projected changes should be used with caution. A higher percentile level may be used to account for uncertainty in sub-daily precipitation projections than what is suggested here.

4.2.2 Percent Changes in Daily and Multi-Daily IDF Curves

Compared to sub-daily IDF values, the multi-day IDF values are used primarily to assess large catchments (where it takes more than 24 hours for flows to peak following a rainfall) and for water management systems (like dewatering and pumping).

The percent changes in daily and multi-day IDF conditions (future periods relative to the model baseline) were estimated for different durations of extreme rainfall events (ranging from 1 day to 120 days). Selected results for the 50th percentile are summarized in Table 32 and Table 33. The methodology is described in Section A.3.3, and the remaining percentiles for all durations and return periods are presented in Appendix B.

Generally, the longest durations of 50-days or greater show a smaller percentage increase compared to the shorter durations of 10-days or less for both the 2050 and 2080 horizons. This suggests that shorter events are more sensitive to climate change effects than the longer events. In most cases the highest percentage changes for a given duration are for higher return period events, meaning that climate change will likely have the greatest influence on extreme precipitation events.

Table 32: Summary of the 50th Percentile of Projected Percent Changes in Rainfall in the 2050s for the South Bruce Study Area

Return Period (years)	1-Day	2-Day	3-Day	4-Day	5-Day	6-Day	7-Day	10-Day	20-Day	30-Day	50-Day	75-Day	90-Day	120-Day
2	7.5%	8.9%	8.9%	9.7%	9.8%	10.0%	9.5%	9.1%	8.7%	9.1%	9.7%	8.5%	8.1%	7.4%
5	8.3%	11.1%	11.4%	11.6%	11.4%	11.6%	11.9%	12.4%	9.8%	10.1%	9.6%	9.3%	9.4%	8.8%
10	9.6%	12.0%	12.9%	12.8%	13.2%	13.2%	12.7%	13.7%	10.6%	10.4%	9.1%	8.9%	9.8%	9.5%
20	11.8%	12.6%	13.0%	12.7%	13.3%	12.7%	13.5%	14.4%	10.9%	10.8%	9.2%	9.8%	10.0%	10.2%
50	12.6%	12.7%	13.0%	14.0%	13.7%	13.5%	14.9%	14.6%	11.0%	10.9%	8.6%	10.4%	10.3%	10.9%
100	13.4%	12.1%	13.8%	13.8%	14.1%	13.7%	15.6%	16.3%	11.1%	11.2%	9.0%	10.7%	10.2%	11.4%
200	15.4%	12.5%	13.4%	13.9%	14.2%	14.2%	16.1%	16.7%	11.1%	11.9%	9.1%	10.8%	10.1%	11.6%
500	16.3%	13.0%	13.8%	14.2%	14.1%	14.0%	16.7%	17.5%	11.5%	12.5%	8.9%	11.0%	10.1%	12.2%
1,000	17.9%	13.0%	13.8%	14.3%	14.3%	13.9%	16.2%	17.8%	12.0%	12.5%	8.9%	10.8%	10.5%	12.2%
2,000	18.9%	12.9%	13.0%	13.6%	14.3%	13.9%	16.0%	18.3%	12.5%	12.8%	8.6%	10.9%	10.7%	13.1%

Table 33: Summary of the 50th Percentile of Projected Percent Changes in Rainfall in the 2080s for the South Bruce Study Area

Return Period (years)	1-Day	2-Day	3-Day	4-Day	5-Day	6-Day	7-Day	10-Day	20-Day	30-Day	50-Day	75-Day	90-Day	120-Day
2	9.3%	11.0%	12.0%	11.9%	11.5%	11.4%	10.1%	11.4%	10.8%	11.2%	10.6%	10.3%	10.2%	10.1%
5	10.6%	13.6%	13.5%	13.3%	13.4%	12.6%	12.3%	11.8%	11.5%	12.8%	11.5%	10.6%	10.9%	10.8%
10	11.9%	14.8%	15.1%	14.7%	14.1%	13.8%	13.7%	12.6%	11.4%	12.2%	11.2%	10.9%	11.4%	10.9%
20	12.5%	16.1%	15.7%	15.9%	16.2%	15.6%	15.2%	13.1%	12.3%	12.6%	11.3%	11.6%	11.4%	10.6%
50	13.9%	15.8%	15.4%	15.4%	16.8%	17.3%	17.3%	14.8%	12.5%	13.8%	11.8%	11.9%	12.0%	11.2%
100	14.4%	15.8%	14.6%	15.7%	16.6%	18.6%	17.8%	15.4%	13.3%	14.2%	11.9%	11.7%	11.7%	11.2%
200	14.5%	16.0%	14.6%	15.9%	17.3%	18.5%	17.6%	16.9%	13.3%	15.1%	11.1%	12.1%	11.7%	11.6%
500	14.7%	16.6%	15.1%	16.5%	17.0%	18.8%	17.9%	17.9%	13.1%	15.7%	11.0%	12.8%	11.8%	12.0%
1,000	15.1%	16.7%	15.2%	16.6%	16.9%	18.5%	18.0%	18.8%	13.4%	16.2%	10.3%	12.9%	12.2%	12.4%
2,000	15.3%	16.7%	14.7%	16.6%	17.3%	19.2%	19.1%	19.4%	13.6%	16.2%	10.0%	12.9%	12.3%	12.9%

4.3 Climate Change Impacts on PMP Estimates

PMP values are typically used to assess the safety of critical infrastructure such as dams, where failure of the infrastructure would cause significant damage and/or loss of life. The projected percentage changes in PMP shown here are for point projections for the site. However, it is expected that the projected percentage changes in PMP will be the same for different size of watersheds. Hence, absolute values for future DAD curves can be obtained by applying the percentage changes in PMP to the DAD curves presented for current climate given in Section 3.3.3.

The percent changes in PMP estimates (future periods relative to model baseline) were estimated for future PMP using the Hershfield and Moisture Maximization methods. Sub-daily climate projections are not available, which are required to generate sub-daily estimates of PMP using these methods. Therefore, percent changes in PMP was estimated for the 1-, 2-, and 3-day durations (Table 34 and Table 35). The 50th percentile results suggest increases in the 1-day PMP of 10.6% for the 2050s and 20.1% for the 2080s. The results agree with the expectation that as temperature increases under future climate conditions, precipitation is expected to increase as more vapor becomes available in the atmosphere (Kunkel et al. 2013), resulting in an increase in the projected PMP. The range of percentage changes in the 1-day PMP (from -28.9% to 102.7% in 2050s and -25.7% to 95.3% in 2080s) suggests that significant uncertainty and hence flexibility may be required in the future for systems designed for the PMP event.

The projected changes in the 50th percentile for 1-day PMP (10.6% in the 2050s and 20.1% in the 2080s; see Table 34 and Table 35) compared to 2000-year 50th percentile 1-day, 2,000-year IDF curves (18.9% in the 2050s and 15.3% in the 2080s; see Table 32 and Table 33) are lower in the 2050s and higher in the 2080s. Although the percentage changes are not always greatest for PMP compared to the 2000-year IDF curves, PMP is still a more conservative estimate of extreme rainfall for the South Bruce study area when absolute values are considered.

Daily rainfall amounts are provided in the climate model ensemble; however, timeseries of sub-daily rainfall in the future projections are not available. Future sub-daily PMP values can be estimated by applying the percentage changes in the 1-day PMP shown in Table 34 and Table 35, to the sub-daily PMP values provided in Table 17 for a given percentile level.

In Table 36 the results of this report were compared to those of Kunkel et al. (2013) and Clavet-Gaumont et al. (2017). Kunkel et al. (2013) used seven GCMs from the CMIP5 to project changes in PMP for the 2050s and 2080s future time periods from the 1971 to 2000 baseline. Clavet-Gaumont et al. (2017) used an ensemble of 12 RCM runs to project the change in PMP between the periods of 1971 to 2000 and 2041 to 2070 time periods for 5 major Canadian water basins. Changes in PMP for the Mattagami river basin (which drains a major portion of northern Ontario) are included in Table 36. The models used and time periods analyzed are different between this study and those in the literature. However, the comparison allows the number to be put into context with the range of those projected previously for a similar area. The estimates from this study are slightly higher than those obtained from Clavet-Gaumont et al. (2017) for the 2050s period (2041 to 2070), and slightly lower than those obtained from Kunkel et al. (2013) for the 2080s period (2071 to 2100).

Table 34: Summary of Selected Percentiles of Projected Percent Changes in PMP Estimates in the 2050s for the South Bruce Study Area

Percentiles	1-Day	2-Day	3-Day
Minimum	-28.9%	-27.9%	-25.0%
5%	-15.3%	-11.1%	-11.1%
25%	3.5%	4.9%	5.2%
50%	10.6%	11.4%	12.7%
75%	20.2%	21.2%	22.3%
95%	38.6%	47.3%	49.2%
Maximum	102.7%	101.7%	115.9%

Table 35: Summary of Selected Percentiles of Projected Percent Changes in PMP Estimates in the 2080s for the South Bruce Study Area

Percentiles	1-Day	2-Day	3-Day
Minimum	-25.7%	-36.9%	-36.8%
5%	-8.7%	-12.0%	-11.0%
25%	6.5%	8.2%	8.8%
50%	20.1%	22.6%	24.5%
75%	41.7%	44.6%	45.4%
95%	66.5%	70.0%	72.8%
Maximum	95.3%	100.6%	96.0%

Table 36: Comparison of PMP Values to those Obtained in the Literature

Duration	**Clavet-Gaumont et al. (2017)**	**Kunkel et al. (2013)**	**[1]Golder**	
	2041-2070	**2071-2100**	**2041-2070**	**2071-2100**
12-hour	—	25% - 35%	—	—
24-hour	8%	—	10.6%	20.1%
48-hour	4%	—	11.4%	22.6%
72-hour	5%	—	12.7%	24.5%

Note: (1) Values shown from this study are for the 1-3 days durations and are assumed to correspond to the 24-72 hour durations provided in the literature.

4.4 Climate Change Impacts on Rainfall on Snow

The daily snowpack/snowmelt analysis used the daily precipitation and temperature projections at South Bruce (using the same ECCC method as for the baseline climate). These results are used to assess large catchments where peak flooding events may be driven by a combination of rain and melt events (rather than by rain alone, as is assumed the case in IDF and PMP). Previous studies have found that the use of combined rainfall and snowmelt statistics instead of only precipitation can help prevent over or under design, and that the impact of this varies based on the location considered (Yan 2018).

The projected changes in the 50th percentile are shown in Table 37 and Table 38 (future periods relative to the model baseline). For shorter durations (1 to 3 days), there is a general increase; this is likely the result of larger shorter duration rainfall events (shown in Table 32 and Table 33 above), which are expected to continue dominating rain-on-snow events. For mid-range durations (10 to 30 days), there is a decrease with general downward trend up to 30-days, larger decreases in the 2080s than in the 2050s, suggesting a general decrease in future snowmelt events which are expected to play a more significant role in the mid-duration rain on snow events. This is also in agreement with an expected decrease in peak snowpack seen in Table 39 (relative to the model baseline from the GCM ensemble over 1979-2019). The long duration events are likely dominated by rainfall due to the occurrence of periods with no snowmelt and are expected to increase for the 2050s (120 days) and 2080s (90 and 120 days). The largest increases were found in the high return period 2080s events.

4.5 Climate Change Impacts on Additional Climate Variables

Analysis of climate variables in addition to extreme rainfall provides contextual climate change information for the South Bruce study area. These include projected changes in annual and monthly temperature and precipitation statistics from which seasonal variation can be inferred. Derived climate variables including rain and snow, snow depth, potential evapotranspiration, drought index, and qualitative information for wind speed and relative humidity. The information provided for wind speed and relative humidity may be interpreted qualitatively, as downscaled climate projections for these variables are limited. Daily future climate timeseries are provided to facilitate additional studies relating to climate change impacts at the South Bruce study area.

4.5.1 Projected Changes in Precipitation and Temperature Statistics

Statistically downscaled projections of daily total precipitation and mean temperature variables are used to estimate the change in monthly mean, minimum, and maximum statistics from the model baseline to the 2050s and 2080s future periods. Changes in precipitation are provided as percentage changes from the current climate baseline, while changes in temperature are provided as absolute values in degree Celsius. This is typically done to facilitate the application of projected changes to the baseline values (Anandhi et al. 2011).

Table 37: Summary of the 50th Percentile Projected Percent Changes in Rain on Snow events in the 2050s for the South Bruce Study Area

Return Period (years)	1-Day	2-Day	3-Day	4-Day	5-Day	6-Day	7-Day	10-Day	20-Day	30-Day	50-Day	75-Day	90-Day	120-Day
2	3.5%	-0.1%	-3.4%	-7.0%	-8.7%	-10.8%	-12.5%	-14.4%	-15.8%	-14.7%	-10.6%	-4.9%	-0.6%	4.4%
5	6.5%	1.7%	-1.3%	-5.4%	-8.8%	-10.5%	-11.8%	-14.3%	-16.0%	-14.7%	-11.9%	-6.4%	-2.5%	4.4%
10	7.1%	3.6%	-1.1%	-4.9%	-8.4%	-10.7%	-12.1%	-14.6%	-16.3%	-15.5%	-12.3%	-7.3%	-3.4%	4.8%
20	7.2%	4.2%	-0.6%	-4.4%	-8.3%	-10.9%	-12.7%	-15.1%	-16.5%	-16.1%	-12.9%	-7.8%	-3.9%	4.8%
50	7.8%	5.4%	0.3%	-3.5%	-8.0%	-10.5%	-13.1%	-15.0%	-17.0%	-16.9%	-13.2%	-8.3%	-4.6%	4.4%
100	8.2%	6.1%	0.9%	-3.4%	-7.8%	-10.2%	-13.2%	-15.1%	-17.1%	-17.0%	-13.5%	-8.3%	-5.0%	4.1%
200	8.7%	6.7%	1.3%	-3.4%	-7.7%	-10.1%	-12.9%	-15.3%	-17.1%	-17.0%	-13.8%	-8.6%	-5.5%	4.0%
500	9.3%	7.0%	1.8%	-3.2%	-7.3%	-10.1%	-12.1%	-15.3%	-17.3%	-17.0%	-14.3%	-9.1%	-6.1%	3.9%
1,000	9.4%	7.2%	2.1%	-3.1%	-6.9%	-10.0%	-11.9%	-15.3%	-17.4%	-16.9%	-14.8%	-9.5%	-6.3%	3.9%
2,000	9.5%	7.2%	2.2%	-2.9%	-6.8%	-9.6%	-11.7%	-15.3%	-17.4%	-16.9%	-15.2%	-9.6%	-6.6%	3.9%

Table 38: Summary of the 50th Percentile of Projected Percent Changes in Rain on Snow Events in the 2080s for the South Bruce Study Area

Return Period (years)	1-Day	2-Day	3-Day	4-Day	5-Day	6-Day	7-Day	10-Day	20-Day	30-Day	50-Day	75-Day	90-Day	120-Day
2	5.7%	0.8%	-4.7%	-8.2%	-11.4%	-13.7%	-14.7%	-17.2%	-19.9%	-17.7%	-11.8%	-4.6%	-0.1%	7.5%
5	11.1%	4.0%	-0.1%	-5.5%	-8.6%	-11.6%	-13.3%	-17.6%	-19.1%	-16.8%	-11.4%	-2.5%	2.0%	11.6%
10	13.0%	6.5%	0.7%	-4.4%	-6.4%	-9.9%	-11.9%	-16.4%	-19.1%	-16.6%	-10.7%	-2.1%	3.7%	14.0%
20	14.5%	8.0%	1.8%	-3.7%	-6.1%	-8.8%	-11.3%	-16.0%	-19.2%	-17.0%	-10.3%	-1.0%	4.5%	16.6%
50	17.1%	10.1%	3.2%	-2.7%	-5.9%	-8.5%	-10.4%	-16.0%	-18.9%	-16.9%	-10.1%	-0.5%	5.1%	17.9%
100	17.6%	12.2%	4.0%	-2.1%	-5.3%	-8.0%	-10.0%	-16.0%	-18.6%	-17.0%	-9.9%	-0.3%	5.4%	18.7%
200	18.8%	13.5%	4.5%	-1.5%	-5.0%	-7.5%	-9.6%	-15.7%	-18.6%	-17.1%	-9.8%	-0.4%	6.4%	19.7%
500	20.5%	14.6%	5.2%	-1.1%	-4.8%	-7.2%	-9.2%	-15.6%	-18.9%	-17.2%	-9.8%	-0.2%	7.1%	20.9%
1,000	21.1%	15.3%	5.8%	-0.6%	-4.8%	-6.9%	-9.1%	-15.6%	-19.0%	-17.3%	-9.5%	-0.1%	7.5%	21.7%
2,000	21.4%	15.9%	6.4%	-0.4%	-4.6%	-6.6%	-9.2%	-15.5%	-18.9%	-17.2%	-9.2%	0.1%	7.6%	22.4%

Table 39: Percent Change in Peak Snowpack Accumulation for the South Bruce Study Area (50th Percentile)

Return Period (years)	2	5	10	20	50	100	200	500	1,000	2,000
Baseline to 2050s	-31.9%	-26.3%	-24.7%	-22.9%	-21.3%	-20.6%	-20.4%	-19.9%	-20.0%	-19.7%
Baseline to 2080s	-43.0%	-37.7%	-35.2%	-33.8%	-32.6%	-31.5%	-30.7%	-29.7%	-29.1%	-28.8%

Annual total precipitation is projected to increase by 7.6% in the 2050s and 9.2% in the 2080s, indicating an upward trend in total precipitation on an annual scale at the 50**th** percentile (Table 40 and Table 41). In the 2050s, monthly total precipitation at the 50th percentile is projected to increase for all months except August which is projected to change by -2.7% (Table 40). The largest projected increase at the 50th percentile is found in the month of January at 12.5%. The total range of projected monthly changes in precipitation for the multi-model ensemble corresponds to -47.1% in August and 67.2% in July. In the 2080s, the months of August and September show projected decreases in precipitation of -2.3% and -0.8% at the 50th percentile while all other months project increasing precipitation amounts (Table 41). The total range of projected monthly changes in precipitation corresponds to -46.5% in September to 66.6% in April. The range of projected changes for monthly total precipitation in Table 40 and Table 41 across calendar months is illustrated in Figure 13.

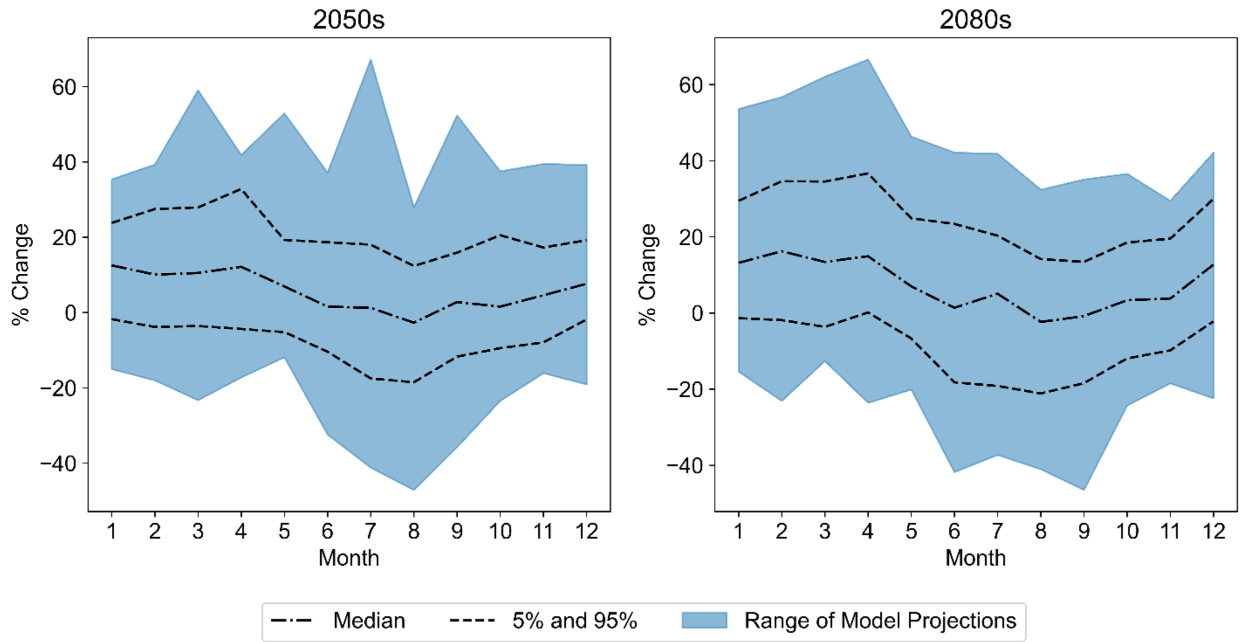

Figure 13 : Range of Projected Changes in Monthly Total Precipitation for the Multi-Model Ensemble for the South Bruce Study Area

The seasonal variation in projected changes (projected decrease in August and greatest project increase in January) have been confirmed with those provided by the Ontario Climate Data Portal (OCDP) for the 2050s and 2080s time periods for the South Bruce study area using a 1986 to 2005 baseline period (OCDP 2020). The reason for the projected decrease in summer precipitation is a consequence of overall surface drying and changes in atmospheric circulation as a result of climate change (Collins et al. 2013). Under the RCP 4.5 scenario, for month of August, the OCDP values show a projected decrease in precipitation of -17%, while in January a 24% increase is projected for the 2050s. The difference in values between those reported here is due to the use of a different multi-model ensemble as well as different baseline periods. Similarly, Bush and Lemmen (2019) show a median annual increase across Ontario of 5.5 % (0.4% to 11.1%, 25th and 75th percentile respectively) for RCP 2.6 and 6.6% (1.8% to 12.4%, 25th and 75th percentile respectively) for RCP 8.5, for the period from 2031 to 2050. This is generally lower than the projected increases for the South Bruce study area but reflects differences in the regions covered and the future time periods considered. The period from 2081 to 2100 shows increases of 5.3% (-0.1% and 10.8% for the 25th and 75th percentiles) for RCP 2.6 and 17.3% (8.5% and 26.1% for the 25th and 75th percentiles) for RCP 8.5, which encompasses most of the monthly median values in Table 40 and Table 41.

The seasonal variation provided in this report (increasing total precipitation in winter and decreasing in summer) is supported by Bush and Lemmen (2019). The values provided in Bush and Lemmen (2019) are based on coarse resolution global climate models; however, in the winter months for the 2031 to 2050 period, Bush and Lemmen (2019) show projected changes in precipitation ranging from 0 to 20%, while in the summer months the ensemble projections range from -10% to 10% for the South Bruce study area. For the 2081 to 2100 period, Bush and Lemmen (2019) show a projected increase of 0 to 30% for the winter months, while the summer months the changes in precipitation range from -10% to 10%.

The range of total monthly precipitation changes is nearly the same between the 2050s and 2080s; however, the projected changes at the 50th percentile are slightly greater (Table 41). The 50th percentile may be used as a screening value for total monthly precipitation, but it should be noted that there is a large range of projections of total precipitation at the South Bruce study area, indicating lack of agreement or uncertainty in the projections. In all months, the multi-model ensemble range covers both projected increase and decrease in total precipitation.

The range of projected changes for annual and monthly mean temperature is provided in Table 42 and Table 43, and illustrated in Figure 14. Annual average temperature is projected to change by 3.4°C in the 2050s and 4.2°C in the 2080s, indicating an increasing trend due to changing climate. The projected changes for the mean monthly temperature are generally greatest for the winter months and early spring months at the 50th percentile. In the 2050s, January and December are projected to be 2.9°C and 2.7°C warmer than the current climate baseline at the 50th percentile, while the month of April has the lowest projected temperature change of 2°C (Table 42). In the 2080s, January also has the highest projected changes in temperature at 4°C, with the months of April and November having the lowest projected change of 3.1°C at the 50th percentile (Table 43). Greater projected changes for the winter months are a common feature of climate change in higher latitudes, as the reductions in snow and ice lead to reductions in albedo and increased heat transport from southern latitudes (Bush and Lemmen 2019). For all months in both time periods, the mean projected change of the multi-model ensemble is greater than the median. This suggests that there are scenarios projecting significantly higher temperatures than the rest of the ensemble.

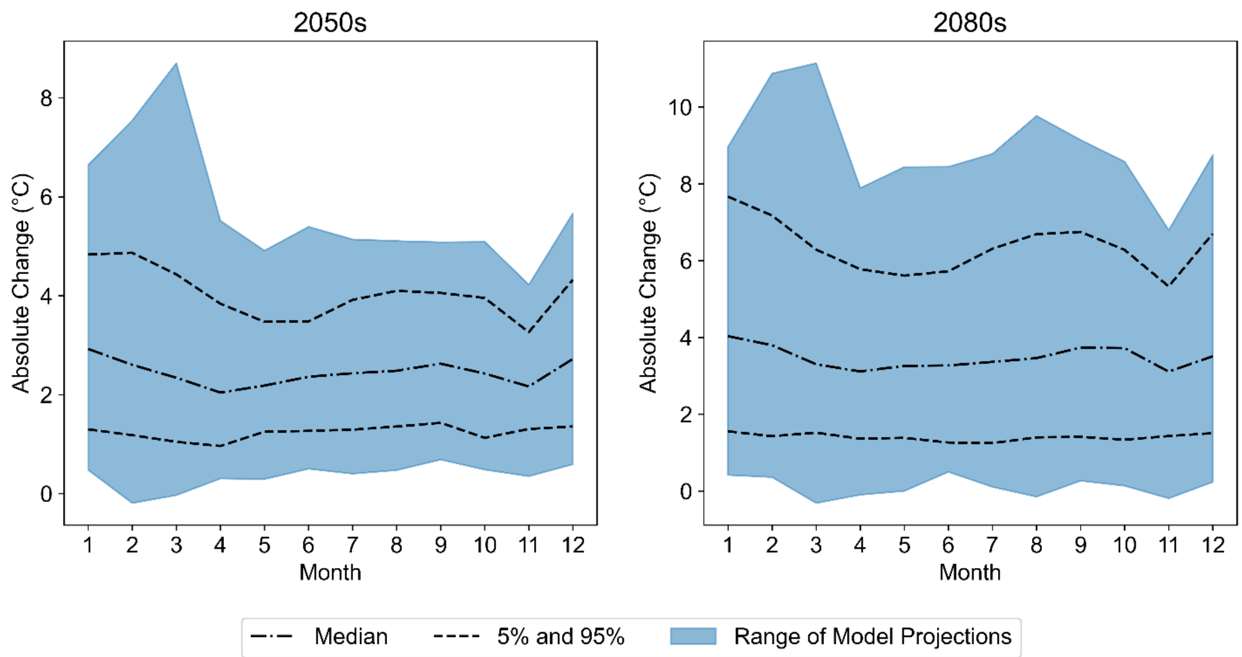

Figure 14: Range of Projected Changes in Monthly Mean Temperature for the Multi-Model Ensemble for the South Bruce Study Area

Similarly, Bush and Lemmen (2019) show a median annual increase across Ontario of 1.5°C (1.1°C to 2.1°C, 25th and 75th percentile respectively) for RCP 2.6 and 2.3°C (1.7°C to 2.9°C, 25th and 75th percentile respectively) for RCP 8.5, for the period from 2031 to 2050. Again, these projections are in line with, but lower than, the projected increases for the South Bruce study area; they reflect differences the regions covered and the future time periods considered. The period from 2081 to 2100 shows increases of 1.7°C (1.0°C and 2.1°C for the 25th and 75th percentiles) for RCP 2.6 and 6.3°C (5.3°C and 6.9°C for the 25th and 75th percentiles) for RCP 8.5, which encompasses monthly median values in Table 42 and Table 43.

Seasonal variation results provided here agree with that of Bush and Lemmen (2019). In Bush and Lemmen (2019), projected changes in temperature range from 1.5°C to 3°C in the winter months and 0.5°C to 3°C in the summer months for the 2031 to 2050 period. In the 2081 to 2100 period, projected changes range from 2°C to 9°C in the winter months and 0.5°C to 7°C in the summer months. Similarly, the values provided in this report show greater projected increases in temperature for the winter months than the summer months.

Table 40: Projected Changes in Monthly Total Precipitation in the 2050s for the South Bruce Study Area (%)

Statistic	Jan	Feb	Mar	Apr	May	Jun	Jul	Aug	Sep	Oct	Nov	Dec	Annual
Minimum	-15.0%	-18.0%	-23.3%	-17.3%	-11.9%	-32.4%	-41.2%	-47.1%	-35.8%	-23.5%	-16.1%	-19.1%	-3.2%
10%	-1.8%	-3.9%	-3.6%	-4.4%	-5.2%	-10.4%	-17.5%	-18.5%	-11.7%	-9.5%	-7.9%	-1.9%	0.2%
25%	4.2%	1.0%	3.4%	2.5%	-0.7%	-4.4%	-7.9%	-9.1%	-3.5%	-5.2%	-2.1%	1.0%	3.8%
50%	12.5%	10.1%	10.5%	12.1%	6.9%	1.6%	1.2%	-2.7%	2.8%	1.6%	4.6%	7.6%	7.6%
75%	18.4%	17.0%	19.0%	22.4%	12.1%	11.3%	9.9%	4.8%	9.3%	14.7%	11.7%	14.1%	11.3%
90%	23.8%	27.5%	27.9%	32.8%	19.3%	18.7%	18.0%	12.4%	15.9%	20.5%	17.3%	19.2%	15.0%
95%	28.9%	32.7%	34.1%	35.7%	24.5%	24.9%	26.4%	20.4%	22.0%	25.6%	19.8%	23.0%	17.7%
99%	32.6%	37.3%	51.1%	41.0%	38.2%	34.7%	35.8%	26.5%	32.6%	33.8%	29.2%	28.8%	19.8%
Maximum	35.4%	39.3%	59.1%	41.9%	52.9%	37.2%	67.2%	28.0%	52.4%	37.5%	39.5%	39.2%	20.4%
Mean	11.6%	10.3%	11.6%	12.5%	7.0%	3.0%	0.7%	-2.7%	2.6%	4.3%	4.7%	7.8%	7.6%
Standard Deviation	10.0%	12.0%	13.2%	13.5%	10.4%	11.8%	15.3%	13.4%	12.4%	12.5%	10.2%	9.2%	5.6%

Table 41: Projected Changes in Monthly Total Precipitation in the 2080s for the South Bruce Study Area (%)

Statistic	Jan	Feb	Mar	Apr	May	Jun	Jul	Aug	Sep	Oct	Nov	Dec	Annual
Minimum	-15.4%	-23.1%	-12.6%	-23.6%	-20.1%	-41.8%	-37.3%	-41.0%	-46.5%	-24.3%	-18.5%	-22.4%	-6.7%
10%	-1.4%	-1.9%	-3.6%	0.1%	-6.7%	-18.2%	-19.2%	-21.1%	-18.4%	-11.9%	-9.8%	-2.2%	0.1%
25%	5.6%	5.6%	3.3%	6.5%	-0.3%	-7.3%	-6.8%	-11.4%	-9.5%	-4.4%	-4.0%	4.8%	4.7%
50%	13.2%	16.2%	13.4%	14.9%	7.0%	1.4%	5.1%	-2.3%	-0.8%	3.4%	3.8%	12.7%	9.2%
75%	22.0%	26.1%	21.5%	25.5%	17.6%	13.0%	12.9%	7.0%	6.1%	9.3%	12.7%	22.7%	13.7%
90%	29.5%	34.6%	34.5%	36.7%	24.9%	23.4%	20.3%	14.2%	13.4%	18.5%	19.5%	30.0%	17.0%
95%	36.5%	41.5%	39.8%	49.5%	30.2%	27.6%	27.1%	17.5%	16.2%	23.0%	22.6%	32.1%	18.9%
99%	48.1%	50.1%	57.1%	58.6%	40.1%	34.8%	36.9%	29.5%	26.3%	33.7%	26.7%	40.3%	20.5%
Maximum	53.6%	56.7%	62.1%	66.6%	46.4%	42.2%	41.8%	32.4%	35.1%	36.6%	29.5%	42.2%	20.8%
Mean	14.0%	16.1%	14.0%	17.4%	8.7%	1.9%	2.7%	-2.9%	-2.3%	2.9%	4.3%	13.2%	9.0%
Standard Deviation	13.0%	14.7%	15.0%	16.2%	12.7%	15.4%	16.1%	14.8%	13.8%	12.0%	11.1%	12.5%	6.3%

Table 42: Projected Changes in Monthly Mean Temperature in the 2050s for the South Bruce Study Area (°C)

Statistic	Jan	Feb	Mar	Apr	May	Jun	Jul	Aug	Sep	Oct	Nov	Dec	Annual
Minimum	0.5	-0.2	0.0	0.3	0.3	0.5	0.4	0.5	0.7	0.5	0.4	0.6	1.2
10%	1.3	1.2	1.1	1.0	1.3	1.3	1.3	1.4	1.4	1.1	1.3	1.4	2.1
25%	2.2	1.8	1.5	1.4	1.6	1.8	1.8	1.9	1.9	1.8	1.7	2.0	2.6
50%	2.9	2.6	2.3	2.0	2.2	2.4	2.4	2.5	2.6	2.4	2.2	2.7	3.4
75%	3.7	3.8	3.1	2.6	2.9	2.8	3.2	3.4	3.4	3.0	2.9	3.7	4.0
90%	4.8	4.9	4.4	3.8	3.5	3.5	3.9	4.1	4.1	4.0	3.3	4.3	4.6
95%	5.7	5.1	5.5	4.5	3.9	4.0	4.0	4.5	4.3	4.3	3.8	4.6	4.9
99%	6.2	7.1	8.2	5.3	4.4	5.0	4.8	5.0	4.9	4.8	4.1	5.6	5.5
Maximum	6.6	7.5	8.7	5.5	4.9	5.4	5.1	5.1	5.1	5.1	4.2	5.7	5.7
Mean	3.1	2.9	2.6	2.2	2.3	2.4	2.5	2.6	2.7	2.5	2.3	2.8	3.3
Standard Deviation	1.3	1.5	1.5	1.1	0.9	0.9	1.0	1.1	1.0	1.0	0.8	1.1	1.0

Table 43: Projected Changes in Monthly Mean Temperature in the 2080s for the South Bruce Study Area (°C)

Statistic	Jan	Feb	Mar	Apr	May	Jun	Jul	Aug	Sep	Oct	Nov	Dec	Annual
Minimum	0.4	0.4	-0.3	-0.1	0.0	0.5	0.1	-0.2	0.3	0.1	-0.2	0.2	1.2
10%	1.6	1.4	1.5	1.4	1.4	1.3	1.3	1.4	1.4	1.3	1.4	1.5	2.1
25%	2.6	2.4	2.1	2.0	1.9	1.9	2.2	2.1	2.2	2.0	2.2	2.4	3.0
50%	4.0	3.8	3.3	3.1	3.3	3.3	3.4	3.5	3.7	3.7	3.1	3.5	4.2
75%	5.6	5.6	4.8	4.3	4.3	4.7	5.1	5.5	5.3	4.8	4.6	5.2	5.7
90%	7.7	7.2	6.3	5.8	5.6	5.7	6.3	6.7	6.8	6.3	5.3	6.7	6.9
95%	7.9	8.0	7.2	6.3	6.3	6.3	7.1	7.4	7.5	7.1	5.9	7.3	7.7
99%	8.9	10.4	10.7	7.4	7.7	7.7	8.7	9.6	8.9	8.2	6.5	7.8	8.3
Maximum	9.0	10.9	11.1	7.9	8.4	8.4	8.8	9.8	9.1	8.6	6.8	8.8	8.4
Mean	4.3	4.2	3.6	3.3	3.4	3.5	3.7	3.9	3.9	3.6	3.3	3.9	4.4
Standard Deviation	2.1	2.2	2.1	1.7	1.7	1.8	1.9	2.1	2.1	1.9	1.5	1.9	1.8

In addition to monthly projected changes in precipitation and temperature, a set of daily future time series are provided; continuous daily climate data series are often needed to drive climate change impact models such as water balance or hydrological models. Directly using climate model outputs is not recommended, as modelled precipitation typically suffers from the effect of drizzle (Werner and Cannon 2016). This mean that there are more wet days with low amounts of precipitation and consequently, lower magnitudes of precipitation for extreme events. The more frequent occurrence of wet days would result in higher antecedent soil moisture conditions prior to rainfall events, while lower values of precipitation extremes may underestimate the magnitude and frequency of peak runoff.

The statistically downscaled climate projections used in the previous sections include bias correction methods to minimize the effect of drizzle present in global climate models and are sufficient for the relative comparisons completed above. However, these effects may still be present when developing daily time series. Furthermore, the historical data sources used in the statistically downscaled climate projections are either spatially interpolated or rely on reanalysis datasets that may not capture site climate conditions. The methodology in Appendix A.3.6.1 is used to overcome these limitations by incorporating the daily infilled dataset for South Bruce (Section 3.1.2). Using this method, a corrected daily timeseries is provided for precipitation, rain, snow, and snow depth. Daily temperature variables as well as potential evapotranspiration are also included in the daily timeseries. All daily future timeseries for each member of the multi-model ensemble are included in Appendix C.

The correction of the distribution of daily precipitation values can be examined using a quantile-quantile plot, which compares the observed and modelled (both corrected and uncorrected) values across the same set of quantiles for the model baseline period of 1979 to 2019 (Figure 15). The observed values in Figure 15 are equivalent to a 1:1 line, while modelled values closer to the 1:1 indicate a distribution that is more statistically similar to what is observed. The shaded area represents the range of climate scenarios across the multi-model ensemble. The uncorrected downscaled climate model projections show slightly higher values for the lowest amounts of observed precipitation indicating the effect of drizzle, while observed precipitation greater than approximately 5 mm/day is typically underestimated. The range of bias corrected precipitation values are shown to overlap the observed precipitation values across the entire distribution. Although the bias corrected values still show an underestimation of precipitation compared to the observations, the effect of drizzle has been reduced and the magnitude and frequency of precipitation extremes are more accurately captured.

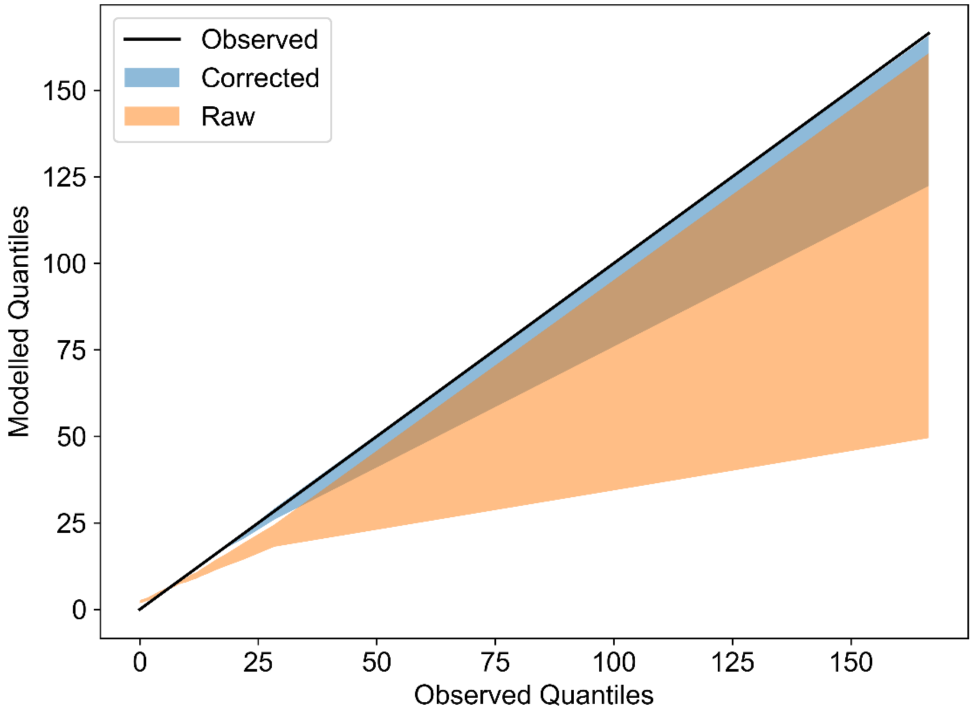

Figure 15: Quantile-Quantile Plot for Corrected and Uncorrected Climate Projections for Daily Precipitation over the Modelled Baseline Period.

The wet and dry day frequencies for modelled precipitation both with and without bias correction compared to observations are shown in Figure 16 and Figure 17. Wet days correspond to days with precipitation greater than 1 mm, while dry days correspond to days with precipitation less than or equal to 1 mm. The mean number of wet days per month is highly variable across the uncorrected climate models, indicated by a large range in the shaded area (Figure 16). The shaded area does not overlap observations for all months except August. In contrast, the bias corrected climate models have a smaller range in the mean number of wet days per month and are much closer to the observations for all months. For the mean number of dry days, the findings are similar (Figure 17). Overall, the range of modelled dry days is smaller and closer to the observations with bias correction, thereby increasing confidence in the use of the modelled daily timeseries.

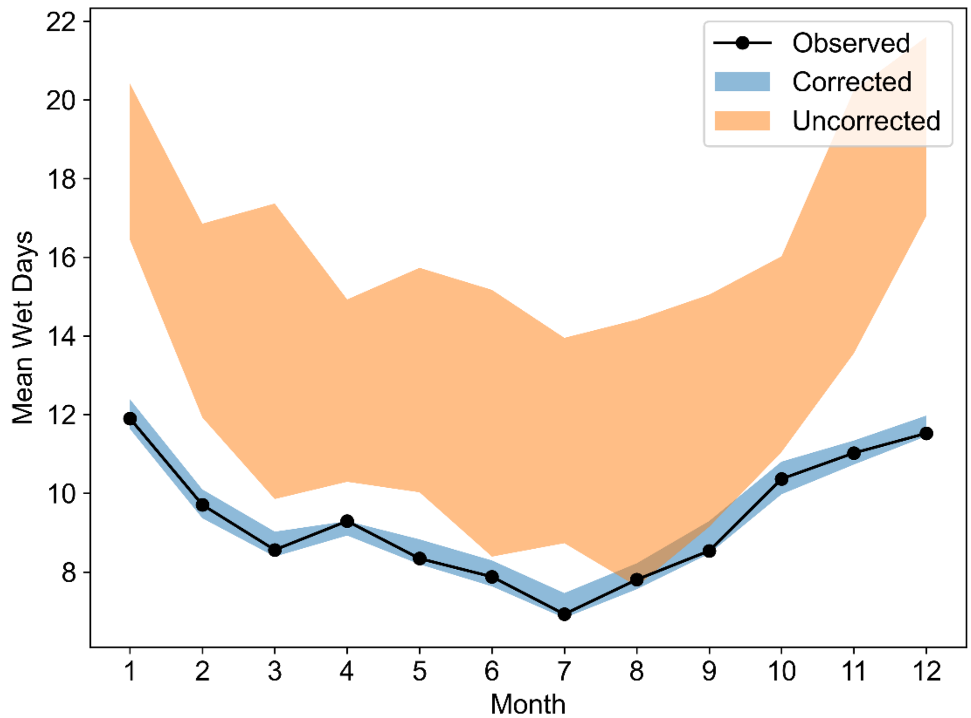

Figure 16: Mean Wet Days Across Calendar Months for Corrected and Uncorrected Modelled Precipitation Compared to Observations

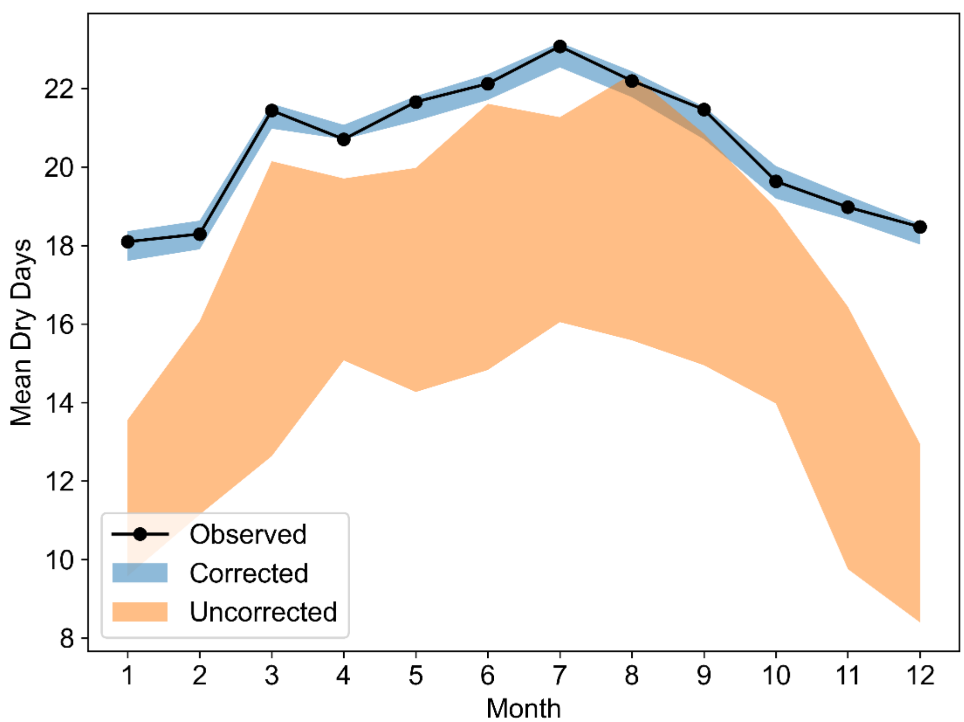

Figure 17: Mean Dry Days Across Calendar Months for Corrected and Uncorrected Modelled Precipitation Compared to Observations

The seasonal variation in precipitation is shown through a comparison of the total monthly precipitation for both corrected and uncorrected values compared to observations, along with derived rain, snow, and snow depth (Figure 18). The corrected and uncorrected values for monthly total precipitation and the derived variables have similar shaded areas. However, the seasonal variation of mean total precipitation is better captured in the corrected values; for mean snow depth, there are significantly less models that overestimate from January to May. If a higher degree of accuracy is required for rain, snow, and snow depth, then an additional bias correction is recommended as additional work on the temperature variables.

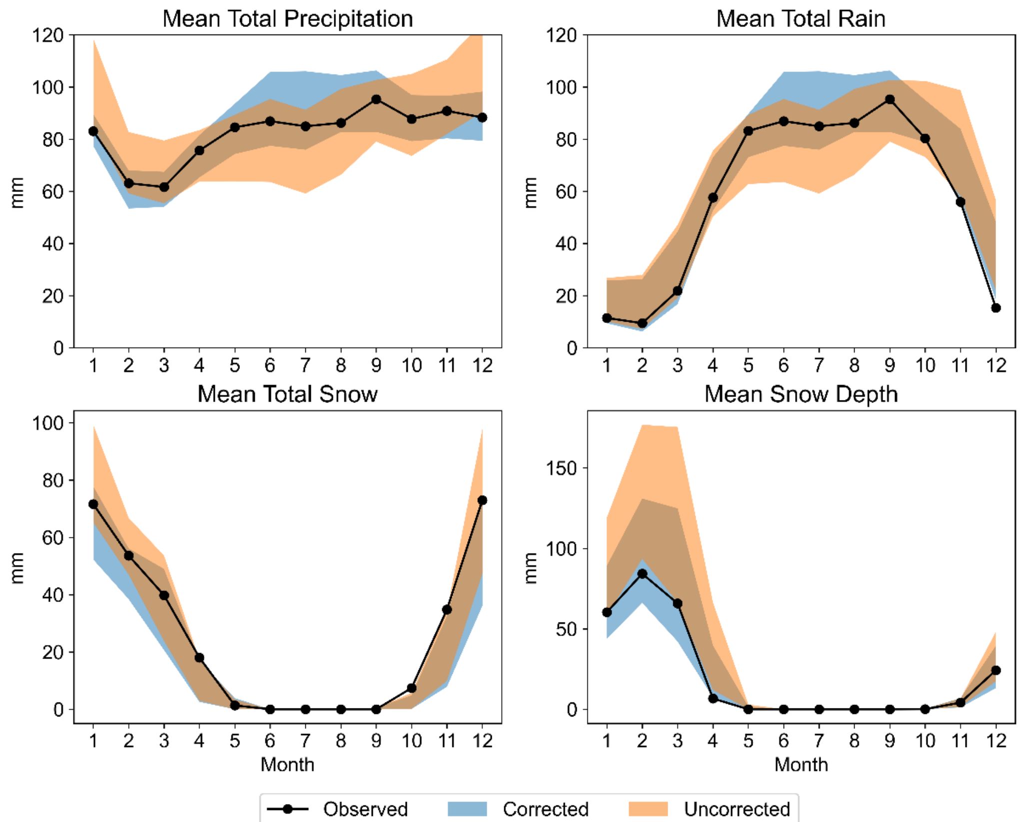

Figure 18: Range of Mean Total Monthly Precipitation Projections and Derived Variables Corrected and Uncorrected Compared to Observations

The application of bias correction to the statistically downscaled climate model outputs for the South Bruce study area has led to improved estimation of precipitation across the distribution of daily values, including daily extremes. Both wet and dry day frequencies are more similar to that of the observed precipitation values, while better capturing the seasonal variation in mean monthly precipitation totals and mean snow depth. Application of bias correction to climate models assume that the same bias between the model baseline and observations will carry forward into the future. This cannot be evaluated as future observations do not exist; however, the results of this bias correction can provide confidence that the daily timeseries of future projections will be more applicable to the site. The complete bias corrected precipitation timeseries from 1950 to 2100 for each of the 136 climate projections, along with the derived rain, snow, snow depth and potential evapotranspiration timeseries are provided in Appendix C.

4.5.2 WMO Climate Indices

The change in WMO climate indices from the model baseline to the 2050s and 2080s future time periods provides an indication on how climate extremes may change under future climate conditions. The distribution of changes to each of the 27 climate indices for the 2050s and 2080s is provided in Table 44 and Table 45 respectively. The projected changes are shown as absolute values to preserve the different units being used for the indices, as some are shown as days, mm, mm/day, and °C. The calculation of various WMO indices was performed considering different time periods within the year (e.g., growing season); therefore, monthly values cannot be provided as the focus is on the project change of the aggregated indices.

In the 2050s with regards to precipitation indices, the projected changes in WMO indices at the 50th percentile appear to indicate a future that is more extreme with regards to precipitation. The number of consecutive wet days only increases by 0.6 days, but the annual amount of precipitation on wet days is projected to increase by 55.9 mm per year on average (up from 984.1 mm per year under current climate conditions), with slightly more days above the 10 mm (heavy), 20 mm (very heavy), and 30 mm precipitation thresholds corresponding to 3, 1, and 0.5 days on average, respectively. Maximum 1- and 5-day rainfall amounts are also projected to increase at the 50th percentile by 3.2 mm and 7 mm, respectively. In the 2080s the same patterns are present and the precipitation amounts and number of days above precipitation thresholds are slightly higher than the 2050s (Table 44).

Under current climate conditions, months of September to November typically have the greatest precipitation amounts (Section 2.5.1), while under future climate conditions, August is projected to have a small decrease in precipitation at the 50th percentile (Section 4.5.1). However, precipitation extremes are projected to increase. This indicates that in August, smaller precipitation events may become less frequent, while larger precipitation events will be more frequent for there to be a projected decrease during these months. In the current climate baseline, the trends in the WMO indices showed no significant trends in extreme precipitation (Table 24), while the change projected for the 2050s and 2080s is showing increasing extremes. This indicates that a shift in rainfall pattern is projected for the South Bruce study area.

Based on these results, future precipitation is expected to yield more frequent intense rainfall events and greater precipitation amounts annually. As noted in Section 4.5.1 for the changes to monthly precipitation amounts, there is a considerable level of uncertainty in the projected changes to precipitation-based indices, as the range of projections across the multi-model ensemble indicates both an increase and decrease for each of the indices. The 50th percentile may be used for screening purposes; however, a different percentile should be considered for design purposes to better capture the desired risk level.

For the temperature-based indices, fewer cold spells and more warm spells are indicated for the 2050s at the 50th percentile (Table 44). Fewer freezing and icing days are projected along with a longer growing season, more summer days, and greater extreme minimum and maximum daily temperatures. In the 2080s, there is further warming indicated by greater increases in growing season, summer days, and extreme minimum and maximum daily temperatures along with further reductions to the number of freezing and icing days at the 50th percentile (Table 45). The temperature-based current climate trends agree with the direction of change projected for future climate except for the number of summer days (average days above 25°C in the year). In the current climate, summer days have been shown to decrease, while they are projected to increase in future climate. This indicates a shift in temperature patterns at the South Bruce study in the summer months, which is confirmed by the projected increases shown in Section 4.5.1.

4.5.3 Potential Evapotranspiration

Changes to potential evapotranspiration rates are a key consideration for water balance assessments of climate change. This section summarizes the distribution of projected changes from the modelled baseline for each calendar month and is provided for the 2050s and 2080s future time periods. The projected changes are provided as a percentage change from the modelled baseline.

Annual total potential evapotranspiration is projected to increase by 13.1% in the 2050s and 14.8% by the 2080s at the 50th percentile, compared to the model baseline. This indicates an increasing trend in potential evapotranspiration due to climate change. In the 2050s all months indicate an increase in potential evapotranspiration for at least 90% of the projections in the multi-model ensemble. The percentage changes range from 7.2% to 19.5% across calendar months at the 50th percentile (
Table 46). The largest changes occur during months where there are typically low amounts of potential evapotranspiration (December through March), indicating that the largest percentage changes correspond with small absolute changes. July was found to be the month with the highest evapotranspiration rates in the current climate baseline (see Section 3.5.3) and is projected to have a 7.7% increase for the 2050s future period at the 50th percentile. Overall, the distribution of projected changes across the climate model ensemble for each month is similar to that of the mean temperature (Section 4.5.1). This is due to the way that potential evapotranspiration is calculated using the Hargreaves equation. Other methods such as the Penman-Monteith equation would take into consideration changes in wind speed and relative humidity; however, these variables are not available for the downscaled multi-model ensemble.

In the 2080s, projected changes in potential evapotranspiration rates are greater for all months at the 50th percentile, ranging from 8.5% to 25.2% (Table 47). This is expected, as in the 2080s period, projected changes in monthly temperatures are greater at the 50th percentile. The projected changes in the 2080s follow the same pattern across months and climate model projections; however, there is a larger spread in projected changes from the model baseline, indicated by the higher standard deviation in projections for each month. Potential evapotranspiration extremes are likely to change in similar manner to the WMO indices due to the dependence on temperature (Section 4.5.2). Therefore, it can be assumed that based on the projections, more warm spells and summer days will result in more periods of elevated potential evapotranspiration rates.

Potential evapotranspiration was calculated on a daily time scale using the temperature projections from the multi model ensemble. The resulting daily dataset is provided in Appendix C.

Table 44: Distribution of Projected Changes in WMO Climate Indices in the 2050s for the South Bruce Study Area

WMO Indices	Min	5%	10%	50%	75%	90%	95%	99%	Max	Mean	Std. Dev.
Consecutive dry days (days)	-2.7	-1.4	-1.2	0.3	1.2	2.2	2.6	3.9	4.9	0.4	1.3
Cold spell duration indicator (days)	-4.9	-3.3	-2.9	-1.3	-0.6	-0.4	-0.2	0.0	0.3	-1.5	1.1
Consecutive wet days (days)	-2.7	-0.9	-0.7	0.6	1.3	1.9	2.6	4.5	5.6	0.6	1.2
Diurnal temperature range (°C)	-0.5	-0.4	-0.3	0.0	0.1	0.3	0.4	0.9	0.9	0.0	0.3
Frost days (days)	-70.3	-52.7	-46.8	-28.3	-20.0	-14.7	-13.6	-10.8	-8.0	-29.9	12.8
Growing season length (days)	2.3	6.7	8.8	20.8	27.8	38.1	47.2	63.6	72.7	22.3	12.8
Ice days (days)	-44.8	-39.7	-35.2	-21.6	-15.5	-12.1	-8.7	-6.2	-5.7	-22.6	9.0
Annual total wet-day precipitation (mm)	-51.4	-14.8	1.1	55.9	91.4	125.0	146.1	160.3	162.3	60.2	46.8
Heavy precipitation days (days)	-2.9	-0.7	0.3	3.0	4.9	6.6	7.4	9.3	10.4	3.3	2.5
Very heavy precipitation days (days)	-0.8	-0.1	0.2	1.0	1.6	2.1	2.6	3.2	3.5	1.1	0.8
Very wet days (mm)	-25.1	-3.5	9.6	41.6	68.2	93.9	101.5	130.6	140.9	47.1	32.7
Extremely wet days (mm)	-18.5	-3.6	0.8	22.6	34.6	44.9	54.5	66.2	86.9	23.4	17.9
Days above 25 mm (days)	-0.5	-0.1	0.0	0.5	0.7	0.9	1.0	1.2	1.7	0.5	0.4
Max 1-day precipitation (mm)	-5.2	-1.5	-0.4	3.2	5.3	7.7	9.7	10.8	11.2	3.4	3.2
Max 5-day precipitation (mm)	-6.8	-1.6	0.9	7.0	10.6	13.5	15.7	20.7	27.9	7.2	5.5
Simple daily intensity index (mm/day)	-0.2	0.0	0.1	0.3	0.5	0.6	0.8	0.9	1.1	0.4	0.2
Summer days (days)	5.6	16.3	17.9	33.7	38.7	45.8	48.9	56.4	58.2	32.2	10.8
Cool nights (% of days)	-9.9	-9.2	-9.0	-7.2	-6.2	-5.3	-4.4	-3.2	-2.8	-7.2	1.5
Warm nights (% of days)	1.7	5.0	5.8	12.1	16.7	20.5	22.2	30.4	31.6	12.8	6.0
Min Tmin (°C)	1.0	1.8	2.1	4.3	5.9	6.9	7.3	10.2	10.8	4.5	2.0
Max Tmin (°C)	-0.5	0.7	0.9	2.1	2.9	3.4	3.7	4.4	4.8	2.2	1.0
Tropical nights (days)	-0.5	2.2	3.2	9.6	14.0	19.0	21.1	30.5	33.8	10.2	6.5
Cool days (% of days)	-9.8	-9.1	-8.9	-7.3	-6.1	-5.1	-4.3	-2.8	-2.4	-7.1	1.5
Warm days (% of days)	2.5	4.6	5.7	13.2	18.5	21.6	23.6	29.1	30.7	13.6	6.3
Min Tmax (°C)	0.8	1.6	1.9	3.6	4.8	5.5	6.4	7.5	7.7	3.7	1.5
Max Tmax (°C)	0.0	1.0	1.2	2.7	3.7	4.4	4.8	6.8	7.1	2.8	1.3
Warm spell duration indicator (days)	3.1	6.0	7.8	22.5	31.7	42.7	50.5	70.5	87.1	24.3	15.2

Table 45: Distribution of Projected Changes in WMO Climate Indices in the 2080s for the South Bruce Study Area

WMO Indices	Min	5%	10%	50%	75%	90%	95%	99%	Max	Mean	Std. Dev.
Consecutive dry days (days)	-2.3	-1.4	-0.8	0.5	1.4	2.3	3.8	6.7	7.2	0.8	1.7
Cold spell duration indicator (days)	-4.9	-3.4	-3.1	-1.2	-0.7	-0.4	-0.3	0.3	0.5	-1.6	1.1
Consecutive wet days (days)	-2.6	-1.3	-0.7	0.5	1.4	2.5	3.3	5.6	7.1	0.7	1.5
Diurnal temperature range (°C)	-1.2	-0.5	-0.4	0.0	0.2	0.4	0.6	0.9	1.0	0.0	0.4
Frost days (days)	-100.2	-87.5	-75.8	-40.3	-25.4	-18.8	-13.2	-7.4	-2.9	-43.7	22.2
Growing season length (days)	-0.2	7.9	12.7	30.5	47.9	71.7	82.1	105.1	109.8	36.5	23.5
Ice days (days)	-61.5	-53.2	-48.4	-29.0	-20.7	-13.9	-10.2	-6.0	-2.9	-30.2	13.1
Annual total wet-day precipitation (mm)	-55.1	-14.7	-3.4	73.9	110.3	144.2	165.8	183.0	212.3	74.1	54.8
Heavy precipitation days (days)	-3.4	-1.1	0.4	3.9	5.8	7.9	9.2	11.7	12.6	4.1	3.1
Very heavy precipitation days (days)	-0.5	0.0	0.3	1.4	2.2	3.1	3.5	4.2	5.5	1.5	1.1
Very wet days (mm)	-25.2	-5.4	4.3	55.0	91.8	119.7	146.7	172.2	222.7	61.1	45.8
Extremely wet days (mm)	-20.7	-3.5	-0.1	26.3	41.2	64.6	75.2	98.7	134.9	30.8	25.2
Days above 25 mm (days)	-0.6	-0.1	0.0	0.6	0.9	1.3	1.6	1.9	2.0	0.6	0.5
Max 1-day precipitation (mm)	-3.6	-1.7	-0.4	3.6	6.1	9.6	11.1	14.1	16.7	4.1	4.0
Max 5-day precipitation (mm)	-10.5	-2.4	-1.1	8.3	13.1	17.8	19.7	22.0	23.9	8.5	6.7
Simple daily intensity index (mm/day)	-0.2	0.0	0.1	0.4	0.7	1.0	1.0	1.1	1.5	0.5	0.3
Summer days (days)	5.2	15.2	19.2	45.3	59.1	69.3	75.9	82.7	83.1	44.5	19.6
Cool nights (% of days)	-10.3	-10.1	-9.9	-8.9	-6.9	-5.5	-4.4	-2.6	-1.8	-8.2	1.9
Warm nights (% of days)	2.1	5.1	6.9	18.4	30.7	37.8	44.6	54.8	56.0	21.1	13.0
Min Tmin (°C)	0.0	1.7	2.3	6.5	9.3	10.7	11.2	15.0	16.1	6.6	3.4
Max Tmin (°C)	-0.3	0.8	1.1	3.2	4.2	5.6	6.1	7.2	7.8	3.1	1.7
Tropical nights (days)	0.7	2.6	3.5	15.5	28.6	44.0	47.6	66.8	72.3	20.0	16.2
Cool days (% of days)	-10.4	-10.1	-10.0	-8.8	-7.1	-5.5	-4.9	-3.3	-2.3	-8.2	1.8
Warm days (% of days)	1.7	5.4	6.3	20.6	29.2	39.8	43.9	52.6	54.7	21.8	12.7
Min Tmax (°C)	0.4	1.6	2.2	5.1	7.2	8.6	9.3	11.1	11.6	5.3	2.5
Max Tmax (°C)	-0.1	1.1	1.5	3.7	5.8	6.8	7.4	10.0	10.7	4.1	2.2
Warm spell duration indicator (days)	2.6	8.0	9.5	38.2	67.9	107.3	127.1	170.7	186.4	49.4	40.1

Table 46: Projected Changes in Total Potential Evapotranspiration in the 2050s for the South Bruce Study Area

Statistic	Jan	Feb	Mar	Apr	May	Jun	Jul	Aug	Sep	Oct	Nov	Dec	Annual
Minimum	-3.5%	-1.0%	0.7%	-1.0%	-0.2%	-0.2%	-0.2%	0.6%	1.8%	-0.9%	-0.3%	0.3%	3.8%
10%	8.6%	7.6%	5.6%	3.7%	4.0%	3.9%	3.6%	4.0%	4.5%	4.4%	4.3%	6.9%	7.4%
25%	14.0%	11.9%	8.9%	6.4%	5.3%	5.1%	5.1%	5.8%	7.2%	8.3%	7.0%	10.2%	9.8%
50%	19.5%	18.7%	14.1%	9.7%	8.1%	7.2%	7.7%	8.7%	10.1%	10.9%	10.6%	15.2%	13.1%
75%	26.0%	29.6%	21.3%	12.9%	10.8%	9.9%	11.2%	12.0%	13.4%	14.2%	14.3%	21.0%	16.4%
90%	35.1%	43.2%	29.7%	17.3%	14.0%	12.3%	12.9%	14.2%	15.3%	17.0%	19.3%	26.3%	18.8%
95%	40.9%	47.8%	40.1%	20.8%	15.7%	13.5%	14.3%	15.0%	16.5%	18.7%	21.9%	29.5%	19.9%
99%	47.1%	58.2%	59.2%	23.5%	17.3%	14.7%	17.7%	19.6%	20.0%	21.7%	24.6%	31.2%	21.4%
Maximum	51.0%	66.0%	70.3%	23.9%	17.9%	16.6%	19.0%	20.2%	23.5%	22.0%	25.4%	31.5%	22.1%
Mean	20.6%	22.2%	16.9%	10.1%	8.4%	7.7%	8.1%	9.0%	10.2%	10.8%	11.1%	15.8%	13.0%
Standard Deviation	10.6%	13.8%	12.0%	5.3%	3.9%	3.3%	3.9%	4.1%	4.2%	4.8%	5.6%	7.4%	4.4%

Table 47: Projected Changes in Total Potential Evapotranspiration in the 2080s for the South Bruce Study Area

Statistic	Jan	Feb	Mar	Apr	May	Jun	Jul	Aug	Sep	Oct	Nov	Dec	Annual
Minimum	0.7%	1.7%	-3.8%	-2.2%	-3.6%	-1.9%	-3.4%	-0.9%	0.3%	0.2%	-3.6%	-1.1%	1.7%
10%	8.8%	8.8%	6.9%	3.5%	3.4%	2.6%	2.7%	2.9%	3.4%	3.6%	4.9%	7.0%	6.8%
25%	15.2%	15.6%	10.8%	7.7%	5.9%	5.2%	5.3%	5.3%	7.0%	7.1%	8.9%	10.6%	10.0%
50%	24.2%	25.2%	17.7%	13.1%	10.0%	8.3%	9.4%	9.6%	12.4%	13.8%	14.0%	18.4%	14.8%
75%	35.8%	36.6%	27.4%	18.2%	14.8%	14.2%	14.3%	15.8%	17.5%	18.8%	20.4%	25.9%	20.4%
90%	46.9%	53.4%	38.4%	22.7%	19.7%	17.2%	17.6%	20.0%	23.4%	25.2%	24.3%	34.0%	26.4%
95%	55.9%	63.3%	53.3%	25.7%	21.9%	19.7%	20.1%	23.4%	27.3%	28.9%	26.1%	37.0%	28.7%
99%	60.2%	87.2%	74.1%	27.6%	25.3%	24.0%	29.0%	32.0%	32.5%	35.6%	31.3%	44.5%	32.4%
Maximum	60.5%	90.2%	80.3%	33.5%	27.3%	27.1%	33.0%	35.2%	35.5%	37.1%	32.5%	45.1%	34.3%
Mean	26.2%	28.8%	20.9%	13.0%	10.5%	9.6%	10.1%	11.2%	13.1%	13.9%	14.6%	19.1%	15.7%
Standard Deviation	14.5%	18.7%	15.0%	7.2%	6.4%	6.0%	6.6%	7.3%	7.8%	8.3%	7.6%	10.6%	7.4%

4.5.4 Drought Index

The drought index was estimated using the standard precipitation and evapotranspiration index (SPEI) of Vicente-Serrano et al. (2010), which is based on the standard precipitation index described in WMO (2012). This method illustrates the number of standard deviations that monthly net precipitation (precipitation less evapotranspiration) is from the median. By using net precipitation, both precipitation and temperature influence the drought index instead of only precipitation. The SPEI was calculated on a monthly timescale using a 12-month calculation interval which accounts for available water deficit in a 12-month rolling window (see Appendix A.3.6.4). Due to the method of calculation, aggregated annual values are not meaningful; therefore, the focus of the results is on the monthly distribution of SPEI. The distribution of projected changes in SPEI for the multi-model ensemble is shown for the 2050s and 2080s future periods in Table 48 and Table 49.

Table 48: Projected Changes in SPEI in the 2050s for the South Bruce Study Area

Month	Min	10%	25%	50%	75%	90%	Max	Mean	Std. Dev.
January	-32.8%	-5.1%	9.1%	26.2%	41.8%	56.6%	98.2%	26.4%	24.8%
February	-90.7%	-30.5%	-9.1%	8.4%	28.5%	51.7%	84.5%	8.2%	33.7%
March	-126.8%	-58.7%	-35.5%	-13.9%	14.2%	37.6%	68.4%	-12.2%	39.8%
April	-149.7%	-62.7%	-30.6%	-7.8%	15.1%	33.0%	75.9%	-12.2%	43.1%
May	-90.6%	-54.2%	-28.8%	-11.9%	9.7%	34.7%	85.2%	-9.5%	33.5%
June	-117.5%	-66.7%	-46.2%	-23.2%	11.1%	34.4%	60.0%	-20.0%	39.4%
July	-163.3%	-104.2%	-72.7%	-36.8%	-8.0%	14.1%	46.5%	-41.9%	44.5%
August	-159.1%	-100.0%	-69.0%	-39.5%	-11.4%	6.9%	51.7%	-41.9%	42.1%
September	-84.2%	-54.5%	-37.0%	-10.0%	9.8%	24.4%	55.5%	-12.4%	29.5%
October	-66.2%	-33.2%	-16.9%	3.4%	28.1%	50.8%	100.7%	5.8%	32.3%
November	-62.9%	-17.2%	-5.0%	13.2%	47.4%	72.4%	106.3%	20.1%	34.4%
December	-43.5%	-13.4%	11.3%	35.6%	60.2%	79.3%	146.6%	36.8%	38.6%

Table 49: Projected Changes in SPEI in the 2080s for the South Bruce Study Area

Month	Min	10%	25%	50%	75%	90%	Max	Mean	Std. Dev.
January	-44.8%	-14.9%	3.2%	26.8%	49.3%	66.3%	100.7%	27.3%	31.4%
February	-88.8%	-42.2%	-21.9%	-4.0%	11.2%	39.0%	115.7%	-3.4%	34.3%
March	-203.0%	-69.2%	-48.5%	-23.2%	1.3%	14.3%	49.2%	-29.1%	43.2%
April	-103.7%	-69.4%	-34.2%	-6.5%	11.5%	34.8%	133.0%	-10.8%	40.3%
May	-97.2%	-53.1%	-35.8%	-4.6%	19.7%	33.3%	100.7%	-6.9%	37.3%
June	-153.6%	-80.5%	-53.1%	-18.5%	11.0%	35.8%	63.0%	-23.3%	46.3%
July	-204.4%	-143.4%	-94.2%	-43.1%	-4.9%	19.4%	69.8%	-52.4%	62.4%
August	-170.8%	-135.9%	-82.3%	-49.2%	-18.4%	3.8%	37.5%	-55.6%	49.7%
September	-138.4%	-80.4%	-49.5%	-23.7%	2.7%	24.0%	84.0%	-24.9%	41.1%
October	-72.5%	-41.1%	-22.2%	-3.8%	16.5%	40.2%	77.7%	-2.8%	31.4%
November	-77.2%	-41.5%	-12.3%	9.7%	29.7%	56.3%	113.7%	8.7%	36.7%
December	-41.3%	-17.0%	5.1%	26.2%	51.7%	75.8%	115.2%	28.0%	34.2%

At the 50th percentile, the months of March to September all have projected decreases in SPEI, indicating drier conditions, while October through February show projected increases for the 2050s (Table 48). At the 50th percentile, July and August show the greatest projected decreases, corresponding to -36.8% and -39.5%, while the greatest increases are shown in the months of December and January, corresponding to 35.6% and 26.2%. For the 2080s, nearly the same months are projected to become drier and wetter as the 2050s, while the projected decreases are slightly greater and the increases are slightly smaller than the 2050s (Table 49). Although projected changes in precipitation are increasing for the summer months (Section 4.5.1), this is offset by greater increases in potential evapotranspiration (Section 4.5.3), ultimately leading to progressively drier conditions in the 2080s versus the 2050s shown here.

Previous studies have analyzed the projected changes in SPEI index across Canada using an ensemble mean of Coupled Model Intercomparison 5 (CMIP5) global climate models. In the region of the South Bruce study area, the SPEI index has been projected to decrease during summer and fall and increase during the winter and spring (Tam et al. 2019). The results shown here for the mean projected changes indicate a decrease in SPEI from spring to early fall (drier conditions), and an increase in SPEI from late fall through the winter months (wetter conditions). The projections for drier summer months agree between the two studies, thereby increasing confidence in the projections. Differences between result provided here and Tam et al. (2019) for the spring months may be due to the use of global climate models from the CMIP5 in Tam et al. (2019), which have a coarser resolution and no bias correction compared to downscaled climate models in this work. The downscaled climate models more accurately capture site conditions for temperature and potential evapotranspiration; therefore, the values provided here are more relevant for the South Bruce study area.

4.5.5 Wind Speed and Relative Humidity

Projected changes in wind speed were obtained from ECCC for an ensemble of 29 GCMs from the CMIP5 (ECCC 2018). The ECCC has provided annual summaries of mean daily wind speed, with each year summarized by the 5th, 25th, 50th, 75th, and 95th percentile. The result of which is shown in Table 50. The projected changes in windspeeds in the 2050s and 2080s range from -21.5% to 1.2% and 45.4% to 1.5%, respectively. The lowest daily mean winds speeds (5th percentile) are projected to have the greatest potential decreases, which are consistent across scenarios and time periods. The projected overall decrease in mean daily windspeeds in the future is consistent with the observed trends discussed in Section 3.5.5.

Jeong and Sushama (2019) projected changes to both mean and extreme wind speeds across Canada under RCP4.5 and RCP8.5 emission scenarios using a regional climate model. From this study it was estimated that the 50-year annual maximum daily wind speed would change between 0% to -8% for the 2071-2100 future period relative to the 1981 to 2010 baseline for the South Bruce study area. For the same time periods, the mean daily wind speed was projected to change between -4% to 4%. This range of projected changes is comparable to that from the ECCC global climate model ensemble at the 50th percentile; however, only one global climate model was used to drive the regional climate model in Jeong and Sushama (2019). Only aggregate statistics were found in the review of applicable literature to the South Bruce study area; therefore, seasonal and monthly statistics for changes in wind speed are not provided.

Table 50: Projected Changes in Mean Daily Wind Speed for the South Bruce Study Area

Time Period	Scenario	5%	25%	50%	75%	95%
2050s	RCP 2.6	-9.3%	-0.2%	-0.1%	1.2%	1.1%
	RCP 4.5	-15.4%	-6.4%	-5.7%	-1.9%	-4.7%
	RCP 8.5	-21.5%	1.0%	-0.9%	0.1%	0.0%
2080s	RCP 2.6	-11.8%	0.6%	-0.5%	1.1%	0.8%
	RCP 4.5	-32.1%	-8.4%	-7.8%	-2.3%	-4.7%
	RCP 8.5	-45.4%	1.5%	-1.6%	-0.9%	0.1%

Climate change is expected to increase levels of atmospheric humidity due to elevated temperatures which increases atmospheric moisture capacity at a theoretical rate of 7% per °C, according to the Clausius-Clapeyron relationship (CSA 2019). Observations have shown that global specific humidity has very likely increased by the 1970s, consistent with observed temperature increase (Hartmann et al. 2013). Increased atmospheric moisture content due to global warming can lead to more intense precipitation events (Bush and Lemmen 2019). Projections of relative humidity in the literature are not available for the South Bruce study area. To provide an estimate of how relative humidity may change in the future, the changes were calculated using the approximations of Alduchov and Eskridge (1996) for the multi-model ensemble of climate projections (see Appendix A.3.6.5).

Annual and monthly percentage changes in relative humidity from the model baseline to the future periods were calculated and presented for the 2050s and 2080s future time periods in Table 51 and Table 52, respectively. Annual average relative humidity is projected to increase by 1.1% in the 2050s and 1.3% in the 2080s at the 50th percentile, indicating an overall upward trajectory. This annual increase is relatively low; however, seasonal variation can be analysed in the form of monthly projected changes to provide more detail.

In the 2050s, average relative humidity in the months of April to November is projected to change by less than 1%, while all other months show a projected increase. The range of projected changes at the 50th percentile correspond to -0.5% to 4.9%, with December to February showing the greatest increase. The months with the greatest changes in relative humidity are consistent with the greatest projected changes in precipitation (Table 40 and Table 41). This is expected, as more atmospheric moisture would likely lead to greater precipitation amounts.

Even though there will likely be more moisture in the atmosphere (Kunkel et al. 2013), the saturation vapor pressure will also increase due to rising temperatures, thereby reducing the relative humidity. This is confirmed in the literature, as decreasing relative humidity trends have been found in the mid latitudes despite increases in specific humidity (Byrne and Gorman 2018). However, in the case of the South Bruce study area, increasing atmospheric moisture will likely dominate over the effect of increasing saturation vapor pressure.

Under current climate conditions, relative humidity in the afternoon (3 pm) is highest during the fall and winter months (Table 51 and Table 52), which also coincides with the greatest projected changes in relative humidity. This indicates that seasonal variation in relative humidity will be greater in the future, with greater contrast between seasons.

Table 51: Projected Changes in Relative Humidity in the 2050s for the South Bruce Study Area

Month	Min	10%	25%	50%	75%	90%	Max	Mean	Std. Dev.
January	0.2%	1.7%	3.3%	4.9%	6.7%	7.7%	11.7%	4.8%	2.3%
February	0.2%	1.4%	2.4%	4.0%	5.3%	6.7%	12.2%	4.1%	2.2%
March	-5.8%	-0.8%	0.3%	1.6%	3.0%	4.4%	9.1%	1.6%	2.3%
April	-4.6%	-2.4%	-1.3%	-0.4%	1.0%	2.2%	5.7%	-0.2%	1.8%
May	-5.7%	-2.2%	-0.5%	0.4%	1.4%	2.7%	6.1%	0.3%	1.9%
June	-5.3%	-3.2%	-1.7%	0.5%	1.7%	2.7%	6.1%	0.1%	2.3%
July	-5.9%	-3.2%	-1.5%	-0.2%	0.9%	1.6%	3.1%	-0.5%	1.9%
August	-5.9%	-3.4%	-1.9%	-0.5%	0.4%	0.8%	2.9%	-0.9%	1.7%
September	-6.3%	-3.1%	-1.9%	-0.3%	0.5%	1.2%	2.6%	-0.7%	1.7%
October	-5.2%	-2.5%	-1.8%	-0.4%	0.7%	1.3%	2.7%	-0.6%	1.6%
November	-3.3%	-1.6%	-0.7%	0.3%	1.5%	2.3%	5.3%	0.4%	1.6%
December	-0.5%	0.9%	1.8%	3.0%	4.8%	5.9%	8.3%	3.3%	1.9%
Annual	-2.3%	-0.3%	0.4%	1.1%	1.8%	2.4%	3.3%	1.0%	1.1%

Table 52: Projected Changes in Relative Humidity in the 2080s for the South Bruce Study Area

Month	Min	10%	25%	50%	75%	90%	Max	Mean	Std. Dev.
January	-0.1%	2.2%	3.8%	6.1%	8.6%	10.2%	16.5%	6.2%	3.1%
February	-0.5%	2.0%	3.2%	5.2%	7.5%	10.7%	14.7%	5.7%	3.2%
March	-5.8%	-0.9%	0.3%	1.8%	3.9%	6.0%	11.9%	2.2%	2.9%
April	-6.0%	-2.8%	-1.3%	0.0%	1.4%	3.0%	8.6%	0.0%	2.2%
May	-7.8%	-2.7%	-0.9%	0.6%	1.9%	3.5%	9.2%	0.5%	2.5%
June	-6.6%	-3.8%	-1.4%	0.7%	2.0%	3.0%	5.7%	0.1%	2.7%
July	-7.7%	-3.8%	-1.8%	-0.1%	1.0%	1.7%	3.9%	-0.6%	2.2%
August	-5.8%	-3.6%	-2.4%	-0.5%	0.5%	1.3%	3.9%	-0.9%	1.9%
September	-5.9%	-3.6%	-2.3%	-0.5%	0.5%	1.5%	3.6%	-0.9%	2.0%
October	-5.4%	-3.2%	-1.7%	-0.2%	0.8%	1.5%	2.4%	-0.6%	1.8%
November	-3.3%	-1.6%	-0.7%	0.6%	1.6%	2.5%	5.0%	0.5%	1.7%
December	-1.0%	0.9%	2.2%	3.7%	5.7%	7.9%	10.6%	4.1%	2.5%
Annual	-2.0%	-0.2%	0.5%	1.3%	2.4%	3.3%	5.7%	1.4%	1.4%

5. QUALITATIVE CLIMATE ASSESSMENT BEYOND THE YEAR 2100

The daily future climate projections used in this report are only available to the year 2100. Future climate assessments beyond 2100 can only be made qualitatively based on the best available information from literature and an understanding of climate change trends up to 2100. Extended concentration pathways (ECPs) provide qualitative estimates of future temperature on a global scale up to the year 2500. It is generally accepted that with increased temperature (through increased radiative forcing), mean global precipitation will also increase by an estimated 1-3% per degree Celsius increase in temperature (IPCC 2013). With this information, the ECP projections can be used to qualitatively inform precipitation trends past 2100 for the site.

The ECP global projections indicate that beyond 2100, the radiative forcing driven by greenhouse gas emissions will gradually slow down and stabilize (Figure 19). The ECP 8.5 scenario results in increasing radiative forcing which slows down and stabilizes by the year 2250. The ECP 4.5 scenario results in stabilized (no change) radiative forcing, while the ECP 3-PD shows gradually decreasing radiative forcing levels. As a conservative measure, projections are provided based on the ECP 8.5 scenario.

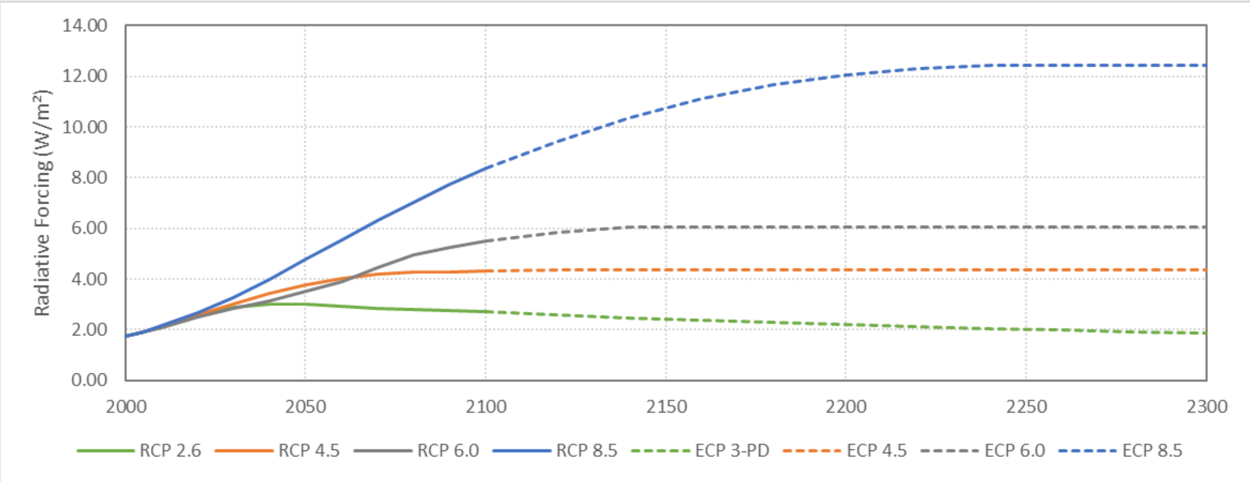

Figure 19: Illustration of RCP and ECP Scenario Radiative Forcing from 2000 to 2300

Two future climate periods (2050s and 2080s) have been used in this report, which allows for the trajectory of the projected changes to be estimated beyond these periods. Comparison of the percentage differences between the 2050s and 2080s time periods shows that on average across durations and return periods:

- Daily and multi-day IDF projected changes are 1.8%
- PMP projected changes are 10.8%
- Rainfall on snow projected changes are 3.5%
- Peak snowpack accumulation projected changes are -10.4%.

This indicates that the overall direction of change for extreme rainfall events is increasing and peak snowpack accumulation is decreasing between the 2050s and 2080s time periods. Based on the ECP 8.5 scenario and the relationship between radiative forcing, temperature and precipitation, these changes may continue well into the future but may slow down and stabilize. There is a delay in the response of global temperatures to radiative forcing; therefore, changes in temperature and precipitation may continue past 2250 when the radiative forcing stabilizes. Due to the large range of radiative forcing in the ECP scenarios, there exists a large amount of uncertainty on how climate will change globally beyond the year 2100, and even more so at the scale of the Project site. Updated climate assessments should be made throughout the project lifecycle to account for updated climate models and scenarios.

By considering the trends in temperature and precipitation beyond 2100 and comparing the estimates for the 2050s and 2080s, it is likely that monthly temperature values will increase beyond 2100. The winter and spring monthly total precipitation may continue to increase, while in the summer months there is less consensus on the continued direction of change. The increasing temperatures will likely result in a continual increase in temperature extremes, while the precipitation extreme indices do not show a clear direction of change between the 2050s and 2080s. Potential evapotranspiration rates may be expected to increase across all months, resulting in drier conditions in April through November and wetter conditions from December through March as indicated by the drought index. The lowest wind speeds (5^{th} percentile) may continue to decrease with little change to the highest wind speeds (95th percentile), while all months show a continued decrease in relative humidity at the 50^{th} percentile. Overall, the climate may continue to become hotter at the South Bruce study area, with wetter conditions in the winter months and drier conditions in all other seasons.

6. UNCERTAINTY OF CLIMATE CHANGE PROJECTIONS FOR PMP, IDF, AND ADDITIONAL CLIMATE VARIABLES

This assessment was based on the current available climate science. The nature of the work undertaken is stochastic with substantial inherent uncertainty around any given data points. The uncertainty associated with any projections or forecasts is increased with a longer time horizon into the future for the projected period. The projections are subject to change with future developments; therefore, this study should be updated, as new climate science is developed and after the release of the latest assessment report by the IPCC. The approach to reduce levels of uncertainty with the future climate projections for this study is based on using multiple projections from multiple models and scenarios (multi-model ensemble approach), as recommended by the IPCC (IPCC 2013), and discussed in Section 4.1. Overall, there is less variability and uncertainty (measured as the agreement within the ensemble or range of projected anomalies) during the 2050s, with variability/uncertainty increasing during the 2080s. In addition, precipitation projections typically have larger uncertainty than temperature projections due to the challenge of capturing precipitation in the climate models (temperature is better understood). Therefore, the level of uncertainty in this assessment, focused on PMP and IDF estimates, is generally higher than that of temperature.

The estimation of PMP (current and future projected) requires moisture content and other variables, which were not readily available from the climate datasets. In order to calculate the moisture content for the model result datasets that do not provide these variables, Golder used the daily minimum temperature projections as a proxy for the dew point temperature and the surface specific humidity as a proxy for the precipitable water. Similar proxies were used to describe additional variables where they were not available from the climate datasets. The selection of proxy data to fill gaps in the climatic datasets added uncertainty around the estimation of PMPs and additional climate variables.

The assessment of additional climate variables carries the same uncertainty inherited from the climate projections; there are also additional uncertainties to consider. The Hargreaves method used to estimate potential evapotranspiration is one of many that are available; however, it was selected partly because it is only dependent on readily available temperature variables as opposed to wind speed and relative humidity. In this report it was shown that relative humidity and wind speed may also change in the future. Therefore, this method does not capture the effects of these changes and adds a level of uncertainty in the future potential evapotranspiration estimates. This uncertainty should also be noted for the drought index, as potential evapotranspiration was used in its calculation. The qualitative analyses for relative humidity and wind speed also carry additional uncertainty, as the available data were either taken from the literature, or from data sources that may not be as applicable to the site compared to the downscaled multi-model ensemble used for precipitation and temperature variables.

7. USING THE RESULTS OF THIS ASSESSMENT IN DECISION MAKING

To better describe the uncertainty around future projections, the estimated percent changes to precipitation (PMP and IDF curves) are described in terms of percentiles, allowing for different levels of acceptable risk. The projections at 50^{th} percentile represent the ensemble median.

When considering the impact of future projected climate on current design parameters, the level of acceptable risk can be selected by using the desired percentile. Selection of future projections for climate change risk assessment should be based on the balance between the extra investment and consequential risks.

Therefore, it is recommended the results in this report be used as follows:

- For the ensemble mean projections, the projections at 50^{th} percentile should be selected as the starting point, which NWMO should consider regarding risk assessment and undertaking planning and engineering design applications of infrastructure in the future.
- To relate the Project phases to the climate assessment periods, the distribution of the projections should be considered by examining the percentiles from the multi-model ensemble. For screening purposes, the 50^{th} percentile may be used from the mid-century climate period for the site characterization, preparation, and construction phase, and the end of century climate period for the operational project phase. For Project phases beyond 2100, a high percentile may be used from the end-of-century climate assessment period as a screening value. Other percentiles may be used to relate to the Project phases. For example, if conservatism is not required, then a lower percentile from the mid-century climate period could be used for the site characterization, preparation, and construction phase.
- For critical infrastructure, selection of future projections at higher percentile and higher return periods should be considered. For example, for critical infrastructure whose failure is considered unacceptable, a 95th percentile could be considered over the typical 50th percentile. With regards to the return period, the storm associated with a return period sufficiently larger than the planning horizon for the infrastructure should be used. In the case of the Project, the decommissioning phase is planned to conclude in 2180, which is approximately 160 years from the publication of this report. Therefore, a return period that is at least larger than 160 years should be used for future extreme rainfall projections. For critical infrastructure it may be more appropriate to select the 1000 or 2000-year return period.
- Projected changes in the future climate assessments (Section 4) may be applied to the corresponding current climate baseline assessments (Section 3). Percentage changes should be multiplied by the corresponding current climate baseline values, while absolute changes may be added to the current climate baseline values. Applying the projected changes in this way help to reduce potential bias in the future climate projections of the multi-model ensemble.
- Where several results overlap specific parameter based on different methods (for instance, the PMP estimates under current climate conditions using the Transposition and Hershfield methods), this report recommends the most conservative method (i.e., the one that generates the largest future rainfall depth) be used.

- The Hargreaves method used to estimate potential evapotranspiration has been shown to perform well at a high-level for the South Bruce study area. However, if a more comprehensive assessment of potential evapotranspiration is needed, then the method should be checked against other methods that use additional climate variables to confirm the validity of this approach. For example, Penman-Monteith based methods incorporate the effects of wind speed and relative humidity which are not included here. Another example may be the incorporation of ice and snow sublimation processes in the winter months.
- The daily future timeseries provided in Appendix C may be used for additional studies at the South Bruce study area. Bias correction of precipitation using the current climate baseline dataset for the area provides future projections that may be used in climate change impact models. A total of 136 projections (one for each member of the multi-model ensemble) is provided for each climate variable. It is recommended all members of the multi-model ensemble be used. If this is not possible, a subset of scenarios should be selected to cover the range of uncertainty in the climate change impact model (see Appendix C for details).
- The qualitative values provided for wind speed and relative humidity should be used with an understanding that they have a higher degree of uncertainty due to lack of data availability and the need for alternative sources to represent the South Bruce study area.
- If a risk is identified for an infrastructure component for the area, a more refined analysis should be performed to further define the risks using the projections at different percentile levels.

8. CONCLUSIONS AND RECOMMENDATIONS

The baseline assessment of the South Bruce study area was completed using publicly available data in the region from ECCC. The current climate baseline dataset was developed using the Wroxeter (6129660) climate station, as it was found to be the most representative station for the study area based on the established assessment criteria (Section 3.1.1). Infilling was performed using the ERA5 reanalysis dataset which was found to adequately capture seasonal and interannual variation in observed regional precipitation and temperature patterns (Section 3.1.2). The Mount Forest (AUT) IDF engineering dataset was used to represent sub-daily rainfall, as it was found to be the most applicable dataset for the study area of the available sub-daily rainfall stations in the region (Section 3.1.3).

Using this baseline dataset, the 24-hours 100-year return period precipitation was estimated at 142.2 mm and the 500-year return period at 174.4 mm from the interpolated IDF curve at the South Bruce study area (Section 3.2.3). The values of IDF estimates were compared with literature sources and found in agreement with previous studies.

Using this baseline dataset, the annual maximum precipitation series was used to calculate PMP using the Hershfield statistical method. The calculation yielded a 1-day value of 405.2 mm, and 457.9 mm for 24-hours. The 2- and 3- day PMP were estimated to be the same as the 1 day due to low variability in the observed 1 to 3-day data, suggesting that most extreme events in the South Bruce study area are associated with relatively short durations of rainfall. If the 2 and 3-day PMP values are key to the future design, further investigation using other methods is recommended. Using the historical observed storms from climate stations in the region, the observed values were transposed to the study area and maximized to develop composite DAD curves (Section 3.3.3). The DAD curves for an area equal to that of the Saugeen watershed (4,025 km^2) gave lower estimates of PMP than the statistical method corresponding to 240.9 mm and 272.2 mm for 1-day and 24-hour durations (Section 3.3.4). Due to the difference in results between methods, it is recommended a conservative approach be taken. Therefore, the greater value for a given duration should be used. The values of PMP estimates by the Hershfield method were compared with literature sources and found in agreement with previous studies.

An analysis of combined rainfall and snowmelt was performed using IDF statistics (Section 3.4). It was found that the 100-year 1-day event corresponded to 85.3 mm, which was less than the same duration and return period for extreme rainfall. This indicates that extreme rainfall events are predominant over the combined rainfall and snowmelt events based on the analysis of the historical observations. However, for longer durations combined rainfall and snowmelt should be considered for designs concerned with volumetric capacity of runoff. The 1-day snowpack was found to be 138.1 mm for a 2-year event and 509.1 mm for a 2000-year event based on modelled snowpack for the current climate baseline period.

Analysis of the additional climate variables for the baseline climate period (1979 to 2019) at the South Bruce study area showed that:

- The months of September to November are typically the wettest, while the months of February and March are typically the driest, representing the average climate conditions over the observed record considered. The wettest month on record was in September 1986 with 251.7 mm (consistent with the average climate conditions) and the driest month on record was in July 1989 with 2.0 mm (outside of average climate conditions). The warmest month on average is the month of July with a mean temperature of 20°C, and the coldest is the month of January with a mean temperature of -6.1°C. The coldest monthly temperature occurred in February 2015 with a mean monthly temperature of -13.7°C, while the warmest monthly temperature occurred in July 2011 with a mean monthly temperature of 22.2°C.
- No statistically significant precipitation related trends were found in the WMO climate indices. Significant temperature related trends detected indicate that days with low temperature are becoming less frequent (fewer frost days, cold nights, and cool days, increasing minimum temperatures), with more warm days and nights.
- The greatest monthly potential evapotranspiration rates were found in July at 136.6 mm on average, with most of the annual potential evapotranspiration occurring between May to August.
- The minimum value of the monthly drought index has occurred in March; however, this event does not exceed the "extremely dry" criteria for the drought index classification. The wettest months were found to correspond with spring rainfall in April and March, as well as fall storms in September.
- Baseline wind speed and relative humidity values were obtained from the WIARTON A climate station, as this station was deemed to be the closest station with climate normal that includes wind speed and relative humidity. The geographical siting of this station is not ideal to represent the site conditions, due to differences in latitude, elevation, and closer distance to Lake Huron compared to the South Bruce study area. The information provided for baseline wind speed and relative humidity should therefore be interpreted qualitatively.

Future projected climate results are presented for the range of models within the "ensemble" and expressed in terms of percentiles. When considering the impact of future projected climate on current design parameters, the level of acceptable risk can be selected by using the desired percentile.

The trends in future climate extremes follow a pathway that is consistent with the trends in climate normals for both the current and future climate projections. From the median (50th percentile) values for the 2050s and 2080s, the projected future climate extremes are indicating a future that is likely to be wetter. The 1-day PMP values are projected to increase by 10.6% and 20.1% in the 2050s and 2080s, respectively, at the 50th percentile (Table 34 and Table 35), relative to the model baseline from the GCM ensemble. The 1-day rainfall events are projected to increase by 7.5% to 18.9% in the 2050s (Table 32) and 9.3% to 15.3% in the 2080s across return periods (Table 33) at the 50th percentile, relative to the model baseline from the GCM ensemble. It was found that the longest durations of 50-days or greater show a smaller percentage increase compared to the shorter durations of 10-days or less, and that the highest percentage changes for a given duration are for higher return period events. This means that climate change will likely have the greatest influence on extreme precipitation events.

Analysis of future climate projections for the additional climate variables showed that:

- Projected changes in temperature ranged from 2.0 to 2.9°C in the 2050s and 3.1 to 4.0°C in the 2080s at the 50th percentile. In the 2050s monthly total precipitation is projected to increase for all months except August at the 50th percentile, ranging from -2.7% to 12.5%. In the 2080s the range of projected changes is slightly larger from -2.3% to 16.2% across calendar months. Bias correction was performed for precipitation in order to provide daily future timeseries of rain, snow, snow depth for the South Bruce study area. The methodology applied was found to greatly improve the estimation of wet and dry day frequencies as well as precipitation extremes. This approach allows for these daily timeseries to be used in further assessments. All precipitation related projection in the set of additional climate variables carry a considerable amount of uncertainty, with little agreement on the direction of change (increase or decrease). Therefore, this uncertainty must be accounted for when using the projected values.
- The future projected changes in WMO indices indicate that future precipitation is expected to yield more frequent intense rainfall events, and greater precipitation amounts annually. Temperature based WMO indices indicate that fewer freezing and icing days are projected along with a longer growing season, more summer days, and greater extreme minimum and maximum daily temperatures.
- Potential evapotranspiration was projected to increase across over 90% of the climate projections using the multi-model ensemble. The pattern of projected changes was similar to that of monthly mean temperature, likely due to the Hargreaves method used for calculation.
- The analysis of the drought index revealed that the period of late fall to mid spring will become wetter in the future while the summer months are projected to become drier. Overall, in the 2080s conditions are expected to continue to become drier and wetter in the same months compared to the 2050s.
- The qualitative assessment of wind speeds at the South Bruce study area imply that they are generally expected to decrease based on available datasets and literature. Relative humidity is also generally expected to decrease due to rising temperatures despite more moisture in the atmosphere due to climate change.

Qualitative assessment of climate change beyond the year 2100 was made using the projections for the 2050s and 2080s time periods and the global ECP scenarios. Overall, extreme precipitation statistics (IDF and PMP) are likely to increase beyond the year 2100 based on the comparison of projections between the 2050s and 2080s time periods. These changes may continue well into the future, as the ECP 8.5 scenario shows increased radiative forcing until the year 2250. It is recommended additional climate assessments be made throughout the project life cycle, so that updated climate projections and scenarios are used to reduce uncertainty associated with projections made far into the future.

The nature of the study has substantial level of inherent uncertainty. The approach to address levels of uncertainty around future climate projections in this study relies on the multi-model ensemble approach recommended by IPCC. Furthermore, the uncertainty associated with any projections is increased with the far future of the projected period, resulting into less variability and uncertainty during the 2050s, when compared to the 2080s. To acknowledge the uncertainty around future projections, the estimate percent changes to precipitation (PMP and IDF curves) is described in terms of percentiles, allowing for different levels of acceptable risk. When considering the impact of future projected climate on current design parameters, the level of acceptable risk can be selected by using the desired percentile. Selection of future projections for climate change risk assessment should be based on the balance between the extra investment and consequential risks.

Based on Golder’s experience in climate change projections, the proposed approaches as described in this study are considered best guidance for the industry.

REFERENCES

Alduchov, O. A. and Eskridge, R. E. 1996. Improved Magnus' Form Approximation of Saturation Vapor Pressure. J. Appl. Meteor., 35, 601–609.

AMEC. 2011. Maximum Flood Hazard Assessment. Nuclear Waste Management Organization Report DGR-TR-2011-35. Toronto, Canada. Available at https://archive.opg.com/pdf_archive/Deep%20Geologic%20Repository%20Documents/DGR%20Submission%20Documents/D175_26.Maximum-Flood-Hazard-Assessment.pdf.

Anandhi, A., Allan, F., Pierson, D.C., Schneiderman, E.M., Zion, M.S., Lounsbury, D. and Matonse, A.H. 2011. Examination of change factor methodologies for climate change impact assessment. Water Resources Research, 47(3). doi: 10.1029/2010WR009104.

Brown, D.W., Moin, S.M.A. and Nicolson, M.L. 1996. A Comparison of Flooding in Michigan and Ontario: 'Soft' Data to Support 'Soft' Water Management Approaches. Canadian Water Resources Journal, 22(2):125-139.

Bush, E. and Lemmen, D.S., editors. 2019. Canada's Changing Climate Report. Government of Canada, Ottawa, Ontario. 444p. Available at https://www.nrcan.gc.ca/sites/www.nrcan.gc.ca/files/energy/Climate-change/pdf/CCCR_FULLREPORT-EN-FINAL.pdf.

Byrne, M.P. and Gorman P.A. 2018. Trends in Continental Temperature and Humidity Directly Linked to Ocean Warming. Proceedings of the National Academy of Sciences, 115(19): 4863-4868. doi: 10.1073/pnas.1722312115.

Canadian Standards Association (CSA). 2019. Draft Standard Plus 4013:19. Technical Guide Development, Interpretation and Use of Rainfall Intensity-Duration-Frequency (IDF) Information: Guideline for Canadian Water Resources Practitioners.

Collins, M., Knutti, R., Arblaster, J., Dufresne, J.-L., Fichefet, T., Friedlingstein, P., Gao, X., Gutowski, W.J., Johns, T., Krinner, G., Shongwe, M., Tebaldi, C., Weaver, A.J. and Wehner, M. 2013. Long-term Climate Change: Projections, Commitments and Irreversibility; in Climate Change 2013: The Physical Science Basis; Contribution of Working Group I to the Fifth Assessment Report of the Intergovernmental Panel on Climate Change, (ed.) T.F. Stocker, D. Qin, G.-K. Plattner, M. Tignor, S.K. Allen, J. Boschung, A. Nauels, Y. Xia, V. Bex and P.M. Midgley; Cambridge University Press, Cambridge, United Kingdom and New York, NY, USA; p. 1029–1136.

Environment and Climate Change Canada (ECCC). 2018. Projected Surface Wind Speed Change Based on CMIP5 Multi-Model Ensembles. Government of Canada. Available at: https://open.canada.ca/data/en/dataset/e0c71149-db7a-4700-acfd-1c8f9d778354.

Environment and Climate Change Canada (ECCC). 2019a. Historical Climate Data. Available at https://climate.weather.gc.ca/historical_data/search_historic_data_e.html. Accessed May 15, 2019.

Environment and Climate Change Canada (ECCC). 2019b. Engineering Climate Datasets. Available at https://climate.weather.gc.ca/prods_servs/engineering_e.html. Accessed June 15, 2019.

Environment and Climate Change Canada (ECCC). 2020. Canadian Climate Normals. Government of Canada. Available at: https://climate.weather.gc.ca/climate_normals/.

Hargreaves, G.H. and Samani, Z.A. 1985. Reference Crop Evapotranspiration from Temperature. Applied Engineering in Agriculture 1(2):96-99. DOI: 10.13031/2013.26773.

Hartmann, D.L., Klein Tank, A.M.G., Rusticucci, M., Alexander, L.V., Brönnimann, S., Charabi, Y., Dentener, F.J., Dlugokencky, E.J., Easterling, D.R., Kaplan, A., Soden, B.J., Thorne, P.W., Wild, M. and Zhai, P.M. 2013. Observations: Atmosphere and Surface; in Climate Change 2013: The Physical Science Basis (Contribution of Working Group I to the Fifth Assessment Report of the Intergovernmental Panel on Climate Change), (ed.) T.F. Stocker, D. Qin, G.-K. Plattner, M. Tignor, S.K. Allen, J. Boschung, A. Nauels, Y. Xia, V. Bex and P.M. Midgley; Cambridge University Press, Cambridge, United Kingdom and New York, NY, USA, p. 159–254. doi:10.1017/CBO9781107415324.008

Hember, R.A., Coops, N.C. and Spittlehouse, D.L. 2017. Spatial and Temporal Variability of Potential Evapotranspiration across North American Forests. Hydrology, 4(5). doi:10.3390/hydrology4010005.

Hosking, J.R.M. and Wallis, J.R. 1997. Regional Frequency Analysis. Cambridge University Press, Cambridge, U.K.

Jeong, D. and Sushama, L. 2019. Projected Changes to Mean and Extreme Surface Wind Speeds for North America Based on Regional Climate Model Simulations. Atmosphere, 10(9):497-516. doi: 10.3390/atmos10090497.

Louie, P. Y. T. and Hogg, W. D. 1980. Extreme Value Estimates of Snowmelt. Proceedings of Canadian Hydrology Symposium 80 (Toronto, ON: 64-78 National Research Council Canada).

Ontario Climate Data Portal (OCDP). 2020. High Resolution Climate Change Projections for Ontario. Laboratory of Mathematical Parallel Systems. York University. Available at: http://lamps.math.yorku.ca/OntarioClimate/index_app_introduction.htm#/.

Ontario Ministry of Natural Resources (OMNR). 2006. PMP for Ontario. Prepared by IBI Group. December 2006.

Pysklywec, D.W., Davar, K.S. and Bray, D.I. 1968. Snowmelt at an Index Plot. Water Resource. 4(5), 937-946.

Tam, B.Y., Szeto, K., Bonsal, B., Flato, G., Cannon, A.J. and Robin, R. CMIP5 Drought Projections in Canada Based on the Standardized Precipitation Evapotranspiration Index. Canadian Water Resources Journal, 44(1): 90-107. doi: 10.1080/07011784.2018.1537812.

Torregrossa, M. 2019. What Caused Foot of Rain in Great Flood 30 Years Ago Today. MLive Michigan, April 2nd, 2019. Retrieved from https://www.mlive.com/weather/2016/09/what_caused_foot_of_rain_in_gr.html.

Vicente-Serrano, S.M., Begueria, S. and Lopez-Moreno, J.I. 2010. A Multiscalar Drought Index Sensitive to Global Warming: The Standardized Precipitation Evapotranspiration Index. Journal of Climate, 23(7):1696-1718. doi: 10.1175/2009JCLI2909.1.

Wan, H., Wang, X.L. and Swail, V.R. 2010. Homogenization and Trend Analysis of Near-Surface Wind Speeds. Journal of Climate, 23(5):1209-1225. doi: 10.1175/2009JCLI3200.1.

Wood. 2019. Climate Change Impacts Review and Method Development. NWMO-TR-2019-05. Toronto, Canada. Retrieved from http://rms.nwmo.ca/Sites/APM/Reports/NWMO-TR-2019-05.pdf.

World Meteorological Organization (WMO). 2009a. Manual on Estimation of Probable Maximum Precipitation (PMP). World Meteorological Organization (WMO). WMO-No. 1045.

World Meteorological Organization (WMO). 2009b. Guidelines on Analysis of Extremes in a Changing Climate in Support of Informed Decisions for Adaptation. World Meteorological Organization (WMO). Climate Data and Monitoring WCDMP-No. 72.

World Meteorological Organization. 2012. Standardized Precipitation Index: User Guide. Washington, DC: World Meteorological Organization. Technical report: WMO No. 1090.

APPENDIX A: DETAILED METHODOLOGY

CONTENTS

Page

LIST TABLES

Page

LIST OF FIGURES

Page

A.1 INTRODUCTION

This appendix outlines in detail the PMP and IDF analyses approach and methodology applied to the South Bruce study area and follows *Climate Change Impacts Review and Method Development* (NWMO-TR-2019-05 from Wood 2019) for PMP analyses. To provide additional context to the changes in PMP and IDF, additional climate variables were analyzed for the South Bruce study area. These include annual and monthly temperature and precipitation statistics from which seasonal variation can be inferred. Derived climate variables are also provided, including WMO indices, rain and snow, snow depth, potential evapotranspiration, drought index, and qualitative information for wind speed and relative humidity. This stepwise approach combines information about the current climate conditions and publicly available projections of how the climate may change under future climate conditions to describe a range of future projections at the site of interest and represents the most recent best guidance found in literature.

Section A.2 provides the detailed methodology followed to develop a current climate observed baseline for PMPs, IDFs, and additional climate variables (Section 3), while Section A.3 outlines the methods based on the GCM ensemble to develop the projected changes in PMP, IDF, and additional climate variables in the future (Section 4).

A.2 CURRENT CLIMATE OBSERVED BASELINE DEVELOPMENT

Understanding the current climate and current climate trends is important when evaluating current design parameters and developing the percentile levels using the future climate projections. The process to develop the observed baselines for PMPs and IDFs is outlined in Figure A.1. Where available, the climate baseline is grounded in observations from local climate stations. Publicly available observations are used to establish the baseline infilled with reanalysis data (to meet data completeness requirements including only considering months and years where at least 90% of the data is available).

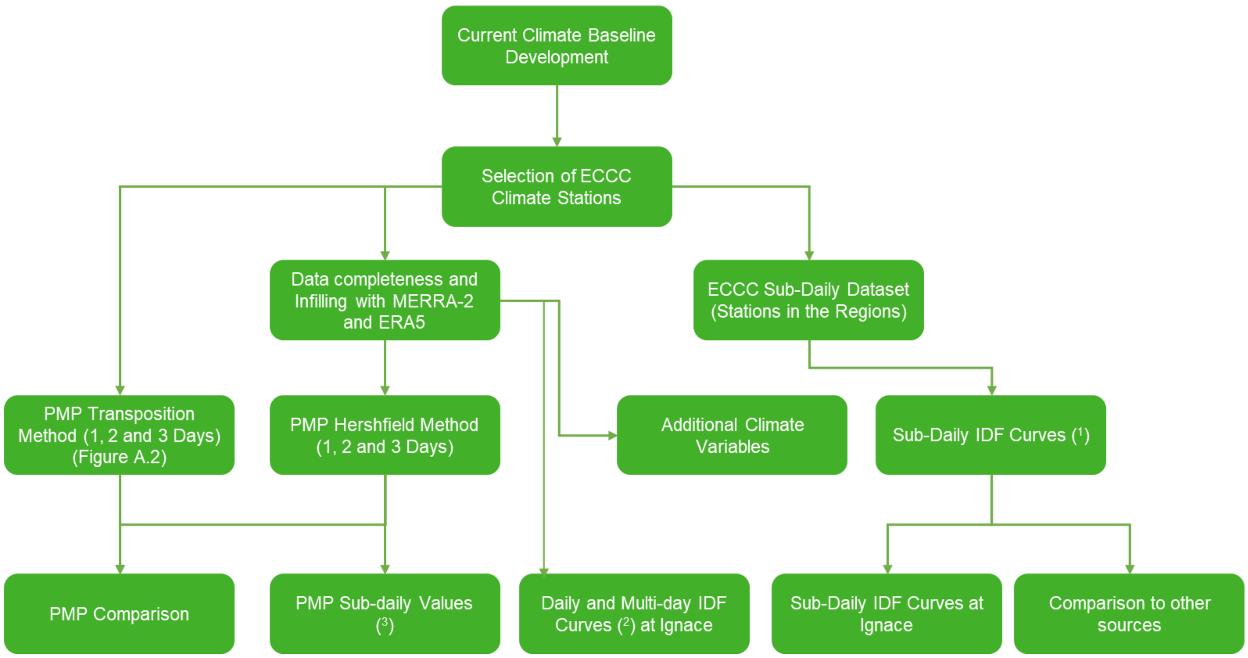

Notes:
1) IDF curves were developed for the following durations: 5, 10, 15, 30 minutes, 1, 2, 6 and 12 hours, and 2, 5, 20, 50, 100, 200, 500, 1000 and 2000 years return period.
2) IDF curves were developed for the following durations: 1, 2, 3, 4, 5, 6, 7, 10, 20, 30, 50, 75, 90, 120 days, and 2, 5, 20, 50, 100, 200, 500, 1000 and 2000 years return period.
3) Sub-daily PMP values were calculated for the following durations: 5, 10, 15, 30 minutes, 1, 2, 6, 12 and 24 hours.

Figure A.1: PMP, IDF and Additional Climate Variables Baseline Analyses Flowchart

Before infilling, the reanalysis data is compared and correlated to the available regional climate station. This step is carried out to create a current climate baseline time series and is used to evaluate PMP, IDF, and additional climate variables for the region of interest. Additional data stations from the region are screened for the study of the extreme events as well as series from the Engineering Dataset for the IDF curves (ECCC 2019). If available, the Adjusted and Homogenized Canadian Climate Data (AHCCD) are used to apply adjustments to the station observations (infilled if necessary) to account for non-climatic shifts in data, mainly due to the relocation of stations and wind undercatch correction (ECCC 2019). Wind undercatch describes the effects of wind on rain gauges that can cause underestimation of rainfall which contributes to inconsistencies in the rainfall dataset (Guo et al. 2001).

The climate station selection is based on the following selection factors to identify the station which best represents the South Bruce study area, meteorologically:

- the length of record (minimum 30 years of data);
- availability of a continuous record;
- proximity to the area of interest;
- age of observations compared to the currently accepted normal period;
- latitude;
- elevation of station;
- geographic siting; and
- monthly data availability threshold of 90% for all years. Based on simplification of WMO (1989), which recommends using the “3/5” rule, where if a month has either 3 consecutive days or 5 random days missing, then that month should not be used in establishing climate normals.

The available climate data from each station must be compared to, and pass, the selection criteria outlined above. Data from most climate stations are constrained by low numbers of observations or a limited life span for the station (data quantity), and varying data quality. Therefore, the station which matches the most selection criteria, with the first three criteria bearing the most weight, is selected. Meeting the monthly data availability is often a challenge over the desired, long observation period. When available climate observations are representative of a site but fail to meet the required data completeness, reanalysis data from the European Centre for Medium-Range Weather Forecasts (ECMWF) Re-Analysis (ERA5) or National Aeronautics and Space Administration’s (NASA’s) Modern-Era Retrospective analysis for Research and Applications (MERRA-2) is used to represent current climate or to infill the missing data.

After the station observations have been reviewed for data completeness, infilling, and any available adjustments, the PMP, IDF, and additional climate variables are calculated. The current climate observed baseline is discussed in Section 3.

A.2.1 Data Sources for Current Climate and Reanalysis

The current climate is based on available long term daily meteorological observations from climate stations near the South Bruce study area. For the South Bruce study area, the selected current climate baseline period is from 1979 through 2019. Meeting the monthly data availability is often a challenge over the desired, long observation period. The data availability is necessary to properly capture the different cycles impacting the observations (e.g., diurnal, seasonal) and avoid potential biases in the analysis of the observations (e.g., consistently missing observations during the nighttime or winter). When available climate observations are representative of a site but fail to meet the required data completeness, reanalysis data from the European Centre for Medium-Range Weather Forecasts (ECMWF) Re-Analysis (ERA5) or National Aeronautics and Space Administration’s (NASA’s) Modern-Era Retrospective analysis for Research and Applications (MERRA-2) is used to represent current climate or to infill the missing data are used to represent current climate or to infill the missing data. The selection of the most appropriate reanalysis dataset to used for infilling missing data is done by:

1) Establishing concurrent periods between observations and reanalysis data, including only the months which are within the 90% data availability criterion of the observed data.
2) Comparing the monthly and annual variation of precipitation between observations and reanalysis datasets for the concurrent periods
3) Calculation and comparison of R^2 statistic between the observed data and both ERA5 and MERRA-2 reanalysis datasets for the concurrent periods

The reanalysis dataset that has the highest level of correlation (R^2 statistic) and the ability to capture the monthly and annual variation of the observed data will be used for infilling.

Infilling the missing data is a two-step process: the first step is to perform a correlation analysis for the concurrent period between the non-missing observations and reanalysis data, and the second step is to scale the reanalysis data using a linear relationship based on the correlation.

Environment and Climate Change Canada (ECCC) has provided the AHCCD dataset that has adjusted measurements to account for non-climatic measurement issues (i.e., wind undercatch) and has combined observations from nearby stations to create longer time series that are useful for trend studies (Mekis and Vincent 2011). The AHCCD dataset includes daily observations for minimum, maximum and mean temperatures and total precipitation. The AHCCD dataset does not always include the most recent observations and as a result, a trending analysis is used to adjust the AHCCD dataset to match the infilled observations to account for any missing observations/years. This adjustment uses monthly factors based on the difference between the two datasets for the concurrent period. A sensitivity analysis is then conducted comparing the datasets to verify that the adjustments are consistent with the infilled dataset.

A.2.2 Calculation of Observed Baseline IDF Curves and Rainfall Statistics

This subsection describes the methodology to calculate the IDF curves for the baseline, divided into different durations (i.e., 1-day, 2-day, and 3-day for the meteorological stations and sub-daily for the stations where sub-daily data is available). The methodology requires fitting curves for several statistical distributions whose parameters are estimated using standard statistical methods. The preferred statistical distribution is then selected based on the results of the goodness-of-fit tests. This section supports the results and summary presented in Section 3.2.

To estimate the IDF values under historical climate conditions, the statistical distribution based on ‘goodness-of-fit’ criteria are used. For this step, three different distributions are assessed, namely: Gumbel, GEV (Generalized Extreme Value) and Log-Pearson type 3 and based on three goodness-of-fit criteria: Anderson-Darling, Kolmogorov-Smirnov and Chi-Squared tests described on the following sub-sections.

A.2.2.1 Sub-Daily and Daily Precipitation

Sub-daily IDF curves apply only to stations with sub-daily observation records. The sub-daily rainfall data was obtained from the ECCC database in the form of annual maximum precipitation for the sub-daily durations provided. Daily IDF are developed by extracting the annual maximum precipitation values from daily historical climate records from the ECCC. The sub-daily and daily annual maximum precipitation values are then fitted to a statistical distribution in order to obtain precipitation corresponding to return periods of 2, 5, 20, 10, 50, 100, 200, 500, 1,000 and 2,000 years.

A.2.2.2 Multi-Day Precipitation

Multi-day precipitation is obtained by taking the moving sum of precipitation values using a window size that corresponds to the duration of interest. Annual maximum precipitation values are then extracted for each multi-day duration and are fitted to a statistical distribution. The 1-day, 2-day, 3-day, 4-day, 5-day, 10-day, 20-day, 30-day, 50-day, 75-day, 90-day and 120-day consecutive rainfall amounts for return periods of 2, 5, 20, 10, 50, 100, 200, 500, 1,000 and 2,000 years are presented.

A.2.2.3 Statistical Distributions

This subsection describes in detail the three candidate statistical distributions used to produce the IDF curve results. The distributions are Gumbel, Generalized Extreme Value (GEV) and Pearson or Log Pearson Type 3.

A.2.2.3.1 Gumbel Distribution (EV1)

The EV1 distribution has been widely recommended and adopted as the standard distribution by Environment and Climate Change Canada for all the Precipitation Frequency Analyses in Canada. The EV1 distribution for annual extremes can be expressed as:

$$Q(T) = \mu + k_T . \sigma$$ **Equation 1**

$$k_T = -\frac{\sqrt{6}}{\pi}\left[0.5772 + ln\left(ln\left(\frac{T}{T-1}\right)\right)\right]$$ **Equation 2**

where *Q(T)* is the exceedance value, μ and σ are the population mean and standard deviation of the annual extremes; T is return period in years.

A.2.2.3.2 Generalized Extreme Value (GEV) Distribution

The GEV distribution is a family of continuous probability distributions that combines the three asymptotic extreme value distributions into one: Gumbel (EV1), Fréchet (EV2) and Weibull (EV3) types. GEV uses three parameters: location, scale and shape. The location parameter describes the shift of a distribution in each direction on the horizontal axis. The scale parameter describes how spread out the distribution is and defines where the bulk of the distribution lies. As the scale parameter increases, the distribution becomes more spread out. The shape parameter affects the shape of the distribution and governs the tail of each distribution. The shape parameter is derived from skewness, as it represents where most of the data lies, which creates the tail(s) of the distribution. The value of shape parameter k = 0, indicates the EV1 distribution. Value of k > 0, indicates EV2 (Fréchet), and k < 0 the EV3 (Weibull). The Fréchet type has a longer upper tail than the Gumbel distribution and the Weibull type has a shorter tail (Overeem et al. 2007 and Millington et al. 2011).

The GEV cumulative distribution function *F(x)* is given by Equation 3 for *k* = 0 (EV1).

$$F(x) = \exp\left\{ - \left[1 - \frac{k}{\alpha}(x-\mu)\right]^{1/k} \right\} \quad \text{for k} \neq 0$$ **Equation 3**

$$F(x) = \exp\left\{ -exp\left[-\frac{1}{\alpha}(x-\mu)\right]\right\} \quad \text{for k} = 0$$ **Equation 4**

where *μ* is the location, α is the scale, *k* is the shape parameter of the distribution, and y is the GEV reduced variate, $y = -\ln(-\ln F)$.

The inverse distribution function or quantile function is given by Equation 5 for k ≠ 0 and Equation 6 for k = 0.

$$Q(x) = \mu + \alpha\{\ 1 - (-lnF)^k\}/k \quad \text{for k} \neq 0$$ **Equation 5**

$$Q(x) = \mu - \alpha\left\{ -exp\left[-\frac{1}{\alpha}(F-\mu)\right]\right\} \quad \text{for k} = 0$$ **Equation 6**

A.2.2.3.3 Pearson and Log Pearson Type 3

The Pearson Type 3 (PE3) distribution is a member of the family of Pearson Type 3 distributions and is also referred to as the Gamma distribution. The PE3 is required for all Precipitation Frequency Analysis in the United States. Like GEV, the PE3 has three parameters, location (μ), scale (σ) and shape (γ). A problem arises with PE3 as it tends to give low upper bounds of the precipitation magnitudes, which is undesirable (Cunnane 1989). The CDF (Cumulative Density Function – *F*) and PDF (Probability Density Function – *f*) are defined in (Hosking and Wallis 1997) as:

If $\gamma \neq 0$, let $\alpha = 4/\gamma^2$ and $\xi = \mu - 2\sigma/\gamma$ **Equation 7**

If $\gamma > 0$ then:

$$F(x) = G\left(\alpha, \frac{x-\xi}{\beta}\right)/\Gamma(\alpha)$$ **Equation 8**

$$f(x) = \frac{(x-\xi)^{\alpha-1}e^{-(x-\xi)/\beta}}{\beta.\Gamma(\alpha)}$$ **Equation 9**

If $\gamma < 0$ then:

$$F(x) = 1 - G\left(\alpha, \frac{\xi-x}{\beta}\right)/\Gamma(\alpha)$$ **Equation 10**

$$f(x) = \frac{(\xi-x)^{\alpha-1}e^{-(\xi-x)/\beta}}{\beta.\Gamma(\alpha)}$$ **Equation 11**

If $\gamma = 0$ then Pearson type 3 follows the Normal distribution:

$$F(x) = \Phi\left(\frac{x-\mu}{\sigma}\right)$$ **Equation 12**

$$f(x) = \phi\left(\frac{x-\mu}{\sigma}\right)$$ **Equation 13**

Where *G* is the incomplete Gamma function and Φ the CDF and ϕ PDF of the Normal distribution.

A.2.2.4 Parameter Estimation Methods

A common statistical procedure for estimating distribution parameters is the use of a maximum likelihood estimator or the method of moments. ECCC uses and recommends the use of the method of moments technique to estimate the parameters for EV1. Golder uses the method of moments to calculate the parameters of the Gumbel distribution. Golder uses L-moments to calculate parameters of the GEV distribution. The following sections describe the method of moments procedure for calculating the parameters of the Gumbel distribution and L-moments method for calculating parameters of the GEV distribution.

A.2.2.4.1 Method of Moments

The most popular method for estimating the parameters of the Gumbel distribution is method of moments (Hogg et al. 1989). In the case of the Gumbel distribution, the number of unknown parameters is equal to the mean and standard deviation of the sample mean. The first two moments of the sample data are sufficient to derive the parameters of the Gumbel distribution in Equation 14 and Equation 15. These are defined as:

$$\mu = \frac{1}{N}\sum_{i=1}^{N} Q_i$$ **Equation 14**

$$\sigma = \sqrt{\frac{1}{N-1}\sum_{i=1}^{N}(Q_i - \bar{Q})}$$ **Equation 15**

Where μ is the mean, σ the value of standard deviation of the historical data, Q_i the maximum precipitation data for year *I*, and $\bar{Q}$ the mean of the precipitation data.

A.2.2.4.2 L-moments Method

The L-moments (Hosking and Wallis 1997) and maximum likelihood methods are commonly used to estimate the parameters of the GEV distribution and fit to annual maxima series. The L-moments are a modification of the probability-weighted moments (PWMs), as they use the PWMs to calculate parameters that are easier to interpret. The PWMs can be used in the calculation of parameters for statistical distributions (Millington et al. 2011). They provide an advantage, as they are easy to work with, and more reliable as they are less sensitive to outliers. L-moments are based on linear combinations of the order statistics of the annual maximum rainfall amounts (Hosking and Wallis 1997 and Overeem et al. 2007). The PWMs are estimated by:

$$b_0 = n^{-1}\sum_{j=1}^{n} x_j$$ **Equation 16**

$$b_1 = n^{-1}\sum_{j=2}^{n} \frac{j-1}{n-1} x_j$$ **Equation 17**

$$b_2 = n^{-1}\sum_{j=3}^{n} \frac{(j-1)(j-2)}{(n-1)(n-2)} x_j$$ **Equation 18**

Where x_j is the ordered sample of annual maximum series (AMS) and b_i are the first PWMs. The sample L-moments can them obtained as:

$$\ell_1 = b_0$$ **Equation 19**

$$\ell_2 = 2b_1 - b_0$$ **Equation 20**

$$\ell_3 = 6b_2 - 6b_1 + b_0$$ **Equation 21**

A.2.2.4.3 L-Moments for the GEV parameters

The GEV parameters: location (μ), scale (α) and shape (*k*) are defined (Hosking and Wallis 1997) as:

$$k = 7.8590c + 2.9554c^2$$

where:

$$c = \frac{2}{3+\ell_3/\ell_2} - \frac{\ln(2)}{\ln(3)}$$ **Equation 22**

$$\alpha = \frac{\ell_2 k}{(1-2^{-k}).\Gamma(1+k)}$$ **Equation 23**

$$\mu = \ell_1 - \alpha\frac{1-\Gamma(1+k)}{k}$$ **Equation 24**

Where Γ is the gamma function, ℓ_1, ℓ_2 and ℓ_3 the L-moments, and μ the location, α the scale and *k* the shape parameters of the GEV distribution.

A.2.2.4.4 L-Moments for the Pearson Type 3 (PE3) and Log Pearson Type 3 (LP3)

The parameters location (μ), scale (σ) and shape (γ) are defined in (Hosking and Wallis 1997) for the Pearson Type 3 distribution are as follows:

$$\gamma = 2\alpha^{-0.5} + sign(\tau_3)$$ **Equation 25**

$$\sigma = \frac{\lambda_2 \pi^{0.5} \alpha^{0.5} \Gamma(\alpha)}{\Gamma(\alpha + 0.5)}$$ **Equation 26**

$$\mu = \lambda_1$$ **Equation 27**

To estimate the value of α:

If $0 < |\tau_3| < \frac{1}{3}$, let $z = 3\pi\tau_3^2$ and use:

$$\alpha = \frac{1 + 0.2960.z}{z + 0.1880.z^2 + 0.0442.z^3}$$ **Equation 28**

If $\frac{1}{3} < |\tau_3| < 1$, let $z = 1 - |\tau_3|$ and use:

$$\alpha = \frac{0.3636.z - 0.59567.z^2 + 0.25361.z^3}{1 - 2.78861.z + 2.56096.z^2 - 0.77045.z^3}$$ **Equation 29**

A.2.2.5 Goodness-of-Fit tests

Goodness of fit tests can be reliably used in climate statistics to assist in selecting the best distribution to fit the given data. These tests are usually applied to reject candidate statistical distributions and provide a sense of how well a given distribution fits the data being tested. These tests describe the differences between the observed data points and the calculated values from the distribution. The performances the three statistical distribution considered are tested by using the following goodness-of-fit tests: Kolmogorov-Smirnov test, Anderson-Darling estimate and Chi-Squared test, described next.

A.2.2.5.1 Kolmogorov-Smirnov Test

The Kolmogorov-Smirnov (KS) test it is used to decide whether the sample being tested originates from a specific continuous statistical distribution. The KS statistic (*D*) is based on the largest vertical difference between the theoretical and the empirical CDFs (Cumulative Distribution Function) and is calculate as:

$$D = \max_{1 \le i \le n} \left(F(x_i) - \frac{i-1}{n}, \frac{i}{n} - F(x_i) \right)$$ **Equation 30**

Where, the samples x_i are assumed to be random, originating from some distribution with CDF of $F(x_i)$, *n* the sample size, and *i* the ith sample, calculated when the data is sorted in ascending order. The hypothesis for this distribution (test) is rejected if the test statistic is greater than the critical value at a chosen significance level. For the significance level of α=5%, the critical value is selected is based on the sample size and tables are available. The value of the statistics *D* is used to rank the distributions.

A.2.2.5.2 Anderson-Darling Test

The Anderson-Darling (AD) test compares an observed CDF to an expected CDF. This method gives more weight to the tail of the distribution than KS test, which in turn leads to the AD test being stronger and having more weight than the KS test. The test rejects the hypothesis regarding the distribution level if the statistic obtained is greater than a critical value at a given significance level (α). The significance level most used is α = 5%, producing a critical value of 2.5018. This number is then compared with the test distributions statistic to determine if it can be rejected or not. The AD test statistic is calculated as:

$$AD = -n - \frac{1}{n} \sum_{i=1}^{n} (2i-1) \ \left[ln\big(F(X_i)\big) + ln\big(1 - F(X_{n+1-i})\big) \right]$$ **Equation 31**

Where *n* the sample size, and *i* the i^{th} sample, calculated when the data is sorted in ascending order, $F(x_i)$ the CDF of the distribution being tested, and the samples x_i are assumed to be random, originating from some distribution with CDF of $F(x_i)$. The value of the *AD* test is used to rank the distributions.

A.2.2.5.3 Chi-Square Test

The Chi-Squared test is used to determine if a sample comes from a given distribution. The test is based on binned data, and the number of bins (k) is determined by:

$k = 1 + logN$ with N the sample size **Equation 32**

The test statistic (χ^2) is calculated as:

$$\chi^2 = \sum_{i=1}^{k} \frac{(O_i - E_i)^2}{E_i}$$ **Equation 33**

Where O_i is the observed frequency, $E_i = F(x2) - F(x1)$ with $x1$ and $x2$ as the limits of the i^{th} bin.

The statistics χ^2 is used to assist in ranking the distributions and the significance level, α = 0.05 produced a critical value of 12.592. For values above this threshold the distribution being tested is rejected.

A.2.3 Calculation of Baseline Probable Maximum Precipitation (PMP)

This section describes the method of the calculation of the baseline values of the PMP using the Transposition method following the recommendation by Wood (2019), and corresponds to steps 1 through 5 from Figure A.2. The Transposition method is based on observed historical events and requires careful analysis and identification of major storms from the available records. The stations in the study area are screened for the largest storms in the observational record and are used to construct the DAD curves, which are then maximized by applying maximization and the transposition factors (described in Section A.2.3.2) to the area of study. These steps are described in the following subsections.

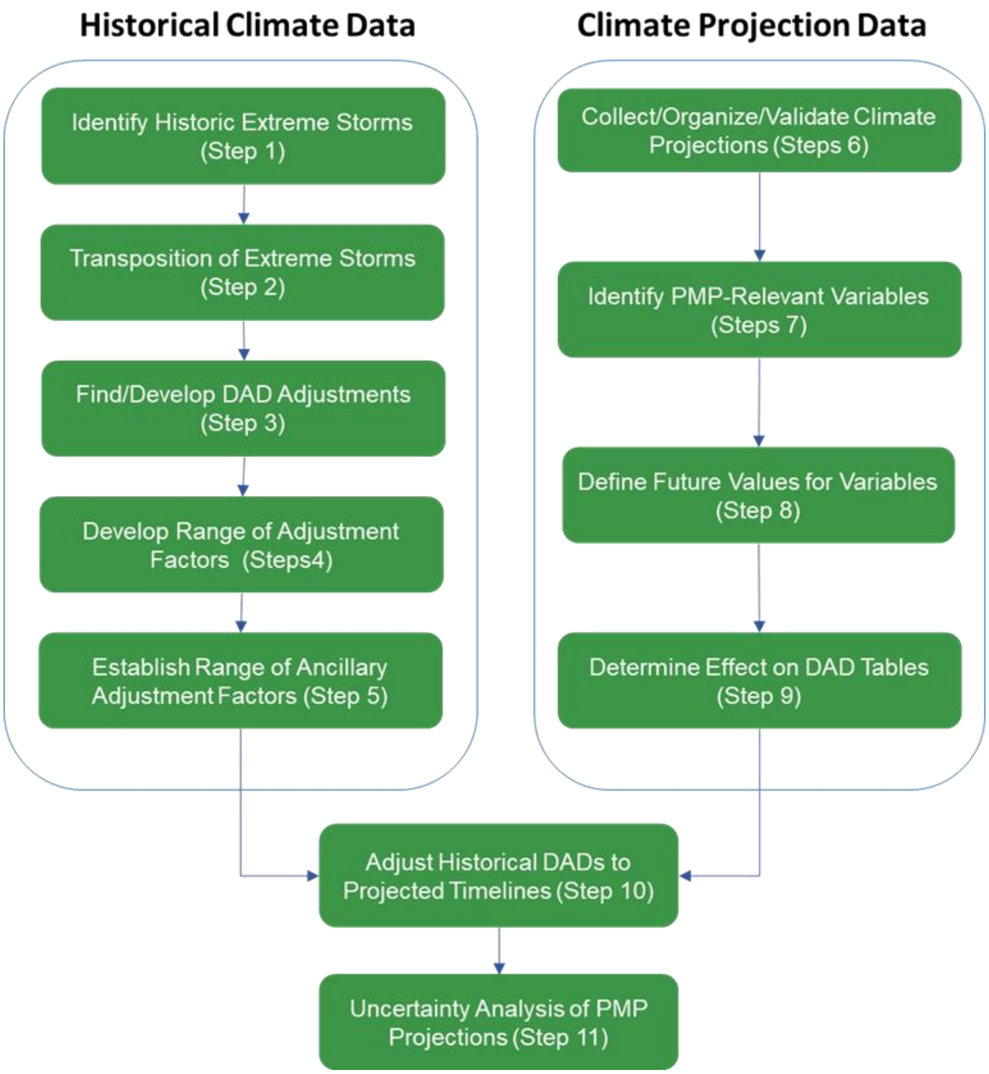

Figure A.2: Baseline and Future PMP Analyses Flowchart

A.2.3.1 Construction of the DAD Curves

The methodology used in this study is based on the one described by WMO (2009a). The precipitation is weighted among stations according to their distance from other stations where the selected storms are recorded using a pairwise comparison. This step is equivalent to an averaged weighting of the precipitation. Averaged weighting is done pairwise with stations that have records for the selected storm, and the centre is defined at the station that recorded the highest precipitation for the selected event with additional meteorological information about the storm. From the centre of the storm, the area is defined using the distance to each station (also in a pairwise approach) defining the set of area/depth points used to develop the DAD curves (as in Section 3.3.3). This approach is a simplification of the methodology using isohyetal maps; however, given the very low density of stations utilized, it is expected to yield similar results to other methods. The depth-area-duration (DAD) curves are then constructed for 1-day, 2-day, and 3-day durations using envelopment (following WMO 2009a) of the area/depth points found as described above. The in-place storm maximization and storm transposition play a large role in the final value of the PMP calculated.

In the case that no one storm dominates precipitation amounts for stations in the region, multiple storms will be selected based on a level of threshold precipitation and the number of stations with recorded precipitation for each storm in the region. This is done to ensure that a number of large storms are captured in the historical record, so that a composite DAD curve can be constructed. The approach taken is the same as if one major storm event is used, however there are more points which that will be considered for the envelopment curves of the 1-day, 2-day, and 3-day durations.

A.2.3.2 Storm maximization and Transposition method

One of the steps of the calculation of the PMP using DAD curves (Transposition method) is the storm maximization using precipitable water (PWC) content of the rainfall event and the transposition to the study area (WMO 2009a). For the storm maximization and transposition, the maximum PWC is estimated using the relationship between dew point temperature and the PWC as shown in Figure A.3. This relationship was determined by OMNR (2006) and is valid for the province of Ontario. The PWC values are based on the 12-hour persistent dewpoint maps (100-year return period with and adjusted statistical distribution as shown in Figure F3.2 from OMNR 2006), and the mean temperature as proxy for the dewpoint temperature, where dewpoint data is not available.

The in-place maximized storms are transposed to the South Bruce area by evaluation of the precipitable water transposition factors. Based on the 100-year return period 12-hour persistent dew-point maps (Figure F3.2) from OMNR (2006), the in-place maximization ratio is calculated as follows:

$$r_{storm} = \frac{PWC_{100-year-A}}{PWC_{storm}} \qquad \textbf{Equation 34}$$

Where $PWC_{100-year-A}$ is the maximum precipitable water for 100-years return period of the 12-hour persistent dew point (using the maps provided by OMNR (2006)) and PWC_{storm} is the maximum precipitable water for the storm event both at the location of the storm center. The daily mean temperature is used as proxy for the dew point, since information on dew point is not available, both at the location of the storm center and at the South Bruce study area.

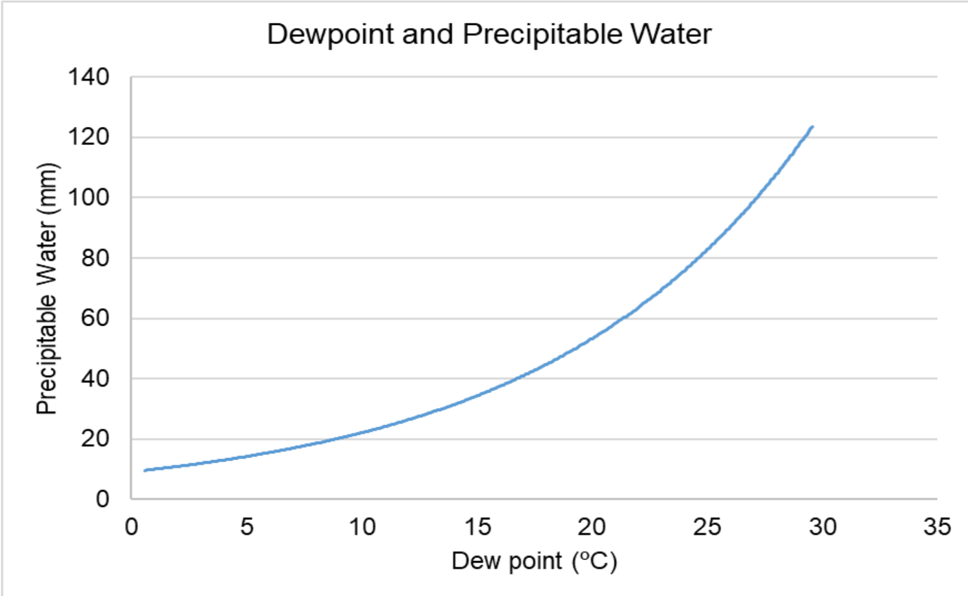

Figure A.3: Precipitable Water and Dew Point relationship (Adapted from: OMNR 2006)

The transposition ratio is calculated as follows:

$$r_{transp} = \frac{PWC_{100-year-B}}{PWC_{100-year-A}}$$ **Equation 35**

Where $PWC_{100-year-B}$ is the maximum precipitable water for 100-years return period of the 12-hour persist dew point at the transposition location (using the maps provided by OMNR 2006).

The final storm maximization factor is calculated as

$$r = r_{storm} \times r_{transp}$$ **Equation 36**

The maximization for the 2- and 3-Day PMP is calculated by adding the delta to the 2 and 3-day DAD from the 1-Day PMP maximization result.

This method is used to derive the final storm maximization factor in Section 3.3.3.

A.2.3.3 Hershfield Method

The WMO acknowledges that there is significant uncertainty regarding PMP calculations and recommends that a comparison of other method and reported values is conducted. A comparison with previous studies completed for the area and the Hershfield method is conducted to validate the result. The Hershfield method, described in WMO (2009a), is a robust statistical method to calculate the PMP values that relies on observations of annual maximum values of daily total precipitation. It is usually recommended for watersheds up to 1,000 km^2 (WMO 2009a). The PMP using the Hershfield method is calculated as follows:

$$PMP = X_n + KS_n$$ **Equation 37**

Where X_n and S_n are the mean and standard deviation (respectively) of the annual maximum 1-day precipitation, and K is a frequency factor that is a function of X_n and rainfall intervals. Adjustments needed to be made to X_n and S_n to account for the length of record used and the maximum observed rainfall event. Multiplicative factors for X_n and S_n were found to be 1.005 and 1.035 respectively when accounting for the length of record used (Figure 4.4 of WMO 2009a). Multiplicative factors for X_n and S_n were found to be 0.997 and 0.971 respectively when accounting for the maximum observed rainfall event (Figure 4.2 of WMO 2009a). The values of K as a function of rainfall duration and mean of the annual maximum series are given in Figure 4.1 of WMO (2009a).

A.2.3.4 Converting Daily PMPs to Sub-Daily

The hourly precipitation data are not available from ECCC and therefore the sub-daily PMP is estimated using ratio factors calculated from the sub-daily IDF curves defined for the study area. The ratios are estimated by taking the 24-hour duration and 100-year return period as reference, and the other sub-daily durations (5, 10, 15, 30 minutes, 1, 2, 6, 12 hours) are scaled accordingly to calculate the sub-daily PMP values. The 100-year return period is selected since it provides a more realistic and reliable estimate among sub-daily durations than higher return period. It is important to note that this estimate has uncertainties and assumes that the PMP follows the same distribution as the IDF curves for 24-hours durations and 100-year return period.

A.2.4 Rain on Snow Procedure

The calculation of the rain on snow follows the methodology adopted by ECCC (Louie and Hogg 1980) to estimate runoff from snowmelt. The methodology uses a degree-day method to separate rainfall and snowfall from precipitation and model the processes of snow accumulation and melt. The following steps are used in the procedure:

1) The snowpack accumulation is estimated based on the daily mean temperature and the total rainfall. If temperature is > 0ºC, precipitation falls as rain and no snowpack is accumulated; if temperature is < 0ºC, precipitation falls as snow and is accumulated to the snowpack.
2) The snowmelt amount (SM) is estimated based on the model presented in Equation 38 for Eastern Canada Forested Basin (Pysklywec et al. 1968) and is depleted from the snowpack.

$$SM = 0.0397\ (Ta - 27.6)\ \left(\frac{inches}{day}\right)$$ **Equation 38**

   Where Ta is the mean daily air temperature in ^{o}F.

3) The calculated snowmelt is added to the rainfall amount, if any (rain + snowmelt).
4) The process is repeated for all days in the data series are calculated.
5) Finally, the daily maximums of the combined rainfall and snowmelt for each year are calculated and a Gumbel distribution is fitted to estimate the several required return periods.

A.2.5 Calculation of Additional Climate Variables

Analysis of additional climate variables is important for providing context to climatic conditions on site and how they are projected to change in the future. This analysis may also provide useful information for further studies conducted at the site. The additional climate variables include monthly temperature and precipitation statistics along with derived climate variables including WMO climate indices, potential evapotranspiration, drought index, and qualitative information for wind speed and relative humidity. A daily future timeseries is also provided for the South Bruce study area that includes bias correction of precipitation. The sections to follow provide detailed methodology for the analysis performed for each of the variables.

A.2.5.1 Monthly Mean, Minimum, and Maximum Temperature and Precipitation

Summary statistics for temperature and precipitation at a monthly time scale allow for seasonal variation in climate to be captured on site. The statistics are calculated in two steps:

1. Resampling – daily climate variables are resampled to a monthly timescale. This is done by taking the sum of daily precipitation and mean of the daily temperatures in each month.
2. Aggregation – each calendar month across all years is aggregated for the resampled monthly total precipitation and temperature variables. The mean, minimum, and maximum are taken to aggregate the monthly values across all years.

To ensure months with insufficient data were not included in these statistics, only months with greater than 90% data availability were considered.

Daily current climate timeseries are provided for total precipitation and mean temperature from the infilled dataset presented in Section 3.1.2 of the main report.

Derived variables including rain, snow, and snow depth are included using the ECCC methods discussed in Louie and Hogg (1980). The snow depth (same as snowpack) is estimated based on the daily mean temperature and the total rainfall. If temperature is > 0ºC, precipitation falls as rain and there is no snow depth. If temperature is < 0ºC, precipitation falls as snow and snow depth is accumulated.

A.2.5.2 WMO Climate Indices

The climate extremes are defined by the World Meteorological Organization's (WMO's) Expert Team on Climate Change Detection and Indices (ETCCDI; WMO 2009b), who recommend 27 indices (ClimDEX) as a means of summarizing daily temperature and precipitation statistics, focusing primarily on aspects of climate extremes. They have been developed to allow comparison of climate conditions on an international basis. Table A.1 provides a summary of these indices and their definitions.

The minimum, maximum, mean, and median of the annual values for each climate index are calculated, as well as trends to help provide a description of the current climate conditions. The trends are calculated using a Theil-Sen estimator, which estimates the slope of a linear trendline using the median of the slopes of all lines through pairs of points. The Mann-Kendall test is used to estimate the significance of the trends. Details on the implementation of these techniques can be found in (Salmi et. al. 2002).

Table A.1: List of WMO Recommended 27 Extreme Indices

ID	Indicator Name	Definitions (1)	Units
CDD	Consecutive dry days	Maximum number of consecutive days with daily precipitation amount less than 1 mm (RR<1 mm)	Days
CSDI	Cold spell duration indicator	Annual count of days with at least 6 consecutive days when daily minimum temperatures are less than the 10th percentile (TN<10th percentile)	Days
CWD	Consecutive wet days	Maximum number of consecutive days with daily precipitation amount greater than or equal to 1 mm (RR>=1 mm)	Days
DTR	Diurnal temperature range	Monthly mean difference between the daily minimum temperature (TX) and the daily maximum temperature (TN)	ºC
FD0	Frost days	Annual count when the daily minimum temperature is less than 0°C (TN<0ºC)	Days
GSL	Growing season length	Annual (1st Jan to 31st Dec in the northern hemisphere, 1st July to 30th June in the southern hemisphere) count between first span of at least 6 days with ground temperatures greater than 5°C (TG>5ºC) and first span after July 1 (January 1 in the southern hemisphere) of 6 days with ground temperatures less than 5°C (TG<5ºC)	Days
ID0	Ice days	Annual count when the daily maximum temperature is less than 0° (TX<0ºC)	Days
PRCPTOT	Annual total wet-day precipitation	Annual total precipitation (PRCP) in wet days where the daily precipitation is greater than or equal to 1 mm (RR>=1 mm)	mm
R10	Number of heavy precipitation days	Annual count of days when precipitation is greater than or equal to 10 mm) (PRCP>=10 mm)	Days
R20	Number of very heavy precipitation days	Annual count of days when precipitation is greater than or equal to 20 mm (PRCP>=20 mm)	Days
R95p	Very wet days	Annual total precipitation (PRCP) when the daily precipitation is greater than the 95th percentile (RR>95th percentile)	mm
R99p	Extremely wet days	Annual total precipitation (PRCP) when the daily precipitation is greater than the 99th percentile (RR>99th percentile)	mm
Rnn	Number of days above nn mm	Annual count of days when precipitation when precipitation is greater than or equal to a user defined threshold (PRCP>= "nn" mm, "nn" is user defined threshold)	Days
RX1day	Max 1-day precipitation amount	Monthly maximum 1-day precipitation	mm
Rx5day	Max 5-day precipitation amount	Monthly maximum consecutive 5-day precipitation	mm

ID	Indicator Name	Definitions (1)	Units
SDII	Simple daily intensity index	Annual total precipitation divided by the number of wet days (defined as PRCP>=1.0 mm) in the year	mm/day
SU25	Summer days	Annual count when the daily maximum temperature is greater than 25°C (TX>25ºC)	Days
TN10p	Cool nights	Percentage of days when the daily minimum temperature is less than the 10th percentile (TN<10th percentile	% of Days
TN90p	Warm nights	Percentage of days when the daily minimum temperature is greater than the 90th percentile (TN>90th percentile	% of Days
TNn	Min Tmin	Daily minimum value of daily minimum temp	ºC
TNx	Max Tmin	Daily maximum value of daily minimum temp	ºC
TR20	Tropical nights	Annual count when the daily minimum temperature is greater than 20°C (TN>20ºC)	Days
TX10p	Cool days	Percentage of days when the daily maximum temperature is less than the 10th percentile (TX<10th percentile)	% of Days
TX90p	Warm days	Percentage of days when the daily maximum temperature is greater than the 90th percentile (TX>90th percentile)	% of Days
TXn	Min Tmax	Daily minimum value of daily maximum temp	ºC
TXx	Max Tmax	Daily maximum value of daily maximum temp	ºC
WSDI	Warm spell duration indicator	Annual count of days with at least 6 consecutive days when the daily maximum temperature is greater than the 90th percentile (TX>90th percentile)	Days

Note:

(1) The abbreviations for the variables used in the definitions are as follows: SH is southern hemisphere; RR is the daily precipitation amount (mm); TX is the maximum temperature (°C); TN is the minimum temperature (°C); TG is the ground temperature (°C); and PRCP is the precipitation amount (mm); RR – daily precipitation amount (mm).

A.2.5.3 Potential Evapotranspiration

Evapotranspiration is the combined process of evaporation and transpiration over a vegetated surface. The principal weather parameters affecting evapotranspiration are air temperature, extraterrestrial radiation, humidity and wind speed, and vegetation parameters. Potential evapotranspiration represents the maximum actual evapotranspiration expected from a given area with no moisture limitations. As only the observed minimum temperature, maximum temperature and total precipitation are available from the daily current climate dataset (no infilled observations of radiation, humidity, and wind speed are produced), an air temperature-based formula, namely the Hargreaves equation (Food and Agriculture Organization [FAO] 2006) will be used.

The Hargreaves equation was developed in 1982 as an alternative to the more complicated energy-balance approach of the Penman-Monteith equation (developed in 1948). The Penman-Monteith method requires significant amounts of climate data including incoming solar radiation, wind speed, and humidity, which are often not available. By contrast, the Hargreaves equation requires only the daily minimum, maximum, and mean temperatures. The Hargreaves equation builds into a more complete model by making assumptions about the solar radiation (based on latitude), accounting for humidity (based on the difference between daily minimum and maximum temperatures) and assuming that the effect of wind is not significant. The FAO has noted that for potential evapotranspiration (ET_o):

> *"Temperatures methods remain empirical and require local calibration in order to achieve satisfactory results. A possible exception is the 1985 Hargreaves' method which has shown reasonable ET_o results with a global validity" (FAO 2006).*

The Hargreaves estimate of daily potential evapotranspiration is arrived at by the following formula:

$$\boldsymbol{E = 0.0023(T_{mean} + 17.8)(T_{max} - T_{min})^{0.5} R_a} \qquad \text{Equation 39}$$

where T_{mean} is the average temperature, T_{max} and T_{min} are daily maximum and minimum temperatures (all in °C), and R_a is the extraterrestrial radiation (MJ/m^2/day). The R_a is calculated as:

$$\boldsymbol{R_a = \frac{24(60)}{\pi} G_{sc} d_r [w_s sin(\varphi) sin(\delta) + cos(\varphi) cos(\delta) sin(w_s)]} \qquad \text{Equation 40}$$

where G_{sc} is the solar constant: 0.0820 MJ/m^2/min;

d_r is the inverse relative distance Earth-Sun (dimensionless): $d_r = 1 + 0.033cos\left(\frac{2\pi}{365}J\right)$;

w_s is the sunset hour angle in radians: $w_s = arccos[-tan(\varphi)tan(\delta)]$;

φ is the latitude of the site in radians;

δ is the solar declination in radians: $\delta = 0.409sin\left(\frac{2\pi}{365}J - 1.39\right)$; and

J is the Julian day.

The daily potential evapotranspiration timeseries is derived from the infilled temperature dataset using the methods described above. It should be noted that with this method, potential evapotranspiration can occur during the winter months due to the inclusion of the diurnal temperature range (maximum temperature – minimum temperature) allowing for some potential evapotranspiration to occur in the winter months, however ice/snow sublimation is not specifically accounted for. Due to the low temperatures and potential evapotranspiration rates during the winter months it is anticipated that this simplification will not have a large impact on the final results.

A.2.5.4 Drought Index

The drought index is estimated using the standard precipitation and evapotranspiration index (SPEI) of Vincente-Serrano et al. (2010), which is based on the standard precipitation index described in WMO (2012). This method illustrates the number of standard deviations that net precipitation (precipitation less evapotranspiration) for a given month is from the median for all months. By using net precipitation, the effects of temperature variation for current climate is also able to impact the drought index instead of only precipitation.

The SPEI is calculated by first taking the difference between monthly total precipitation and evapotranspiration, D_i where i corresponds to a given month in the monthly baseline timeseries. Next, 1-dimensional convolution is performed on D_i according to the selected calculation interval, resulting in X_i. The calculation interval used is selected as 12 months, so that each monthly value contains the sum of the previous 12-months. The drought index is calculated using a running deficit/surplus of net precipitation; therefore, the calculation interval of 12 months is used to account for seasonal variability in net precipitation. The scale and shape parameters of a two-parameter gamma distribution is found for X_i. Using these parameters, the non-exceedance probabilities, P_i for each value in X_i is extracted from the cumulative distribution function of the gamma distribution. The SPEI values are then obtained by taking the quantiles of a normal distribution with mean of 0 and standard deviation of 1 that correspond to P_i. With this method, the mean and standard deviation of the SPEI will have values of 0 and 1 due to the normalization step.

A drought is indicated by a negative SPEI value, which indicates a deficient of available water in a given location. Due to the standardized nature of this drought index, generalized classification systems have been developed. The drought classification system provided by WMO (2012) can be used to interpret the SPEI values (Table A.2). SPEI values are summarized using a set of percentiles for each calendar month. This allows for the distribution of water deficit/surplus across calendar months to be examined.

Table A.2: SPEI Classification System

SPEI Value	Classification
2.0+	extremely wet
1.5 to 1.99	very wet
1.0 to 1.49	moderately wet
-0.99 to 0.99	near normal
-1.0 to -1.49	moderately dry
-1.5 to -1.99	severely dry
-2 and less	extremely dry

A.2.5.5 Wind Speed and Relative Humidity

The closest published climate normals from ECCC (2020) are used to characterize wind speed and relative humidity at the site and are compared to published literature values, where available. Information on daily mean wind speed trends is obtained from Wan et al. (2010). In this study, wind speed observations are homogenized across Canada using the ECCC digital data archive for the period of 1979 to 2019. Homogenization was carried out by first adjusting for the effects of non-standard anemometer heights, detecting and adjusting for systematic errors (location and exposure of the observation site, anemometer type, instrument malfunctions, etc.), and identification and adjustment for discontinuities in wind speed timeseries. Linear trends were then estimated using the monthly mean series of the homogenized daily mean wind speed data.

A.3 FUTURE CLIMATE PROJECTIONS DEVELOPMENT

Future climate projections are important for understanding how climate is projected to change from the climate baseline. The future climate projections come from publicly available statistical downscaled future climate projections on a daily scale. Recognizing the inherent uncertainty with projections, multiple projections from multiple models and scenarios are included in the analysis. Therefore, the future projected changes in climate are provided in terms of percentiles. An exception to this is the provision of daily future timeseries for South Bruce. In this case, daily values are provided for each climate scenario to allow future studies to select and run scenarios in different types of climate impact modelling studies.

The following sub-sections describe the methodology to develop future climate change projections and to incorporate these projections to the PMP estimates, IDF curves, and additional climate variables. The methodology presented in these subsections supports the analyses and results for the future projections for PMP, IDF curves and additional climate variables presented in Section 4.

A.3.1 Data Sources for Future Climate

Future climate projections are important for understanding how climate is projected to change from the climate baseline. The Intergovernmental Panel on Climate Change (IPCC) is generally considered to be the definitive source of information related to past and future climate change as well as climate science. In 1988, the IPCC was formed by the World Meteorological Organization (WMO) and the United Nations Environment Program (UNEP) to review international climate change data. The IPCC is generally considered to be the definitive source of information related to past and future climate change as well as climate science. As an international body, the IPCC provides a common source of information relating to emission scenarios, provides third party reviews of models, and recommends approaches to document future climate projections. Periodically, the IPCC issues assessment reports summarizing the most current state of climate science. The Fifth Assessment Report (AR5) (IPCC 2013) represents the most current complete synthesis of information regarding climate change. The Sixth Assessment report (AR6) is due for release in May 2022 and will include updated climate scenarios and projections (IPCC 2020). The updated projections are anticipated to be in line with the AR5 but will include additional emissions scenarios to be assessed.

A.3.2 Global Climate Change Projections

Future climate is typically projected using general circulation models (GCMs; also used interchangeable with global climate models) that involve the mathematical representation of global land, sea and atmosphere interactions over a long period of time. GCMs are one of the tools available that allows us to estimate and understand changes in climatic conditions for future periods. In order to provide global projections of climate, the spatial and temporal resolution of GCMs (hundreds of kilometers and monthly) is coarse compared to meteorological models (kilometers and hourly).

These GCMs have been developed by various government agencies, but they share a number of common elements described by the IPCC. The IPCC does not run the models but acts as a clearinghouse for the distribution and sharing of the model forecasts. Future climate projection data are available from about 30 GCMs. GCMs require extensive inputs to characterize the physical processes and social development paths that could alter climate in the future. In order to represent the wide range of the inputs possible to global climate models, the IPCC has established a series of RCPs that help define the future levels of radiative forcing terms. The IPCC identified four greenhouse gas (GHG) emission scenarios, namely, RCP 2.6, RCP 4.5, RCP 6.0, and RCP 8.5 (business-as-usual). The pathways are named after the radiative forcing projected to occur by 2100.

Beyond 2100, the radiative forcing is described using extensions of the RCPs called Extended Concentration Pathways (ECPs) that help define the trajectory of greenhouse gas concentrations out to the year 2300. It should be noted that the ECPs (i.e., climate change model projections beyond 2100) contain a high degree of uncertainty. These four RCPs and ECPs have been described more fully by van Vuuren et al (2011) in their paper "The representative concentration pathways: an overview" and have been summarized in Table A.3. The IPCC identified four RCPs; however, this report focuses on the three RCPs (RCP 2.6, RCP 4.5, and RCP 8.5) currently available from ClimateData.ca (ClimateData.ca 2019).

Table A.3: Characterization of Representative Concentration Pathways

Name	Radiative Forcing in 2100 and 2300	Characterization
RCP 8.5, ECP 8.5	8.5 W/m² (2100) 12 W/m² (2300)	Increasing greenhouse gas emissions over time, with no stabilization, representative of scenarios leading to high greenhouse gas concentration levels (business-as-usual GHG emissions); and comparable to the SRES A2/A1FI scenarios. Past 2100, greenhouse gas emissions stabilize near 2250 at 12 W/m².
RCP 6.0, ECP 6.0	6.0 W/m²	Without additional efforts to constraint emissions (baseline scenarios); and comparable to SRES B2 scenario. Past 2100, greenhouse gas emissions stabilize near 2150 at 6.0 W/m².
RCP 4.5, ECP 4.5	4.5 W/m²	Total radiative forcing is stabilized shortly after 2100, without overshoot. This is achieved through a reduction in greenhouse gases over time through climate policy; and comparable to SRES B1 scenario. Past 2100, greenhouse gas emissions stabilize near 2150 at 4.5 W/m².
RCP 2.6, ECP 3PD	2.6 W/m²	"Peak and decline" scenario where the radiative forcing first reaches 3.1 W/m² by mid-century and returns to 2.6 W/m² by 2100. This is achieved through a substantial reduction in greenhouse gases over time through stringent climate policy. Past 2100, greenhouse gases remain constant at concentrations in 2100.

Note: Summarized from van Vuuren et al. (2011); W/m² = watt per square metre.

A.3.2.1 Regional Climate Change Projections

GCMs resolution is generally too coarse for direct use, as it does not resolve weather and extreme weather patterns or climatology at local scales. Outside of using the GCM output directly, there are different options to analyze climate projections at a regional scale. Most downscaled climate datasets include minimum temperature, maximum temperature and precipitation. The focus is on statistical or dynamically downscaled datasets which have a higher temporal and spatial resolution of the data; however, they may have limited variables available. The availability of daily downscaled data allows for better characterization of climate extremes, especially for precipitation. The availability of high spatial resolution (10 km instead of hundreds of km in global climate models or GCMs) provides better data to represent site-specific information for the study.

The climate change impact assessment for this study considers 136 bias-corrected climate projections from two distinct data sources:

- BCCAQ v2: Pacific Climate Impact Consortium (ClimateData.ca) data using Bias Correction/Constructed Analogues with Quantile mapping reordering (BCCAQ) version 2– (ClimateData 2019)
- GDO-DCP LOCA: Bias Correct models using Localized Constructed Analogs (LOCA, Pierce et al. 2014 and Reclamation 2013)

The BCCAQv2 data consists of 24 models (72 projections), using RCP 2.6, RCP4.5, and RCP8.5, and the LOCA data consists of 32 models for RCP 4.5 and RCP 8.5 only (64 projections), for a total of 136 projections for the dataset (hereinafter referred as the ensemble). The GCMs that were incorporated into each downscaling method are shown in Table A.4. Additional information on each model including the associated institution and resolution and methods used for each model component are provided in Appendix A of Flato et al. (2013). The downscaled projections are available for two different horizontal resolutions: 1/8 degree or approximately 12 km (BCCAQv2) and 1/16 degrees or approximately 6 km (LOCA). Both datasets provide downscaled climate model results from 1950 to 2100 for daily total precipitation, minimum temperature, and maximum temperature.

Table A.4: Global Climate Models used in BCCAQv2 and LOCA Downscaling Methods

Dataset Characteristic	ClimateData.ca (BCCAQv2)	GDO-DCP Archive (LOCA)
Climate Models		
ACCESS1-0	—	X
ACCESS1-3	—	X
bcc-csm1-1	X	X
bcc-csm1-1-m	X	X
BNU-ESM	X	—
CanESM2	X	X
CCSM4	X	X
CESM1-BGC	—	X
CESM1-CAM5	X	X

Dataset Characteristic	ClimateData.ca (BCCAQv2)	GDO-DCP Archive (LOCA)
CMCC-CM	—	X
CMCC-CMS	—	X
CNRM-CM5	X	X
CSIRO-Mk3-6-0	X	X
EC-EARTH	—	X
FGOALS-g2	X	X
GFDL-CM3	X	X
GFDL-ESM2G	X	X
GFDL-ESM2M	X	X
GISS-E2-H	—	X
GISS-E2-R	—	X
HadGEM2-AO	X	X
HADGEM2-CC	—	X
HadGEM2-ES	X	X
INMCM4	—	X
IPSL-CM5A-LR	X	X
IPSL-CM5A-MR	X	X
MIROC5	X	X
MIROC-ESM	X	X
MIROC-ESM-CHEM	X	X
MPI-ESM-LR	X	X
MPI-ESM-MR	X	X
MRI-CGCM3	X	X
NorESM1-M	X	X
NorESM1-ME	X	—
Spatial Resolution		
6 km	—	X
12 km	X	—
Years Available		
1950 - 2100	X	X
Climate Variables		
Minimum Temperature	X	X
Maximum Temperature	X	X
Mean Temperature	X	X
Total Precipitation	X	X

Both data sources provide spatially downscaled data; however, the BCCAQv2 approach has some drawbacks that makes it difficult to find good analog days for the entire domain as the domain size increases. It is also more likely that the model can miss days with precipitation and localized extreme precipitation events that are important to capture. These drawbacks are discussed in detail in *Downscaled CMIP3 and CMIP5 Climate Projections* by Bracken (2016). The LOCA approach was developed to address these issues of BCCAQv2 and was therefore used in this analysis.

The ClimateData.ca portal provides statistically downscaled daily Canada-wide climate scenarios, at a gridded resolution of 300 arc-seconds (or roughly 10 km) for the simulated period of 1950-2100 (ClimateData.ca 2019). The climate variables available from ClimateData.ca data include minimum temperature, maximum temperature and precipitation. The selection of data for this project is based on the available temporal and spatial resolution of the data. The availability of daily downscaled data allows for better characterization of the climate extremes, especially for precipitation. The availability of high spatial resolution (10 km instead of hundreds of km in GCMs) provides better representation for site-specific studies like this project.

The LOCA data is retrieved from the GDO-DCP archive, which provides fine spatial resolution translations of climate projections using three downscaling techniques including daily LOCA for the United States. The archive uses global climate projections from the World Climate Research Programme's (WCRP) CMIP3 and CMIP5 multi-model dataset that was used for the IPCC fifth assessment report (GDO-DCP 2019).

GCM projections are downscaled to a finer resolution using the Bias Correction/Constructed Analogues with Quantile mapping reordering version 2 (BCCAQv2) developed by the Pacific Climate Impacts Consortium (PCIC) (ClimateData.ca 2019). This downscaling method is a statistical algorithm that disaggregates the GCM outputs to a finer spatial and temporal resolution; in other words, they take the gridded data and calculate values that reflect the local conditions that cannot be simulated by the GCM. The Bias Correction/Constructed Analogues with Quantile mapping reordering interpolates spatially to a finer scale daily. More detailed description and model performance can be found in Werner and Cannon (2016).

Since no one model or climate scenario can be viewed as completely accurate, the IPCC recommends that climate change assessments use as many models and climate scenarios as possible, or a "multi-model ensemble". For this reason, the multi-model ensemble approach is used in this study to delineate the probable range of results and better capture the actual outcome (an inherent unknown). Best practices recommend using all plausible futures for greenhouse gases that includes to best- and worst-case scenarios (RCP 2.6, 4.5, 6.0, and 8.5) when considering long timescales to address uncertainty. In addition, a multi-model ensemble is also recommended since the mean of an ensemble is generally closer to the observed values for past climate than any given individual model or scenario (Charron 2016).

Before beginning the future climate projections, the 136 potential members of the multi-model ensemble are reviewed to observe whether the general temperature and precipitation ranges reasonably match the observed ranges of climate for the region. Monthly averages are used to capture the known seasonality of the region. From this evaluation, all scenarios from the ensemble demonstrated typical behaviour within the current climate normal for the region and within the monthly averages.

The downscaled data has a daily temporal resolution (GCMs typically have monthly temporal resolution) which allows for the characterization of future climate extremes. In addition, the improved horizontal resolution of 10 km in the downscaled data could better improve the representation of the study area, given the complex terrain in study area.

A.3.2.2 Uncertainty of Climate Change Downscaling Methods

To address the inherent uncertainty associated with climate change projections, multiple projections from multiple models and scenarios are used in this study. ECCC (2016) recommends that multiple climate models and emission scenarios should be used to overcome the range of natural climate variability and uncertainties regarding future greenhouse gas emissions pathways and climate response. Instead of selecting one single projection, projections from all available model runs are used to describe the probable range of results. The future projections are provided in terms of percentiles of the range of future climate projections.

A.3.3 Projecting Future Rainfall Statistics (IDF Curves)

This subsection describes the methodology to estimate IDF curves using modelled data from the ensemble and the methodology to assess changes to future rainfall (i.e., 2050s and 2080s), when compared to model baseline from the ensemble. This section, specifically, describes in detail Golder's IDF curve updating methods, including the Quantile Delta Method (QDM) and the Ratio Method (RM). This section supports the results and analysis presented in Section 4.2 of the main report.

The ensemble approach is used to obtain daily precipitation (1950 to 2100) to develop IDF curves representative of the model baseline (ideally same period as the current climate baseline) and the desired future periods, following the methods described in Section A.2.2. Specifically, IDF curves are developed for multi-day precipitation (methodology described in Section A.2.2.2.) and for sub-daily and daily observations applied only at stations with sub-daily observation records (methodology described in Section A.2.2.1). Statistical distributions (A.2.2.3) and goodness-of fit tests (A.2.2.5) are completed for each IDF developed under this task.

Once the IDF curves are developed for each climatic projection (model baseline and desired future periods), each model within the ensemble (approximately 136 models sourced from ClimateData.ca and LOCA) and each duration (e.g., multi-day precipitation or sub-daily and daily precipitation), future IDF curves are then compared to model baseline IDF curves. The QDM and RM methods are selected to produce a statistical range for the percentage change in absolute values.

The difference in IDF estimates between the QDM and RM models, across the entire ensemble is used to present the changes from the model baseline over a range of percentiles for selected return periods and duration of storm. Percent changes in precipitation associated with the 50th percentile are presented in Section 4.2. Detailed percentile differences across the dataset are presented Appendix B.

The projected change in the IDF curves can be applied to the observed estimates in order to obtain absolute values adjusted for climate change. This is represented by the equation given below:

$$IDF_{future} = IDF_{observed} \cdot (1 + IDF_{change})$$ **Equation 41**

Where the absolute value for the future IDF estimate (IDF_{future}) is obtained using the observed IDF estimate ($IDF_{observed}$) and the percentage change (IDF_{change}) projected under the selected future conditions. All changes should be applied for the same return periods and durations between the future percentage changes and the observed IDF estimates. For example, if the observed IDF estimate ($IDF_{observed}$) is 109.8 mm for the 1-day 100-year return period and the projected percentage change at the 50th percentile (IDF_{change}) is 14.3% for the 1-day 100-year return period, the estimated future IDF absolute value (IDF_{future}) is 109.8 mm * (1 + 0.143) = 125.5 mm.

A.3.3.1 Quantile Delta Mapping (QDM)

This method is based on the Equidistant Quantile Matching (EQM) algorithm (Li et al. 2010, Piani et al. 2010, Hassanzadeh et al., 2014, Srivastav et al., 2014, Cannon et al. 2015 and Schardong et al. 2018). First, the current climate baseline (based on observations), model baseline, and modelled future annual maximum rainfall datasets are fitted with statistical distributions. This method is generic to any of the four potential statistical distribution to be tested. Next, the current climate baseline annual maximum rainfall and model baseline annual maximum rainfall are equated using a functional relationship. This relationship establishes a mathematical connection between daily modelled and sub-daily observed annual maximum precipitation. Projected changes in climate (Δ_m) are calculated between the quantiles of the model baseline ($IDF_{baseline}$) and future (IDF_{future}) distributions corresponding to selected return periods of the IDF curve. This is done using the following equation for a given sub-daily duration i,

$$\Delta_{m_i} = \frac{IDF_{future_i}}{IDF_{baseline_i}} - 1$$ **Equation 42**

The projected future sub-daily IDF ($IDF_{projected}$) is then calculated using the functional relationship (f) established previously, along with the projected changes in climate (Δ_m) for each sub-daily duration.

$$IDF_{projected_i} = f\left(IDF_{baseline_i}\right) \cdot \Delta_{m_i}$$ **Equation 43**

After the distribution of the future sub-daily IDF has been obtained, extreme values are then extracted using the inverse cumulative distribution function with the probability of the selected return periods.

Downscaled climate projections from the data portals used here are limited to daily temporal resolutions. Therefore, sub-daily rainfall projections are not available, and it is assumed here that the projected changes in the 1-day modelled IDFs is uniform across the sub-daily durations. This allows for Δ_m to be constant for each sub-daily rainfall duration. Applying changes in daily to sub-daily precipitation extremes has been done in the past; however, it should be noted that changes in atmospheric processes governing rainfall production will unlikely be uniform for short to long time durations (e.g., convective scale processes at shorter durations versus large scale synoptic systems at longer durations) (CSA 2012). Therefore, the projected changes in sub-daily extremes should be interpreted with caution, and values used for design purposes should select a higher percentile to account for uncertainty related to the projected changes in sub-daily precipitation extremes.

The QDM, as well as the EQM, follows the steps presented in the flowchart of Figure A.4.

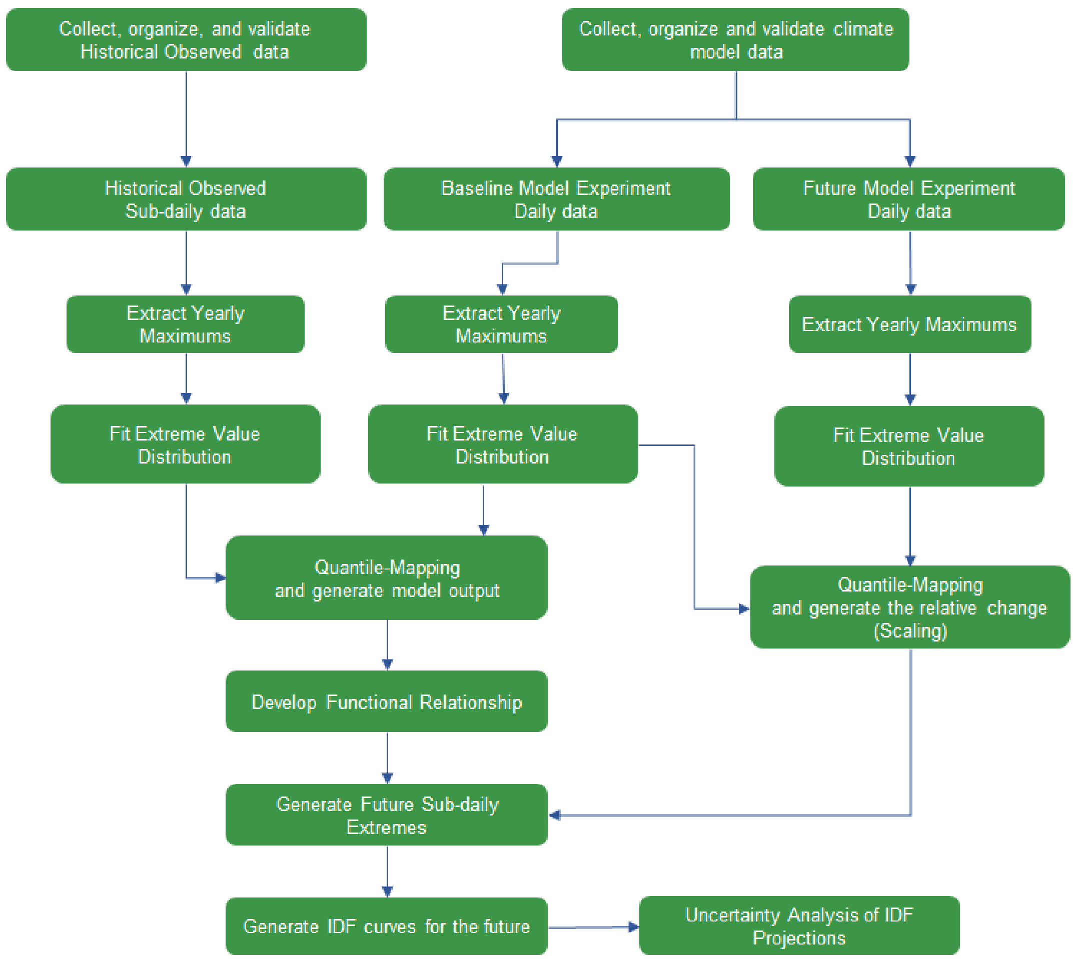

Figure A.4: QDM Method Flowchart (Adopted from Schardong and Simonovic 2019)

A.3.3.2 Ratio Method (RM)

The Ratio Method (RM) (Olsson et al. 2009) is generic for any statistical distribution selected and allows for analysis of any return period, including the 500-year return period. Details on how RM has been used in this work are shown in Figure A.5. Ratios are calculated between the model baseline and future projected IDF curves which signify the projected changes due to climate change. Since this method uses only the daily GCM results to estimate a percentage change between baseline and future conditions, the smallest timestep for which a percent change is generated is one-day. The 1-day changes are then applied uniformly to each sub-daily duration. The inclusion of the RM method in addition to the QDM method captures an additional source of uncertainty pertaining to the method used for updating the IDF curves for climate change, as the results of both methods are used when generating percentile levels from the multi-model ensemble.

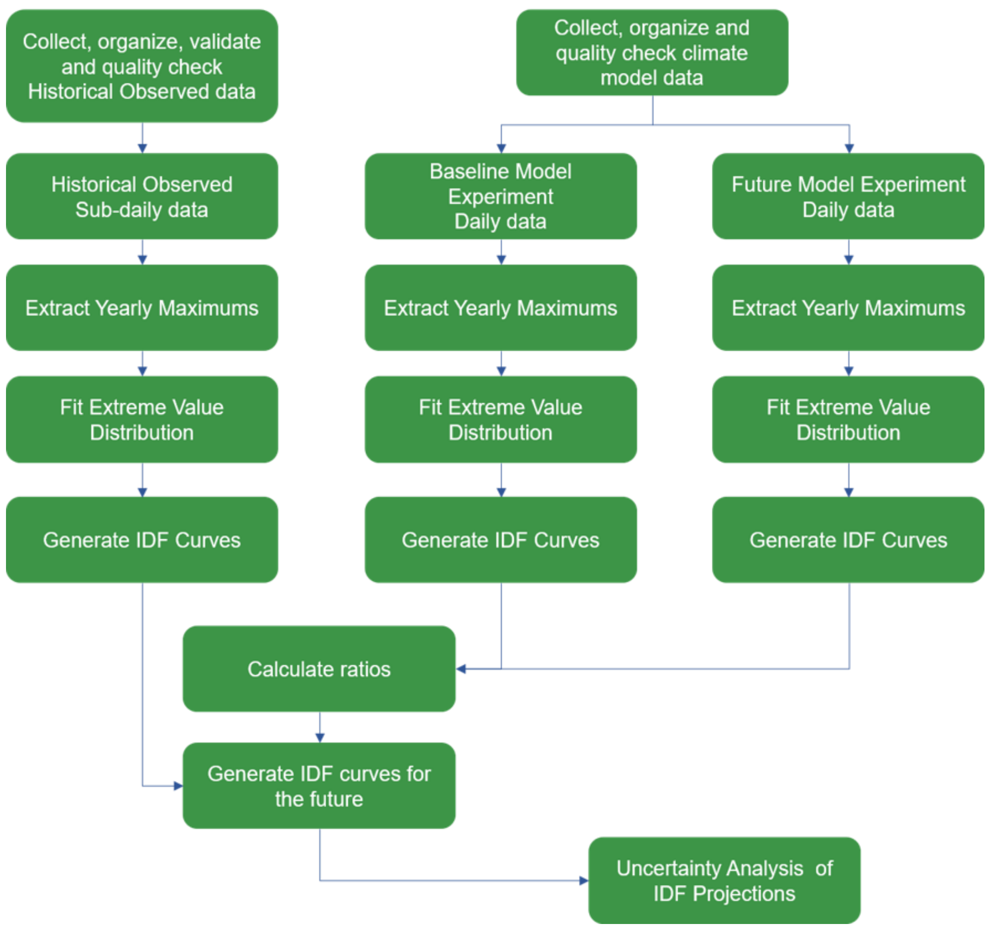

Figure A.5: Ratio Method Flowchart

A.3.4 Projecting Future Changes in PMPs

Future climate projections follow the steps outlined in Figure A.2. First, downscaled daily climate projections are obtained (Step 6). Next, variables relevant to the estimation of PMP using the Moisture Maximization and Hershfield methods are extracted which include daily total precipitation and daily minimum temperature (Step 7). The results for the future time periods using these methods are calculated (Step 8). Percentiles are calculated across the results of both methods used for all members of the multi-model ensemble. The percentage changes for each percentile are then applied to the DAD tables for current climate presented in Section 3.3.3 (Steps 9 and 10). All percentiles for the DAD tables are given in Appendix B, which provide an indication of the level of uncertainty associated with the climate projections on the DAD tables (Step 11).

The change in PMP for the future are presented as percent changes between the model baseline period (1950- 1993) and the selected future periods (2050s and 2080s) across all models within the ensemble. The Hershfield method follows the same approach used to develop PMP estimates for current climate (see Section A.2.3).

The Moisture Maximization method requires the moisture content and other variables, which are not readily available from the modelled climate datasets. In order to calculate the moisture content for the model result datasets that do not provide this variable, the daily minimum temperature projections from the multi-model ensemble are used as a proxy for the dew point temperature, which is used to estimate saturation vapor pressure. The saturation vapor is then used as a proxy for the precipitable water. No additional proxies are required to be used to describe other variables. Uncertainty regarding the projected changes in PMP from the multi-model ensemble is shown using percentiles which demonstrate how the PMP projections are distributed. The minimum and maximum projections were calculated, along with those corresponding to the 5^{th}, 25^{th}, 50^{th}, 75^{th}, and 95^{th} percentiles.

The projected change in the PMP values can be applied to the observed estimates in order to obtain absolute values adjusted for climate change. This is represented by the equation given below:

$$PMP_{future} = PMP_{observed} \cdot (1 + PMP_{change})$$ **Equation 44**

Where the future value for the PMP estimate (PMP_{future}) is obtained using the observed PMP estimate ($PMP_{observed}$) by the percentage change (PMP_{change}) in the value for the PMP.

A.3.5 Projecting Future Changes in Rain on Snow and Snowpack

The method for projecting changes in rain on snow and snowpack follows the method applied to the baseline climate described in Section A.2.4. Daily snowpack and snowmelt is estimated for each of the models in the ensemble methodology adopted by ECCC (Louie and Hogg 1980), and snowmelt is added to assumed rainfall to estimate rain on snow. The method uses a degree-day method, which assumes that in the case of sub-zero temperatures, precipitation falls as snow, which can accumulate to form snowpack. For temperatures above zero, precipitation falls as rain and accumulated snow begins to melt. The resulting annual maximum series for rainfall and snowmelt for each model and baseline/future period is then fitted to a Gumbel distribution to estimate the return period, and the resulting return values are then compared within each model to estimate a percentage change between the baseline and the future periods.

A.3.6 Projecting Future Changes in Additional Climate Variables

The method for projecting changes in the additional climate variables follows the method applied to the baseline climate described in Section A.2.5. For each of the additional climate variables projected changes are obtained using the approach outlines in the following sections.

A.3.6.1 Projecting Future Changes in Monthly Mean, Minimum, and Maximum Temperature and Precipitation

Minimum and maximum daily temperature from the multi-model ensemble of climate projections are first averaged into the mean temperature for all calendar months across all years in the model baseline and future time periods corresponding to the 2050s and 2080s. For each calendar month, the difference between the model baseline and future time periods is calculated. In the case of precipitation, the daily precipitation totals are first summed into monthly totals, then the average of the monthly totals is taken for each calendar month. The percentage difference from the model baseline to the future time periods is provided for each calendar month.

Daily future timeseries are provided from the multi-model ensemble for both precipitation and temperature climate variables. For precipitation, a bias correction step is needed to account for artifacts in the modelled daily values. Although statistically downscaled climate models discussed in Section A.3.2.1 have a higher spatial resolution than GCMs (10 km instead of hundreds of km), there are still issues with the statistically downscaled projections including:

- Artifacts from the GCMs, resulting in drizzle (more frequent low intensity precipitation), and under representation of precipitation extremes.
- The data used for bias correction of the statistically downscaled climate products may be inappropriate for the location of the site due to interpolation of point values in the gridded datasets used in the downscaling process.

In the analyses for future climate presented in the previous sections, the changes between the model baseline and future climate periods are calculated to mitigate bias that remains present in the downscaled climate products. Here, a bias correction methodology is presented to obtain the most representative data for the site climate. The bias correction is applied to precipitation only, as temperature is generally well represented by climate models and downscaled climate products.

The Quantile Delta Mapping (QDM) method of Cannon (2015) is used for bias correction, as the correction can be applied to different segments of the precipitation distribution. This allows for the correction of drizzle in days with low amounts of precipitation, as well as days with extreme precipitation amounts. The QDM bias correction is applied using on a monthly timescale, which is interpolated for each day of the year. This allows for seasonal bias to be corrected without introducing additional artifacts near the boundary between months or seasons. The QDM method for bias correction is similar to that used for updating future rainfall statistics in Section A.3.3.1, but there are key differences. First, the relationships are built between the observed and model baseline data and are applied to the future projections to correct for bias. Second, quantiles are extracted from the empirical distribution using linear interpolation, rather than fitting a statistical distribution to each dataset. The method is applied using the following steps:

1. For a calendar month extract data for all years.
2. Extract a set of Q_{m_i} evenly spaced quantiles from the observed and model baseline empirical cumulative distributions across the range of non-exceedance probabilities, P_i.
3. Compute bias-correction factors, CF_{m_i} for each Q_i by taking the difference between those obtained from Step 2.
4. Apply linear interpolation of monthly correction factors to daily correction factors (for each day of the year) from the center day of each month, resulting in the set of correction factors CF_{d_i}.
5. For each day in the future projected dataset, find the closest probability to those in the set of P_i from Step 2, and apply the corresponding CF_{d_i} using addition.
6. Repeat Steps 1 to 4 for each day of the year. The future dataset is now corrected for bias with the fundamental assumption that the difference between observed and model baseline datasets will be preserved in the future (Wang and Chen 2014).

The calculation (Step 3) and application (Step 5) of additive correction factors allows for wet and dry day frequencies to be corrected as multiplicative correction factors will not be applied in regions of the precipitation distribution where there are all zeros for either the observed or modelled baseline datasets. Anandhi et al. (2011) recommends that when using additive correction factors, the set of evenly spaced quantiles should be greater than 25 to minimize differences between additive and multiplicative correction factors. In this work, 50 evenly spaced quantiles are used in order to correct for bias in precipitation extremes.

The corrected daily timeseries of precipitation and derived variables including rain, snow, and snow depth are provided. Daily timeseries for temperature and potential evapotranspiration are included but are not bias corrected as mentioned above.

A.3.6.2 Projecting Future Changes in WMO Climate Indices

The WMO climate indices are first calculated for the modelled baseline and future periods using the method described in Appendix A.2.5.2. Projected changes in the WMO climate indices are obtained by taking the difference in the maximum, minimum, mean, and median values calculated across years between the modelled baseline and the 2050s and 2080s future time periods.

A.3.6.3 Projecting Future Changes in Potential Evapotranspiration

Projected change in potential evapotranspiration are estimated by first calculating potential evapotranspiration using the statistically downscaled minimum and maximum temperature projections from the multi-model ensemble. Monthly totals are then taken and averaged across calendar months. The percentage change between the monthly values between the model baseline and future time periods is calculated for each member of the multi-model ensemble. The distribution of percentage changes across the multi-model ensemble is then provided using a set of percentiles. Daily future timeseries are provided for potential evapotranspiration using the downscaled temperature projections from the multi-model ensemble, using the same methodology as Appendix A2.5.3.

A.3.6.4 Projecting Future Changes in the Drought Index

The drought index is first calculated with the method describes in Appendix A.2.5.4 using statistically downscaled precipitation and temperature projections for each member of the multi-model ensemble. The percentage change is taken for each month and percentile between the modelled baseline and future time periods.

A.3.6.5 Qualitative Changes in Wind Speed and Relative Humidity

Changes in windspeed and relative humidity are provided using the best available information applicable to the South Bruce study area. Both windspeed and relative humidity climate variables are not available in the set of statistically downscaled climate projections from Climatedata.ca. However, the ECCC provides projected surface wind speed changes based on an ensemble of 29 global climate models from the CMIP5 on a 1°x1° grid across Canada (ECCC 2018). The projected changes from the grid cell closest to the South Bruce study area are extracted, and percentiles across the multi-model ensemble are presented for each future period and climate scenario available. This information should be interpreted qualitatively, as the global climate models have a very course spatial resolution and may not be representative of the study area.

In the absence of literature values, relative humidity can be estimated using the August-Roche-Magnus approximation, which implies that saturation vapor pressure changes approximately exponentially with temperature under typical atmospheric conditions (Alduchov and Eskridge 1996),

$$Relative\ Humidity = \frac{\exp\left(\frac{17.625 \cdot t_D}{243.04 + t_D}\right)}{\exp\left(\frac{17.625 \cdot t}{243.04 + t}\right)} * 100\%$$ **Equation 45**

Where t is the mean daily temperature and t_D corresponds to the dewpoint temperature, which is assumed to be the minimum daily temperature (all in °C). This assumption was also made for storm maximization in DAD curve development (Appendix A.2.3.2). Relative humidity is calculated using this equation for each member of the multi-model ensemble. Monthly mean values are then calculated and summarized using a set of percentiles.

REFERENCES

Alduchov, O. A. and Eskridge, R. E. 1996. Improved Magnus' Form Approximation of Saturation Vapor Pressure. J. Appl. Meteor., 35, 601–609.

Anandhi, A., Allan, F., Pierson, D.C., Schneiderman, E.M., Zion, M.S., Lounsbury, D. and Matonse, A.H. Examination of Change Factor Methodologies for Climate Change Impact Assessment. Water Resources Research, 47(3). doi: 10.1029/2010WR009104.

Bracken, C. 2016. Downscaled CMIP3 and CMIP5 Climate Projections – Addendum, Release of Downscaled CMIP5 Climate Projections (LOCA) and Comparison with Preceding Information. Bureau of Reclamation. Retrieved from https://gdo-dcp.ucllnl.org/downscaled_cmip_projections/techmemo/Downscaled_Climate_Projections_Addendum_Sept2016.pdf.

Canadian Standards Association (CSA). 2012. Draft Standard Plus 4013-12 Technical Guide Development, Interpretation and Use of Rainfall Intensity-Duration-Frequency (IDF) Information: Guideline for Canadian Water Resources Practitioners. Toronto, Canada.

Cannon, A.J., Sobie, S.R. and Murdock, T.Q. Bias Correction of GCM Precipitation by Quantile Mapping: How Well Do Methods Preserve Changes in Quantiles and Extremes? Journal of Climate, 28(17): 6938-6959. doi: 10.1175/JCLI-D-14-00754.1.

Charron, I. 2016. A Guidebook on Climate Scenarios: Using Climate Information to Guide Adaptation Research and Decisions, 2016 Edition. Ouranos, 94 pages.

Cunnane, C. 1989. Statistical Distributions for Flood Frequency Analysis. Operational Hydrology Report no. 33, World Meteorological Organization.

Environment and Climate Change Canada (ECCC). 2016. Climate Data and Scenarios for Canada: Synthesis of Recent Observation and Modelling Results. Environment and Climate Change Canada. Available at: https://www.canada.ca/en/environment-climate-change/services/climate-change/publications/data-scenarios-synthesis-recent-observation.html.

Environment and Climate Change Canada (ECCC). 2019. Engineering Climate Datasets. Available at https://climate.weather.gc.ca/prods_servs/engineering_e.html. Accessed June 15, 2019.

Environment and Climate Change Canada (ECCC). 2020. Canadian Climate Normals. Government of Canada. Available at: https://climate.weather.gc.ca/climate_normals/.

FAO (Food and Agriculture Organization). 2006. FAO Irrigation and Drainage Paper NO. 56 Crop Evapotranspiration. Available at http://www.fao.org/docrep/X0490E/X0490E00.htm

Flato, G., Marotzke, J., Abiodun, B., Braconnot, P., Chou, S.C., Collins, W., Cox, P., Driouech, F., Emori, S., Eyring, V., Forest, C., Gleckler, P., Guilyardi, E., Jakob, C., Kattsov, V., Reason, C. and Rummukainen. M. 2013. Evaluation of Climate Models. In: Climate Change 2013: The Physical Science Basis. Contribution of Working Group I to the Fifth Assessment Report of the Intergovernmental Panel on Climate Change [Stocker, T.F., D. Qin, G.-K. Plattner, M. Tignor, S.K. Allen, J. Boschung, A. Nauels, Y. Xia, V. Bex and P.M. Midgley (eds.)]. Cambridge University Press, Cambridge, United Kingdom and New York, NY, USA

GDO-DCP. Downscaled CMIP3 and CMIP5 Climate and Hydrology Projections. Accessed 2019. Retrieved from https://gdo-dcp.ucllnl.org/downscaled_cmip_projections/#Welcome.

Guo, J.C.Y, Urbonas, B. and Stewart, K. 2001. Rain Catch under Wind and Vegetal Cover Effects. Journal of Hydrologic Engineering, Vol. 6, Issue 1. https://doi.org/10.1061/(ASCE)1084-0699(2001)6:1(29).

Hassanzadeh, E., Nazemi, A. and Elshorbagy, A. 2014. Quantile-Based Downscaling of Precipitation Using Genetic Programming: Application to IDF Curves in the City of Saskatoon. J. Hydrology. Eng., 19(5), 943-955.

Hogg, W. D., Carr, D.A. and Routledge, B. 1989. Rainfall Intensity–Duration–Frequency Values for Canadian Locations. Ottawa: Environment Canada, Atmospheric Environment Service.

Hosking, J.R.M. and Wallis, J.R. 1997. Regional Frequency Analysis. Cambridge University Press, Cambridge, U.K.

Intergovernmental Panel on Climate Change (IPCC). 2013. Climate Change 2013: The Physical Science Basis. Contribution of Working Group I to the Fifth Assessment Report of the Intergovernmental Panel on Climate Change. Retrieved on March 15, 2017 from https://www.ipcc.ch/report/ar5/wg1/.

Intergovernmental Panel on Climate Change (IPCC). 2020. The IPCC and the Sixth Assessment Cycle. Retrieved on May 8th, 2020 from https://www.ipcc.ch/site/assets/uploads/2020/05/2020-AC6_en.pdf.

Li, H., Sheffield, J. and Wood, E.F. 2010. Bias Correction of Monthly Precipitation and Temperature Fields from Intergovernmental Panel on Climate Change AR4 Models Using Equidistant Quantile Matching. Journal of Geophysical Research, 115(D10), D10101.

Louie, P. Y. T. and Hogg, W. D.1980. Extreme Value Estimates of Snowmelt. Proceedings of Canadian Hydrology Symposium 80 (Toronto, ON: 64-78 National Research Council Canada).

Mekis, É. and Vincent, L.A. 2011. An Overview of the Second Generation Adjusted Daily Precipitation Dataset for Trend Analysis in Canada. Atmosphere-Ocean 49, 163–177. https://doi.org/doi: 10.1080/07055900.2011.583910.

Millington, N., Das, S. and Simonovic, S.P. 2011. The Comparison of GEV, Log-Pearson Type 3 and Gumbel Distributions in the Upper Thames River Watershed under Global Climate Models. Water Resources Research Report no. 077, Facility for Intelligent Decision Support, Department of Civil and Environmental Engineering, London, Ontario, Canada, 53 pages. ISBN: (print) 978-0-7714-2898-2; (online) 978-0-7714-2905-7.

National Aeronautics and Space Administration (NASA). 2019. Modern-Era Retrospective analysis for Research and Applications, Version 2. Retrieved from https://gmao.gsfc.nasa.gov/reanalysis/MERRA-2/.

Olsson, J., Berggren, K., Olofsson, M. and Viklander, M. 2009. Applying Climate Model Precipitation Scenarios for Urban Hydrological Assessment: A Case Study in Kalmar City, Sweden. Atmos. Res., 92:364–375, doi:10.1016/j.atmosres.2009.01.015.

Ontario Ministry of Natural Resources (OMNR). 2006. PMP for Ontario. Prepared by IBI Group. December 2006.

Overeem, A., Buishand, A., and Holleman, I. 2007. Rainfall Depth-Duration-Frequency Curves and Their Uncertainties. Journal of Hydrology. 348(1-2),124-134. doi: 10.1016/j.jhydrol.2007.09.044.

Piani, C., Weedon, G.P., Best, M., Gomes, S.M., Viterbo, P., Hagemann, S. and Haerter, J.O. 2010. Statistical Bias Correction of Global Simulated Daily Precipitation and Temperature for the Application of Hydrological Models. Journal of Hydrology, 395(3-4),199–215.

Pysklywec, D.W., Davar, K.S. and D.I. Bray. 1968. Snowmelt at an Index Plot, Water Resource, 4(5), 937-946.

Reclamation. 2013. Downscaled CMIP3 and CMIP5 Climate Projections: Release of Downscaled CMIP5 Climate Projections, Comparison with Preceding Information, and Summary of User Needs. U.S. Department of the Interior, Bureau of Reclamation, Technical Service Center, Denver, Colorado, 116 p. Available at: http://gdo-dcp.ucllnl.org/downscaled_cmip_projections/techmemo/downscaled_climate.pdf.

Salmi, T., Määttä, A., Anttila, P., Ruoho-Airola, T. and Amnell, T. 2002. Detecting Trends of Annual Values of Atmospheric Pollutants by the Mann-Kendall Test and Sen’s Slope Estimates – The Excel Template Application MakeSens. Publications on Air Quality, No. 31.

Schardong, A. and Simonovic, S.P. 2019. Application of Regional Climate Models for Updating Intensity-Duration-Frequency Curves under Climate Change. International Journal of Climate Change. 9(5): 311-330. DOI: 10.9734/ijecc/2019/v9i530117.

Srivastav, R.K., Schardong, A. and Simonovic, S. P. 2014. Equidistance Quantile Matching Method for Updating IDF Curves under Climate Change, Water Resources Management, 28(9): 2539-2562.

Wan, H., Wang, X.L. and Swail, V.R. 2010. Homogenization and Trend Analysis of Near-Surface Wind Speeds. Journal of Climate, 23(5):1209-1225. doi: 10.1175/2009JCLI3200.1.

Wang, L. and Chen, W. 2014. Equiratio Cumulative Distribution Function Matching as an Improvement to the Equidistant Approach in Bias Correction of Precipitation. Atmospheric Science Letters, 15:1-5. doi: 10.1002/asl2.454.

Werner, A.T. and Cannon, A.J. 2016. Hydrologic Extremes – An Intercomparison of Multiple Gridded Statistical Downscaling Methods. Hydrology and Earth System Sciences., 20: 1483-1508. doi: 10.5194/hess-20-1483-2016.

Wood. 2019. Climate Change Impacts Review and Method Development. Nuclear Waste Management Report NWMO-TR-2019-05. Toronto, Canada. Available at: http://rms.nwmo.ca/Sites/APM/Reports/NWMO-TR-2019-05.pdf.

World Meteorological Organization. 1989. Calculation of Monthly and Annual 30-Year Standard Normals. Washington, DC: World Meteorological Organization. Technical report: WMO-TD No. 341, WCDP-10. Geneva, Switzerland.

World Meteorological Organization (WMO). 2009a. Manual on Estimation of Probable Maximum Precipitation (PMP). World Meteorological Organization (WMO). WMO-No. 1045. Geneva, Switzerland

World Meteorological Organization. 2012. Standardized Precipitation Index: User Guide. Washington, DC: World Meteorological Organization. Technical report: WMO No. 1090. Geneva, Switzerland.

APPENDIX B: ADDITIONAL FUTURE CLIMATE STATISTICS

Additional future rainfall statistics tables are provided in a companion spreadsheet for this report. This format was selected in order to allow for the results to be more readily accessible and improve the readability of the report. The minimum, maximum, mean, standard deviation, and percentiles ranging from 5% to 99% provide information on the distribution of the projected changes in climate from the multi-model ensemble. These statistics are provided for daily, and multi-day IDF curves, as well as PMP, combined rainfall and snowmelt, and peak snowpack accumulation for the multi-model ensemble climate projections. Projections for both the 2050s and 2080s time periods for all the additional statistics are included.

APPENDIX C: DAILY CLIMATE TIME SERIES

Daily current climate timeseries are provided for the baseline period of 1979 to 2019. This includes the daily infilled dataset discussed in Section 3.1.2 of the main report, which includes the infilled daily precipitation, and minimum, maximum, and mean daily temperatures. Derived variables for potential evapotranspiration, rain, snow, and snow depth are also included.

Daily future timeseries are provided for the bias corrected precipitation and derived variables including rain, snow, and snow depth. Minimum, maximum and mean daily temperatures are also provided as well as potential evapotranspiration. For the climate variables, a daily timeseries is provided for each member of the multi-model ensemble for the period of 1979 to 2100. This corresponds to a total of 136 daily timeseries for each of the climate variables. It should be noted that for the period that overlaps the daily current climate timeseries, the daily current climate timeseries should be preferred, as it is based on observations instead of modelled results.

If possible, it is recommended each member of the multi-model ensemble be used to capture the full range of uncertainty in the climate projections. If this is not possible (due to computational time constraints for example), a subset of the daily timeseries may be selected in a way that reasonably captures the range of uncertainty in the impact model. For example, if rainfall on snow in the month of April is a critical design parameter for a flood management model, a subset of the daily timeseries that captures the range of rainfall and snowmelt in the month of April may be selected if it is not possible to run all of the climate scenarios. This assessment will be dependant on the use of the data.